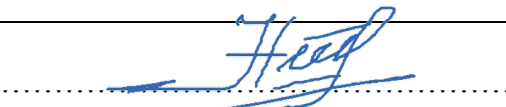




University of  
Stavanger

**FACULTY OF SCIENCE AND TECHNOLOGY**

## **MASTER'S THESIS**

Study program/Specialization:  Petroleum Engineering / Natural Gas Technology	Spring semester, 2018  Open
Author: Alisher Narzulloyev	 (signature of author)
Internal supervisor: Dag Chun Standnes External supervisors: Ingun Skjevraak (Equinor ASA) Knut Kristian Meisingset (Equinor ASA)	
Title of master's thesis: <b>Dashboard for visualization, evaluation and modeling of wellbore and field H<sub>2</sub>S production</b>	
Credits (ECTS): 30	
Key words: Spotfire Dashboard Data Visualization and Analysis Reservoir Souring Hydrogen Sulfide Sulfate-Reducing Bacteria Seawater Ion Analysis	Number of Pages: 83  + supplemental material/other None  Stavanger, June 15/ 2018

Title for Master's Thesis

Faculty of Science and Technology



I dedicate this work to my parents, to the memory of my  
grandparents, and my wonderful brothers,  
Bekhruz and Akobir.

# Acknowledgments

I would first like to express my profound gratitude to my supervisors, Dr. Ingun Skjevrak and Dr. Knut Kristian Meisingset, for their continuous guidance, technical and administrative support as well as readiness to help. I would also like to thank my co-supervisor, Dr. Dag Chun Standnes, for his valuable comments and discussions in the review of my thesis. I am privileged and grateful for the opportunity of working under their supervision.

I take this opportunity to express my gratitude to all of the Department of Remaining Resources Recovery in Stavanger (ST RRR) at Equinor, including Thibaut Forest, Jørgen Bergsagel Møller, Øystein Lie, Martin Iding, Øystein Tesaker, Kjersti Håland for their kind help and support. I would like extend my thanks to my fellow student, Mr. Andrew Mburu for a wonderful semester and productive discussions on the subject.

Last but by no means least, I am sincerely grateful to my parents for the unceasing encouragement, support and attention. I thank you for allowing me to pursue my passion and providing all to achieve my goals.

Alisher Narzulloyev  
University of Stavanger, Norway

# Abstract

For several years, continuously increasing amounts of hydrogen sulfide ( $H_2S$ ) are being produced from numerous fields on the Norwegian Continental Shelf as a result of reservoir souring. Reservoir souring – increasing concentration of  $H_2S$  in production fluids from initially sweet reservoirs – is, typically, encountered after the breakthrough of seawater that is injected for higher recovery purposes. Failure to control and mitigate elevated  $H_2S$  production may result in serious health issues of operating personnel, loss of production liquid quality and amount, as well as escalated operational expenditures. Despite the importance of the question, modeling and prediction attempts of reservoir souring suffers from less reliable outcomes let alone its mitigation approaches, which could be attributed to the limited understanding of factors governing increased  $H_2S$  production.

To address the challenge of understanding the factors influencing and/or prohibiting  $H_2S$  production, the aim of building a dashboard for visualization of relevant reservoir souring data has been set. Thus, the main objectives of the work to achieve the goal are defined as follows:

- Gather necessary data for  $H_2S$  production evaluation;
- Build a platform in Tibco's Spotfire tool based on the collected data that allows charting interactive and flexible 2D visualizations;
- Propose a structure for the evaluation of  $H_2S$  production;
- Incorporate developed  $H_2S$  production models (correlations).

Current work presents a workflow for building dashboard for  $H_2S$  production evaluation where gathering, cleaning and manipulation of necessary data are done within Spotfire. The evaluation of  $H_2S$  production data is performed in three interactive levels, namely field, reservoir and wellbore levels. Field level contains the analysis for overall comparison of fields in question. Reservoir level illustrates the relationship between water cut and  $H_2S$  production per formation. Most of the analysis was carried on wellbore level owing to data availability and quality. Cumulative  $H_2S$  vs. cumulative seawater plots are generated for all wellbores and cumulative  $H_2S$  is mapped per wellbore where areal variety in oil composition can be investigated. Besides, ion data analysis is also carried out and more accurate seawater fraction calculation is suggested.

Developed empirical correlation for matching  $H_2S$  production history is integrated into the dashboard and finally, a workflow for integration of dashboard with SourSim<sup>®</sup>RL prediction results through  $H_2S$  production optimization tool is proposed.

# Table of Contents

Acknowledgments .....	i
Abstract.....	ii
Table of Contents .....	iii
List of Figures.....	v
<b>1 Introduction .....</b>	<b>1</b>
<b>2 Literature Review .....</b>	<b>3</b>
<b>2.1 Background of Reservoir Souring.....</b>	<b>3</b>
2.1.1 What is reservoir souring? .....	3
2.1.2 Mechanisms of reservoir souring .....	3
2.1.3 Sulfate-reducing bacteria .....	5
2.1.4 Factors controlling SRB growth .....	5
2.1.5 Hydrogen sulfide scavenging in the reservoir.....	8
2.1.6 Well location and water movement .....	8
2.1.7 Hydrogen Sulfide Partitioning .....	9
<b>2.2 Overview of Existing Models for H<sub>2</sub>S Production .....</b>	<b>10</b>
2.2.1 Mixing type souring model.....	10
2.2.2 Biofilm model .....	12
2.2.3 Thermal Viability Shell model.....	14
2.2.4 Mechanistic Model of Burger .....	16
2.2.5 SourSim <sup>®</sup> RL.....	18
<b>2.3 Reservoir Souring Case Histories.....</b>	<b>20</b>
2.3.1 South Arne Field – Denmark .....	20
2.3.2 Snorre Field (platform A) .....	22
2.3.3 Gullfaks Field.....	22
<b>3 Methodology.....</b>	<b>24</b>
<b>3.1 Data Science Concept of the Present Thesis .....</b>	<b>24</b>
<b>3.2 Data Structuring for Visualization.....</b>	<b>27</b>
<b>3.3 Calculations Involved Behind the Scenes .....</b>	<b>28</b>

3.3.1	Outlier detection and removal.....	28
3.3.2	H <sub>2</sub> S Calculator.....	30
3.3.3	Ion data analysis.....	32
3.3.4	Wellbore geo-location.....	34
<b>4</b>	<b>Results and Discussion .....</b>	<b>36</b>
<b>4.1</b>	<b>Field Level Visualization and Data Analysis.....</b>	<b>36</b>
4.1.1	Cumulative H <sub>2</sub> S over the field lifetime.....	36
<b>4.2</b>	<b>Reservoir Level Visualization and Data Analysis.....</b>	<b>39</b>
4.2.1	Water Cut vs. H <sub>2</sub> S per formation .....	39
<b>4.3</b>	<b>Wellbore Level Visualization and Data Analysis.....</b>	<b>43</b>
4.3.1	Cumulative H <sub>2</sub> S vs. Cumulative Seawater.....	43
4.3.2	Injection – Production data joint analysis .....	46
4.3.3	Wellbore location on map.....	49
4.3.4	Ion data analysis.....	50
4.3.5	Effect of different SWC calculations on the analysis .....	55
<b>4.4</b>	<b>Incorporating H<sub>2</sub>S production models (correlations) in the dashboard .</b>	<b>57</b>
<b>5</b>	<b>Conclusion .....</b>	<b>61</b>
<b>5.1</b>	<b>Summary and Recommendations.....</b>	<b>61</b>
<b>5.2</b>	<b>Future Development of the Dashboard.....</b>	<b>63</b>
<b>6</b>	<b>Bibliography.....</b>	<b>65</b>
	<b>Nomenclature .....</b>	<b>69</b>
	<b>Appendix A .....</b>	<b>70</b>
	<b>Appendix B .....</b>	<b>72</b>
	<b>Appendix C .....</b>	<b>73</b>
	<b>Appendix D .....</b>	<b>74</b>

# List of Figures

<b>Figure 1: The setup for H<sub>2</sub>S production is not well defined</b> .....	2
Figure 2: Factors controlling SRB activity in reservoirs.....	6
Figure 3: Schematic representation of bacterial reservoir souring.....	11
Figure 4: H <sub>2</sub> S Production using mixing zone model.....	12
Figure 5: Schematic representation of biofilm reservoir souring.....	13
Figure 6: Development of TVS model.....	16
Figure 7: Nutrient supply .....	17
Figure 8: Workflow of SourSim®RL .....	19
Figure 9: Sulfate in produced water versus seawater cut ( <i>Source: Robinson et al. 2010</i> )..	21
Figure 10: Schematic illustration of observed dual souring mechanism.....	23
Figure 11: Workflow for building the current dashboard .....	25
Figure 12: Visualization levels.....	28
Figure 13: Outlier detection .....	29
Figure 14: Outlier removal procedure.....	30
Figure 15: Schematic illustration of a well .....	35
Figure 16: Cumulative H <sub>2</sub> S production since field start-up.....	36
Figure 17: a) Cumulative H <sub>2</sub> S production and b) H <sub>2</sub> S concentration in produced seawater since field start-up.....	37
Figure 18: Field level cumulative H <sub>2</sub> S vs. cumulative seawater chart.....	38
Figure 19: H <sub>2</sub> S concentration (ppm) vs. water cut trellised by reservoir.....	40
Figure 20: Decreased gas rate effect on H <sub>2</sub> S concentration.....	41
Figure 21: Comparison of total H <sub>2</sub> S produced against gas phase concentration.....	41
Figure 22: Dual reservoir effect in formation level.....	42
Figure 23: Field I-X cumulative H <sub>2</sub> S production per well-bore.....	43
Figure 24: H <sub>2</sub> S concentration in gas phase (ppm) vs. SWC.....	44
Figure 25: Cumulative H <sub>2</sub> S (kg) vs. cumulative seawater production.....	44
Figure 26: Cumulative H <sub>2</sub> S vs. Cumulative seawater production for all wellbores of Field I.	45
Figure 27: Wellbore examples of each “Type” .....	46
Figure 28: Injection – Production data joint analysis.....	48



Figure 29: Map chart (Field I example), cumulative H <sub>2</sub> S and seawater, oil composition for the entire history.....	49
Figure 30: Map chart, cumulative H <sub>2</sub> S and seawater, oil composition for 1998-2008 period .	50
Figure 31: Sulfate mass balance.....	51
Figure 32: Well X generated and produced H <sub>2</sub> S .....	52
Figure 33: Other well examples on generated and produced H <sub>2</sub> S comparisons .....	53
Figure 34: Well X seawater fraction calculated from different methods .....	55
Figure 35: Well X cumulative H <sub>2</sub> S vs. cumulative seawater .....	56
Figure 36: Simplified model match in example of Type II wellbores .....	59
Figure 37: Simplified model match for Type I and III wellbores .....	60
Figure 38: Workflow for H <sub>2</sub> S Production Forecast and Control.....	63

# 1 Introduction

Reservoir souring is defined by increasing concentration of H<sub>2</sub>S in production fluids from initially sweet reservoirs. It has become one of the major problems in offshore oilfields where seawater injection is employed as a secondary recovery method.

The economic significance of reservoir souring can be very critical if due cognizance is not paid during the planning period of field development, meaning that upgrading of all equipment to sour service material after the onset of increased H<sub>2</sub>S production can escalate the cost by orders of magnitude. Moreover, oil and gas export lines have specific maximum limit of H<sub>2</sub>S concentration that is allowed to transport. Should the concentration exceed the maximum limit, subsequent profit loss from fluid export would be expected. To lower field-wise concentration of H<sub>2</sub>S in export fluid, wells with high H<sub>2</sub>S amount are usually shut in causing lost or delayed production.

Besides economic impact, reservoir souring can result in serious health and safety issues. H<sub>2</sub>S is a colorless, flammable and highly toxic gas that has a smell of “rotten eggs” at low concentrations and is a second most common cause of inhalation death after carbon monoxide (Johnson et al., 2017). In terms safety, after the onset of H<sub>2</sub>S its monitoring becomes mandatory with strictly disciplined safety procedures (Eden et al., 1993).

In the view of aforementioned impacts of reservoir souring, a project with an objective of enhanced understanding of the phenomenon for reduced uncertainty in H<sub>2</sub>S prognosis has been launched. As a part of the project the development of a Spotfire dashboard for evaluation and modeling of H<sub>2</sub>S production is also initiated. However the setup of the dashboard was not so well defined (Figure 1) that optimal predictions for new wells and fields can be made on the basis of existing data. Thus, current work of building a dashboard has the following main objectives:

- Propose a structure for H<sub>2</sub>S development and forecast, which involves:
  - Gathering, cleaning and manipulation of data necessary for H<sub>2</sub>S production evaluation;
  - Building a platform in Tibco’s Spotfire tool for charting interactive 2D visualizations;
- Evaluate the development of H<sub>2</sub>S on field, reservoir and wellbore levels;
- Incorporate developed H<sub>2</sub>S production models (correlations).

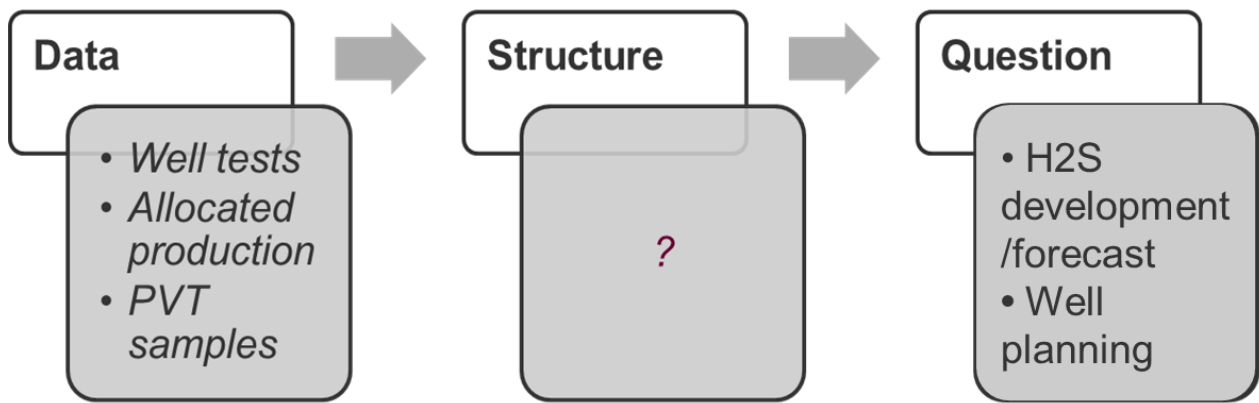


**Figure 1: The setup for H<sub>2</sub>S production is not well defined**

To understand reservoir souring and be able to identify relevant data for further analysis a detailed review of background information on reservoir souring, developed models for H<sub>2</sub>S generation and several case histories from North Sea fields is carried out. The literature review section is then followed by the methodology section where the actual work fulfilled to build the dashboard for H<sub>2</sub>S production evaluation, to extract data from different sources, its cleaning and manipulation for calculating the necessary parameters is presented.

In “Results and Discussions” chapter of the work detailed explanation of the dashboard’s workflow is presented. The dashboard illustrates the data in three interactive levels of visualization drilling down from field to formation/reservoir and to well-bore levels. Plots for cumulative H<sub>2</sub>S production has been generated for several hundred wells of different fields with seawater injection, proving a correlation between the produced H<sub>2</sub>S and seawater. To analyze injection effects, joint visualization of injection, production and H<sub>2</sub>S development data is also established.

Ion data analysis has also been performed to show how much of sulfate (mg/l) had been lost in a reservoir to generate H<sub>2</sub>S and how much of H<sub>2</sub>S had been scavenged within the reservoir delaying its appearance at the producers. The impact of oil composition on H<sub>2</sub>S generation is investigated by visualizing cumulative H<sub>2</sub>S and seawater per wellbore on a map chart.

Lastly, the in-house developed models for H<sub>2</sub>S production forecast is integrated into the Spotfire dashboard, since the need for a suitable tool is obvious in the view of the economic importance of H<sub>2</sub>S prediction.

## **2 Literature Review**

### **2.1 Background of Reservoir Souring**

#### **2.1.1 What is reservoir souring?**

A phenomenon of undesirable increase in the concentration of hydrogen sulfide in production fluids is referred as reservoir souring. This generally occurs in reservoirs where seawater-flooding is introduced for secondary recovery, pressure maintenance and/or produced water disposal operations. An increase in the concentration of H<sub>2</sub>S usually starts after the breakthrough of the injected water at the producing wells. Dual porosity reservoirs, however, may have H<sub>2</sub>S breakthrough prior to injection water breakthrough (Vance & Thrasher, 2005). Industry has reported varying concentrations of H<sub>2</sub>S measured at the wellhead being as high as several thousand parts per million per volume (ppmv) (Khatib & Salanitro, 1997; Larsen, 2002). On the other hand, reservoirs are considered to be sour once the hydrogen sulfide concentration rises above 3 ppmv (Eden et al., 1993).

If due actions are not taken at the right moment, reservoir souring may result in serious problems including corrosion and sulfide stress-cracking of installations, loss of economic value of crude, increased cost of refining, lost or deferred production due to shutting in the wells with extreme H<sub>2</sub>S concentrations as well as health and safety concerns because of its high toxicity and inflammability.

#### **2.1.2 Mechanisms of reservoir souring**

Two main groups of reservoir souring mechanisms – biotic and abiotic – have been proposed. The latter mechanism of reservoir souring is believed to be less important and includes thermochemical reduction of sulfate to sulfide, thermal decomposition of organic sulfur, pyrite dissolution and redox reactions involving bisulfite oxygen scavengers (Herber, 1987; Eden et al., 1993; Khatib & Salanitro, 1997). Microbial reduction of sulfate to sulfide, however, is widely accepted to be the most predominant mechanism of H<sub>2</sub>S production in water-flooding employed reservoirs (Ligthelm et al., 1991; Sunde et al., 1993).

## **Abiotic mechanism of reservoir souring**

A brief summary of non-microbiological reservoir souring mechanisms (also referred as geochemical souring) is given by Immanuel et al. (2015). They also emphasized why some of these mechanisms of geochemical souring cannot be considered as pivotal:

- Thermochemical sulfate reduction. This is the most plausible mechanism of geochemical approach for reservoir souring and in the presence of pre-existing H<sub>2</sub>S as a catalyst the temperature limits for the occurrence of the current mechanism is demonstrated to be 77 – 121°C.
- Thermal decomposition of organic sulfur. In this case the process requires elevated temperatures above normal reservoir conditions and it is not associated either with sulfate reduction or related to seawater injection (Eden et al., 1993).
- Pyrite (FeS<sub>2</sub>) may be considered as a geological hydrogen sulfide source in formation rocks. However, pyritic mineral dissolution in reservoir requires oxidant at high potential that is unlikely to occur in reservoir environment.
- Oxygen scavengers are implemented during water-flooding operations where seawater contains sulfate in a varied amount. These chemicals are redox poisoning agents. But low concentrations of them cannot explain high amount of H<sub>2</sub>S produced and thus the probability of this mechanism being responsible for H<sub>2</sub>S growth is very low.

## **Microbial reservoir souring**

Microbial (biotic) reservoir souring is mostly encountered in reservoirs where seawater and/or produced water reinjection is carried out to maintain reservoir pressure and sweep the oil towards the production wells. Sulfate-reducing bacteria (SRB) and sulfate-reducing archaea (SRA) collectively referred as sulfate-reducing prokaryotes (SRP), are the main driving force of microbial H<sub>2</sub>S growth. At the primary production stage these bacteria may initially be present in the reservoir in a passive state or introduced during drilling operations. As a consequence of water-flooding more favorable environment establishes owing to redistribution of temperature profile and availability of nutrients like phosphorous and nitrogen (Haghshenas, 2011). For the rest of the present thesis microbial mechanism will be meant when referring to reservoir souring.

### **2.1.3 Sulfate-reducing bacteria**

First conclusion on the existence of SRB in production waters was drawn by Edson S. Bastin and his colleagues in 1926. A microbiological investigation of several wellhead samples from oilfields showed that SRB were common inhabitants of this environment. Since then numerous articles came out regarding bacterial communities that can reside in deep reservoirs (Rosnes et al., 1991; Pedersen, 2000). However, the question about the origin of these bacteria i.e. whether they have been in the reservoir since its deposition or were introduced lately from other sources is still challenging<sup>1</sup>.

Sulfate-reducing bacteria and archaea represent a ubiquitous group of strictly anaerobic prokaryotes that use sulfate as a terminal electron acceptor and organic compounds or hydrogen as electron donors for anaerobic respiration (Vance & Thrasher, 2005). Metabolic potential of SRB is very broad and they can oxidize various organic compounds present in reservoirs including volatile fatty acids (VFA), alcohols, hydrocarbons and aromatic compounds, carboxylic acids using sulfates that are introduced to reservoirs during water injection (Immanuel et al., 2015). One should bear in mind that the present list for organic compounds is probably not exhaustive.

Different members of SRB have been encountered from oilfield reservoirs and they are categorized based on the maximum temperature that they can tolerate. Mesophilic bacteria have a moderate temperature range of growth and will not multiply above 45°C (Eden et al., 1993). Thermophilic isolates are active at temperature as high as 80°C and they are envisaged to be autochthonous to oil reservoirs (Beeder et al., 1994). Hyperthermophilic SRB have optimal growth temperatures above 80°C and are also found in oil reservoirs (Beeder et al., 1995).

### **2.1.4 Factors controlling SRB growth**

As it was already discussed, sulfate and organic compounds are required for metabolism and SRB growth in the role of electron acceptor and electron donor respectively. However, even when these requirements are accomplished, there are still numerous physical conditions which have to be met for microbial sulfidogenesis to take place. A simple overview of different factors controlling SRB growth is shown in Figure 2. A thorough comprehension and apparently

---

<sup>1</sup> Whether the bacteria found in these (oilfield) waters today are lineal descendants of forms living on the sea-bottom at the time the sediments were laid down or have been introduced later by ground waters descending from the surface to the oil-bearing horizons is an interesting question that it may never be possible to answer – Edson S. Bastin (1926)

quantification of these factors in the reservoir environment makes it possible to develop a model to forecast the likelihood of reservoir souring (Herbert et al., 1985).

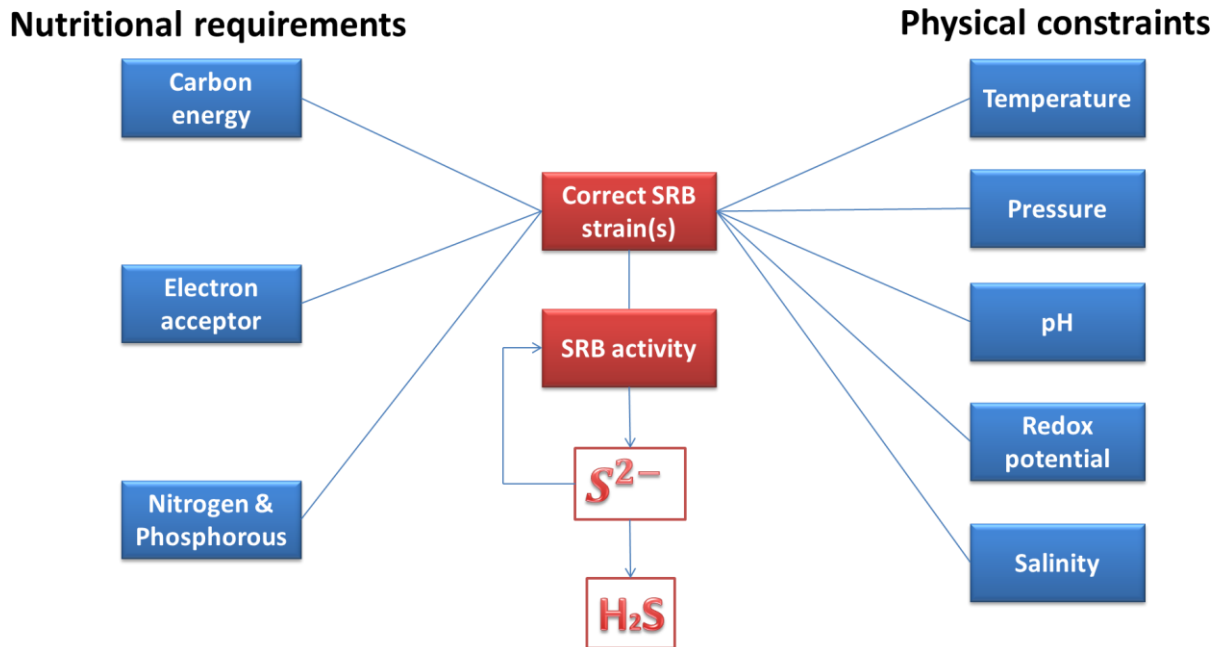


**Figure 2: Factors controlling SRB activity in reservoirs**

Below a contribution and/or prevention of each of the nutritional and environmental factors are summarized from Johnson et al. (2017) and Herbert et al. (1985) reports unless otherwise stated.

**Nutritional requirements:**

- Carbon source, typically VFA, is essential to provide the electron donor for respiration and for incorporation into cells as biomass. Besides VFA, some SRP can utilize other organic compounds biodegraded from oil, such as acetate.
- Sulfates are usually considered as electron acceptors, even though certain microorganisms can reduce other oxidized sulfur compounds such as elemental sulfur and thiosulfate. Sulfate containing injection waters may become rich of available electron acceptors due to the usage of such compounds as oxygen scavengers. Concentration of sulfate and carbon varies largely within and between reservoirs, and thus directly impacts the amount H<sub>2</sub>S production.
- Nitrogen and Phosphorous are particularly important for bacteria and archaea growth and reproduction. They form essential components of varying cellular molecules (proteins,

nucleic acids etc.). Despite the importance for metabolism and growth, only trace amounts of these elements are needed.

**Physical constrains:**

- **Temperature.** The initial temperature of a reservoir is considered to have a great impact on the activity of sulfate-reducing micro-organisms and thus on the concentration of generated H<sub>2</sub>S. As it was previously presented, SRB are classified with regards to temperature ranges within which they are able to react. Birkeland (2005) and Immanuel et al. (2015) have tabulated sulfate-reducing micro-organisms recovered from oil field production waters and it can be seen that the overwhelming majority of them belong to mesophilic and thermophilic groups that can tolerate temperatures up to 80°C. Hence reservoirs with high initial temperatures experience less souring (only hyperthermophilic SRB (>80°C) growth), at least prior to cooling of reservoir as a result of water-flooding.
- **Pressure.** Depending on the depth of the reservoir this factor varies greatly and thus as a result of adaptation to the environment sulfate-reducing micro-organisms can tolerate greater pressure ranges. To investigate the effects of pressure on micro-organisms is quite challenging when they are isolated from a reservoir, i.e. in laboratories. However, conducted researches show that pressures above 15000 psi [ $\approx$ 1034.2 bar] have detrimental impact on their growth.
- **pH.** Sulfate-reducing micro-organisms have a narrow window of 6 - 8.6 in their pH requirements for growth due to the effects of reduced or elevated pH on their trans-membrane proton gradient. Most of the sulfate reducers have an optimum of close to pH 7. pH is essential factor in controlling the H<sub>2</sub>S partitioning behavior between gas, oil and water phases both at reservoir and surface conditions.
- **Redox potential.** Reduction-oxidation potential is a measure (in volts (V) or millivolts (mV)) of the tendency of a chemical species to acquire electrons and thereby be reduced (Reduction potential). In order to function SRB require a negative redox potential (-100 mV or less).
- **Salinity** is often referred as the major factor impacting reservoir souring. The effect of salinity is inversely proportional to the concentration of total dissolved solids (TDS), i.e. the higher the TDS, the lower is the likelihood of SRB growth. Although the metabolism of sulfate reducers can occur over a wide range of TDS, their activity is usually limited to salinities of fresh water up to 150000 mg/l TDS.



- **Sulfide Concentration.** Sulfide is extremely toxic to all life including sulfate-reducing micro-organisms, despite the fact that it is the by-product of energy metabolism. There is a hydrogen sulfide concentration build-up limit after which it starts to inhibit metabolism of sulfate, sulfur and thiosulfate. Resistance level of sulfate-reducing micro-organism to sulfide toxicity is conventionally considered greater than 250 mg/l after which sulfide inhibits the activity of bacteria. However, H<sub>2</sub>S concentration higher than 200 mg/l is rarely observed in Norwegian Continental Shelf (NCS) wells (Knut Kristian Meisingset).

### **2.1.5 Hydrogen sulfide scavenging in the reservoir**

Above mentioned factors control the overall amount of H<sub>2</sub>S generated by microbial sulfate reduction. However, there are numerous other factors that serve as a sink for generated H<sub>2</sub>S and influence its total amount in produced fluids. For instance, the ability of rocks containing iron-minerals such as siderite (FeCO<sub>3</sub>), hematite (Fe<sub>2</sub>O<sub>3</sub>) and magnetite (Fe<sub>3</sub>O<sub>4</sub>) to bind the sulfide and thus cause a reduction in the concentration of H<sub>2</sub>S is a very important loss mechanism (Vance & Thrasher, 2005). On the other hand, these iron containing minerals to some extent may dissolve in the formation water and consequently react with H<sub>2</sub>S containing in water phase and precipitate in the form of pyrite (FeS) resulting in a partial removal of H<sub>2</sub>S. The higher the concentration of ions in the formation water, the less H<sub>2</sub>S will be produced (Håland et al., 1999). These scavenging mechanisms of H<sub>2</sub>S, in practice, are considered to occur at the rock surface, i.e. even if the bulk rock contains large amounts of iron minerals, their scavenging capacity is bound to surface area available for interaction with water flowing through pores (Vance & Thrasher, 2005). These factors are generally referred as retention and/or adsorption terms in most of the predictive models developed for reservoir souring. For instance, Sunde et al. (1993) incorporated both of the these scavenging mechanisms in the adsorption term of their biofilm model which will be revisited in the following chapter in a more detail.

In general, scavenging capacities of a sandstone formation is expected to be relatively high, depending on the available mineralogy, whereas carbonate formations have extremely low scavenging capacities (Johnson et al., 2017).

### **2.1.6 Well location and water movement**

Besides formation mineralogy, water injection rate and the vicinity of injection and production wells affect injected water breakthrough time and thus H<sub>2</sub>S appearance at the production wells. Generally, production wells with relatively short injector – producer travel

distance coupled with high injection rates show earlier breakthrough of injected seawater as compared to those with extended travel path length. Besides, parameters such as rock permeability and porosity might be expected to impact on H<sub>2</sub>S transit time.

### **2.1.7 Hydrogen Sulfide Partitioning**

Partitioning of H<sub>2</sub>S between oil, gas and water phases is a thermodynamic process that is a function of temperature, pressure, fluid composition, and water pH and ionic strength (Burger et al., 2013). H<sub>2</sub>S generated within the reservoir partitions between almost immobile oil phase and relatively faster moving water phase resulting in a delay in its appearance in production wells. Partitioning coefficients (K-values) was measured by Ligthelm et al. (1991) for a simulated North Sea oil and seawater under different temperature/pressure ranges (from 25°C/35MPa to 100°C/15MPa). However, the results over these conditions were almost stable ranging from 18 to 19.5 meaning that the amount of H<sub>2</sub>S partitioned in residual oil is nearly insensitive to reservoir thermo-baric conditions. Vance and Thrasher (2005) show and conclude that the concentration of H<sub>2</sub>S partitioned into residual oil behind the floodfront is significantly less than H<sub>2</sub>S sunk in the mineralogy scavenging. Hence, it is anticipated that in terms of reservoir loss of biogenic H<sub>2</sub>S, the mineralogy aspects dominate over dissolution into residual fluids.

Changes in temperature/pressure alongside the production line cause the partitioning of H<sub>2</sub>S between gas, oil and water phases at the test separator. While hydrogen sulfide concentrations are measured in gas phase, the quantitative determination of overall H<sub>2</sub>S mass rate actually being produced in multiphase systems needs to be carried out in order to assess the actual souring level. Gas/oil ratio (GOR) and water/total liquid ratio (water cut) alterations during the lifetime of a field may raise different levels of souring when measured at the wellhead. In these cases, no additional H<sub>2</sub>S is generated, but changes in the relative volume of produced water (where most of the H<sub>2</sub>S is dissolved) and the production gas (into which most of the H<sub>2</sub>S partitions) result in a higher concentration appearing in gas phase (Vance & Thrasher, 2005).

In addition, for wells where gas-lift operations are performed, a due cognizance should be paid since it can dilute hydrogen sulfide concentrations in gas from the mainstream.

## 2.2 Overview of Existing Models for H<sub>2</sub>S Production

*“All models are wrong – some models are useful”* – George E. P. Box

Quantifying and incorporating all of the above-mentioned parameters into a model to describe and predict H<sub>2</sub>S generation and production may prove unmanageable and even unnecessary. The purpose of the model should always be to learn about the behavior of the real phenomenon, in this case H<sub>2</sub>S generation and production. Each of these factors may improve model's description of the real world, however one should always bear in mind that whether it is worthwhile, i.e. value-creating, to include a specific parameter into a model. To do this, sensitivity analysis or in cases where no reasonable mathematical model is developed a comparison of analogue wells, formations and fields with different development approaches may be applied.

### 2.2.1 Mixing type souring model

Mixing zone souring pattern, often referred as mixing model, is a 1D analytical model for H<sub>2</sub>S generation and transportation in an oil reservoir due to bacterial activity (Ligthelm et al., 1991). The model assumes that SRB growth takes place in a mixing zone where injection water and formation water mix within the reservoir (Figure 3). Injection water, mainly seawater, has high concentrations of sulfate but lacks organic compounds. Formation water, on the other hand, contains organic compounds including fatty acids (nutrients) owing to the contact between the oil and formation water. As the displacement of formation water by injection water continues, mixing zone will develop because of diffusion and dispersion. Ligthelm et al. assumed that the generation of H<sub>2</sub>S due to bacterial activity occurs in a narrow pulse  $\Delta x$  within the mixing zone that moves along the reservoir.

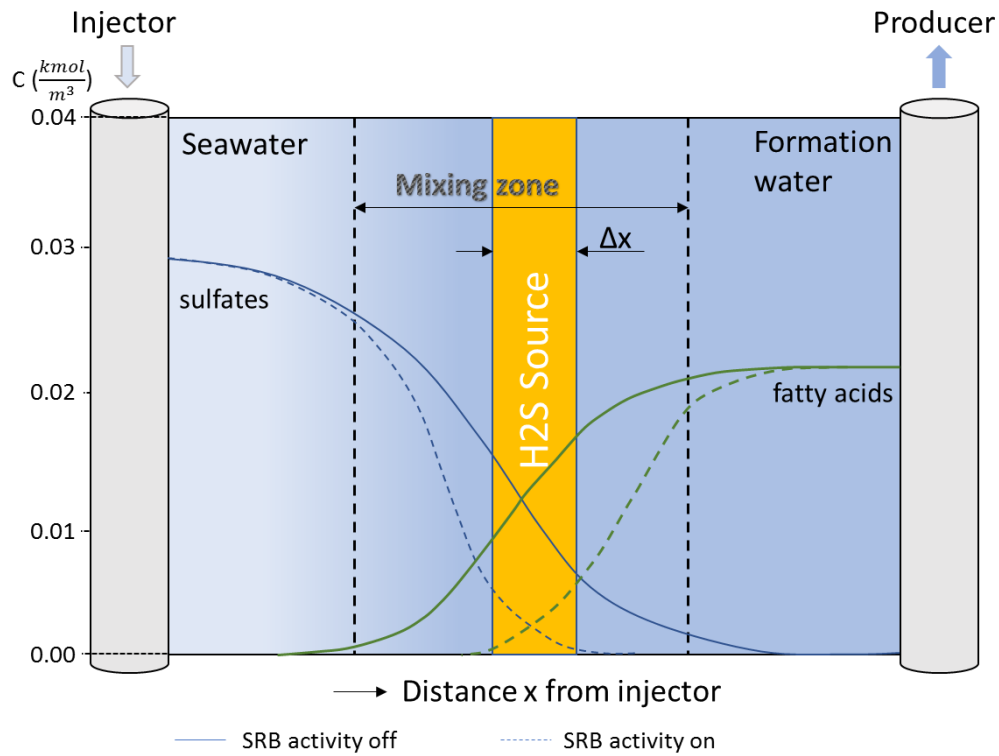


**Figure 3: Schematic representation of bacterial reservoir souring**  
 (Source: Redrawn from Haghshenas (2011))

In case there are no bacterial reactions, error functions describe the concentration profiles. The mixing zone between seawater and formation water is given by  $4\sqrt{Dt}$ , where  $D$  is the dispersion coefficient and  $t$  is the time for displacement process. In the presence of bacterial activity, however, the reaction length  $\Delta x$  is defined as  $2\sqrt{D\tau_b}$ , where  $\tau_b$  is the time that SRB convert sulfates and fatty acids into  $H_2S$ . This time-scale is the measure of how long does it take to reach the balance in biological reactions. In order to make  $\tau_b$  small as compared to time  $t$  ( $t \gg \tau_b$ ), it is assumed that the number of bacteria is large enough so that this balance is reached very quickly. It is assumed that  $H_2S$  source with a constant width  $\Delta x$  moves with the same speed as the water phase and gives a uniform  $H_2S$  production rate of  $R_H^w$ , which is proportional to the reaction region width and defined as:

$$R_H^w = \left[ \frac{C}{4\sqrt{\tau_b}} \right] \frac{1}{\sqrt{t}} \quad (1)$$

where  $C$  is an empirical constant that depends on the initial compositions of seawater and formation water. The  $H_2S$  source term is inversely proportional to the square root of time and at the initial stage of water injection it takes very high values.

According to the mixing model, H<sub>2</sub>S production begins with small quantities after water breakthrough and increases gradually. Once the bacterial reaction zone  $\Delta x$  is produced from the reservoir, the production of H<sub>2</sub>S should eventually stop (Figure 4). However, as the practice shows it is not the case in many reservoirs, where H<sub>2</sub>S production continues long after water breakthrough. Although the partitioning of H<sub>2</sub>S between the fluid phases and the possibility of scavenging by iron-containing minerals has been included, mixing model of Ligthelm et al. does not consider temperature and limiting nutrients effects on SRB growth.

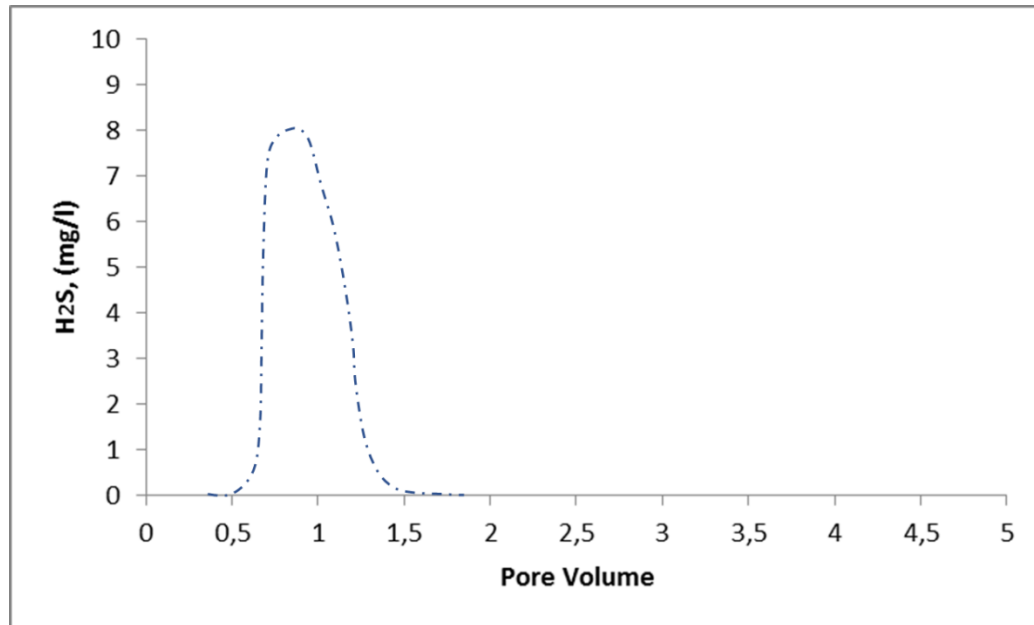


**Figure 4: H<sub>2</sub>S Production using mixing zone model**

### 2.2.2 Biofilm model

Sunde et al. (1993) developed a 1D numerical transport model based on conservation equations. Current model takes into account microbial growth rates, the effect of nutrients, seawater and formation water mixing, transport and adsorption of H<sub>2</sub>S in the reservoir formation. Unlike mixing model, biofilm model assumes that the generation of H<sub>2</sub>S due to immobile bacterial activity takes place in a biofilm near the water injection well (Figure 5). Lack of nutrients, especially nitrogen (N) and phosphorous (P), in injected seawater was considered to be a limiting factor. Thus, the model is based on the growth characteristics of SRB in biofilm and the nutritional conditions of injection water and reservoir water.

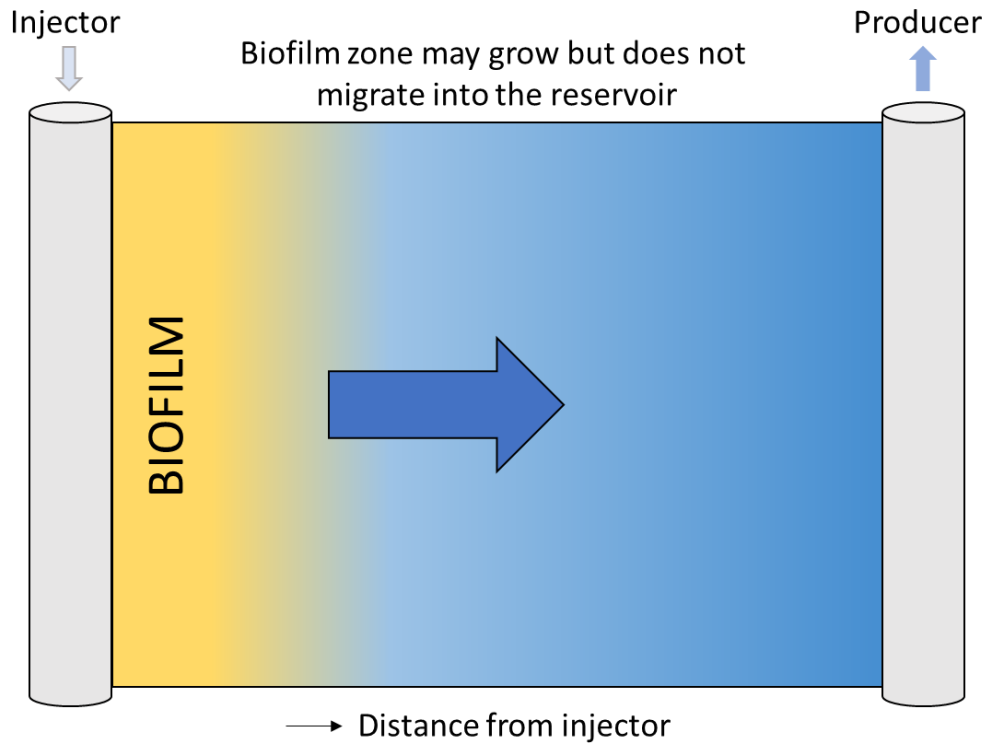


**Figure 5: Schematic representation of biofilm reservoir souring**

The model solves the convection – diffusion – reaction – adsorption equations in one dimensional domain assuming a homogeneous reservoir, constant temperature and incompressible fluid flow. It should also be noted that Sunde et al. implemented an idea of considering two level of adsorption; first – dissolved metal ions and salts being the strongest affinity of the two levels, and second – reactions with minerals that occur after the first level reaches its maximum concentration. The latter level of adsorption will increase the retardation time and justify the delay in the  $H_2S$  production profile. The authors claim that the capacity of reservoir rock to adsorb determines the number of pore volumes produced prior to the souring of producers. The reaction term in the model expresses the relationship between concentrations of sulfate, substrates and nutrients, and the specific growth/reduction rate of SRB. Haghshenas (2011) showed a simplified case of bacteria growth rate in the case of one sulfate, one substrate and one nutrient is given as follows:

$$\mu = \mu_{max} \left( \frac{C_{sulphate}}{K_{sulphate} + C_{sulphate}} \right) \left( \frac{C_{substrate}}{K_{substrate} + C_{substrate}} \right) \left( \frac{C_{nutrient}}{K_{nutrient} + C_{nutrient}} \right) \quad (2)$$

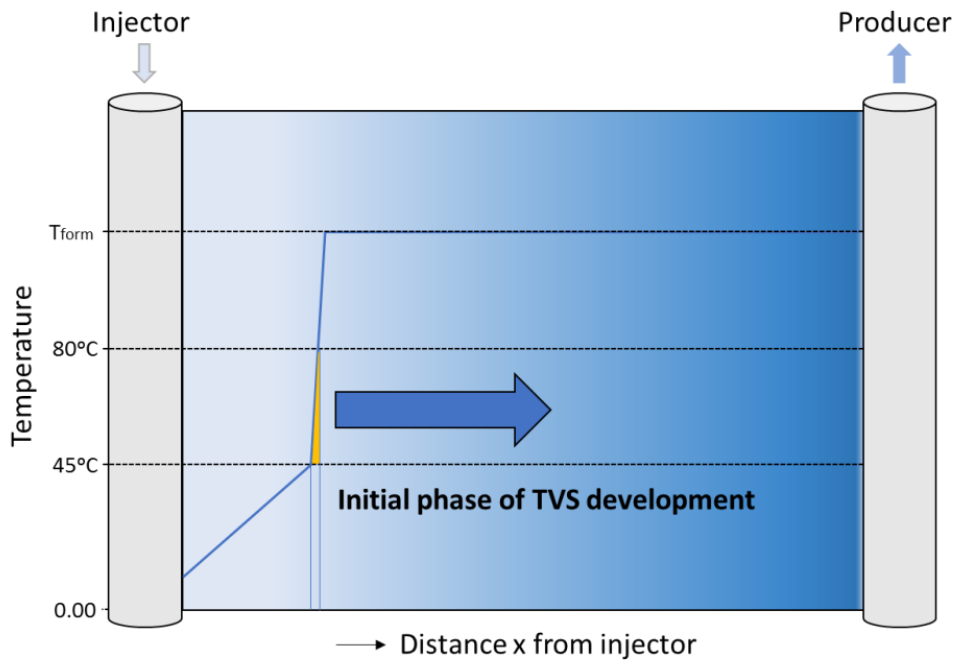
where,  $\mu_{max}$  is the maximum growth/reduction rate,  $C$  is concentration of corresponding components,  $K_j$  is half saturation constant.

The biofilm model treats nutrients in the injection water as a main limiting factor for hydrogen sulfide production. In cases where seawater is injected above oil-water contact or where seawater is mixed with produced water prior to injection, biofilm model would be valid, since both sulfate and organic compounds are sufficiently available for continuous SRB growth. This model, however, does not explain uninterrupted increase in the amount of H<sub>2</sub>S generated when seawater is injected below the oil-water contact and where organic compounds' source for SRB growth is limited to only residual oil in aquifer zone. In this case one would expect a small pick and thereafter a decline when organic carbon is depleted.

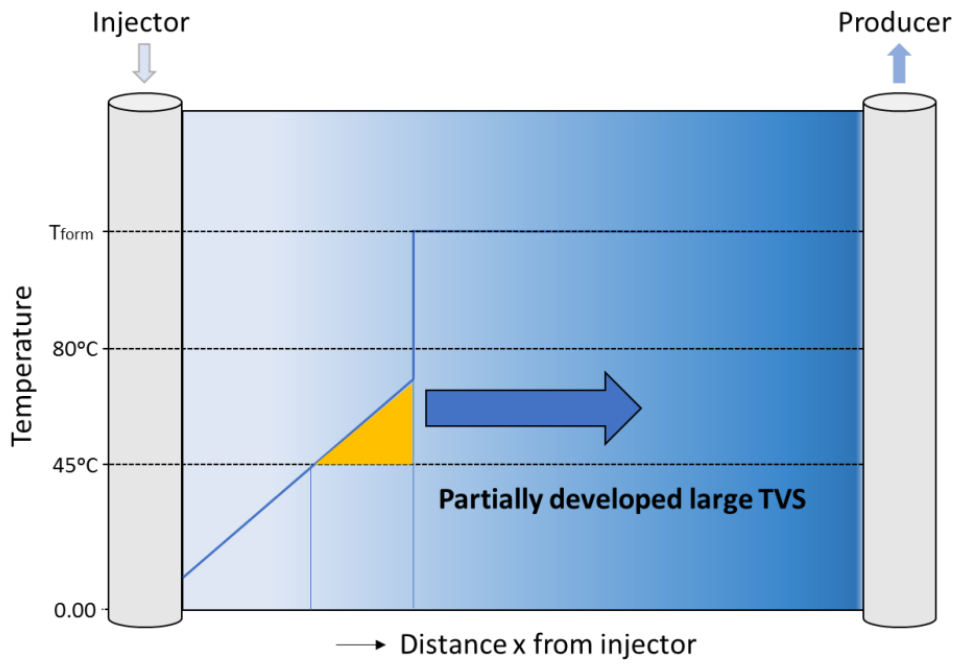
### **2.2.3 Thermal Viability Shell model**

In Thermal Viability Shell (TVS for short) model the main accent is given to the effect of temperature and pressure on SRB growth in the reservoir. The essential concept of the model is that H<sub>2</sub>S is generated in a fragment of a reservoir that has a favorable temperature and pressure for microbial activity. Eden et al. (1993) stated that the tendency of sweet reservoir to show souring is dependent upon the establishment of a dynamic viability shell in either the mesophilic (20-40°C) (m-SRB) or thermophilic (40-80°C) SRB (t-SRB) temperature ranges (Eden et al., 1993). The model suggests that souring from thermophilic sources is potentially more anticipated than from mesophilic ones. These bacteria type based temperature limits are then used to characterize and calculate the volume of thermal viability shell (reaction zone). The amount of H<sub>2</sub>S is found by integrating the sulfide production rate over time within a TVS, which in turn is calculated from an empirical correlation for sulfate consumption rate.

Figure 6-a, b and c demonstrate how thermal viability shell (form is similar to flattened torus) grows within the reservoir, reaches its maximum size when cold front crosses the upper bound (80°C) and remains at that size regardless of the continuously injected seawater amount. The onset of biogenic souring depends on both initiation of TVS and injection seawater breakthrough transporting the metabolically produced H<sub>2</sub>S to the producer. The velocity of growing TVS is much slower than the seawater passing through its boundaries, and thus H<sub>2</sub>S generated in a TVS will be carried to the producer by seawater. Eden et al. (1993) emphasized that first seawater produced will not have passed through a TVS and any biogenic H<sub>2</sub>S appearing at the producer at this time will have been generated in the moving thermal zone (mixing zone). As a result, one expects a decrease in its concentration before a production of hydrogen sulfide from a TVS takes place.

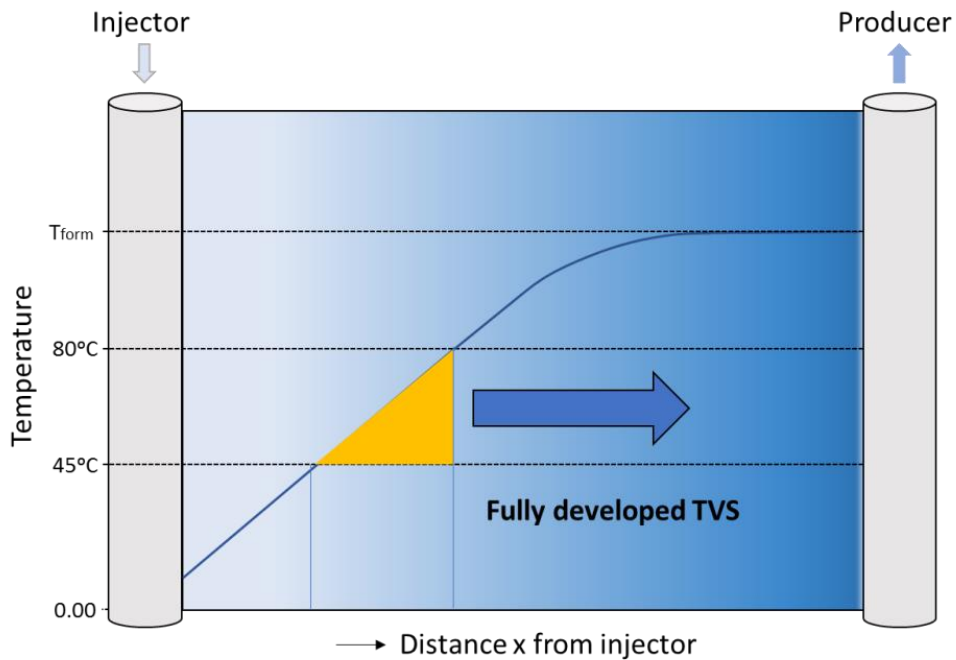


**A: Initial phase of TVS development**



**B: Partially developed large TVS**





**C: Fully developed TVS**

**Figure 6: Development of TVS model**

The main drawback of model could be that it does not take into account partitioning and adsorption of hydrogen sulfide that actually has serious impacts on the amount of  $H_2S$  produced. Furthermore, by establishing the temperature limits for t-RSB growth, Eden et al. completely disregarded the role of m-SRB. Despite the understanding of the importance of water composition in the established stable region around the injector, where all thermo-baric conditions for t-SRB growth are met, they did not incorporate the composition of seawater and formation water in their model.

#### 2.2.4 Mechanistic Model of Burger

Mechanistic model is a modification of existing in-house model developed by ARCO Alaska to predict the effects of reservoir souring in Prudhoe Bay and Kuparuk River fields. Burger et al. (2005 and 2006) published a pair of reports on mechanistic modeling of reservoir souring in seawater injected and produced water re-injected chalk reservoirs. Their model considers the water-flooded region of the reservoir as a macroscopic element with one injector and one producer, and divides the reservoir into equally sized horizontally spaced elements representing the total pore volume. The assumption behind the model is that a biofilm grows only on the fracture faces and that all reactions by SRB take place within the fractures where required

nutrients are provided by injected water and the fluids within the formation. Temperatures only below 95°C are assumed to be favorable for SRB growth.

To determine the coefficients of an equation that calculates the H<sub>2</sub>S bio-generation in each element, a history match process was performed. The expression for H<sub>2</sub>S bio-generation in case of seawater injection only, represented as follows:

$$\text{moles H}_2\text{S|SWI} = K_1 * [1 - \exp(-K_2/P_v)] * C_{\text{SO}_4} * V * K_3 \quad (3)$$

where  $K_1$  and  $K_2$  are constants determined by history match,  $K_3$  is a temperature-dependent function found in laboratory studies,  $C_{\text{SO}_4}$  is the concentration (moles/L) of the sulfate in the element's fracture,  $P_v$  is the number of pore volumes of water that have flowed through the element at a given time, and  $V$  is the volume (liters) of the fracture. This algorithm shows that biogenic H<sub>2</sub>S production remains relatively constant for some duration of time, which strongly depends on  $K_2$  - the effective rate of nutrient supply, and starts declining exponentially when the amount of organic carbon in connate water and residual oil is depleted (Figure 7).

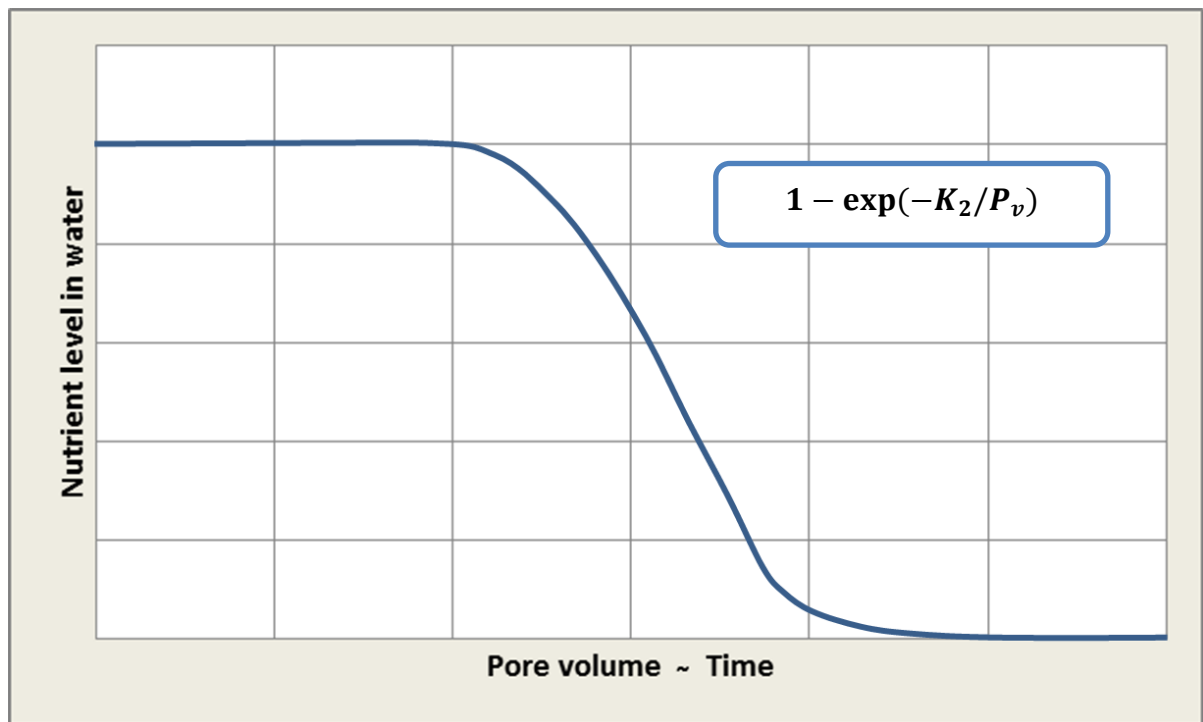


**Figure 7: Nutrient supply**

On the other hand, when produced water reinjection is carried out all necessary chemicals for SRB growth are already available in the injection water. To determine conversion of sulfate

and depletion of dissolved organic carbon (DOC) the water can be analyzed in the laboratory prior to the injection. In this case Burger et al. came to the following conclusion:

$$\text{moles H}_2\text{S|PWRI} = [C_{\text{DOC}}/K_4] * V * K_3 \quad (4)$$

where  $C_{\text{DOC}}$  is the concentration of DOC in the re-injected water,  $K_4$  is the laboratory determined stoichiometric metabolism of re-injected DOC with sulfate (DOC per moles of sulfate) (Burger et al., 2006).

By combining the expressions for seawater injection and produced water reinjection one can get the equation that predicts biogenic  $\text{H}_2\text{S}$  production either from seawater or produced water re-injected reservoirs.

$$\begin{aligned} \text{moles H}_2\text{S|SWI} = & \{K_1 * [1 - \exp(-K_2/P_V)] * C_{\text{SO}_4} + \\ & + C_{\text{DOC}}/K_4\} * V * K_3 \end{aligned} \quad (5)$$

While the second generation term representing the concentration of DOC is zero in case of seawater injection only, both terms take positive values when produced water reinjection is carried out.

Having history matched with production data, the mechanistic model of Burger gives the predicted values for hydrogen sulfide production. As described above, the trend for  $\text{H}_2\text{S}$  production in the case of seawater injection follows exponential decline and should eventually stop, i.e. at some stage there will be very low or even no  $\text{H}_2\text{S}$  production. In practice, however, in most of wells this is not the case. Another thing worth mentioning is that before applying the model for different reservoirs, correlations for fluid flow and  $\text{H}_2\text{S}$  modeling have to be adjusted for each specific reservoir.

### 2.2.5 SourSim<sup>®</sup>RL

As for today several simulators with full 3D transient capabilities have been developed including SourMax, Dynamic TVS,  $\text{H}_2\text{S}$  Model, REVEAL and SourSim<sup>®</sup>RL (Johnson et al., 2017).

The SourSim<sup>®</sup>RL model was developed during a number of Joint Industry Projects. The software implies that the souring problem is solved by coupling it to the existing reservoir simulators to incorporate full 3D transient. Thus, reservoir parameters and wells' operating

conditions provided by the reservoir simulator are brought to the souring simulator to provide the final souring solution (OilPlusLTD). This one-way coupling approach enables to avoid re-building of the reservoir simulation, and makes simulation run times shorter since pressure and flow equations do not have to be solved (Evans et al., 2006).

The H<sub>2</sub>S generation criteria used in SourSim model is based on laboratory and field measurements of SRB growth at different conditions. The model introduces a term of “biomass potential” which represents biomass accumulation with a given H<sub>2</sub>S generation potential in different locations of a reservoir. The implemented criteria of H<sub>2</sub>S generation can replicate the different stages of biomass development, including lag phase, exponential growth phase, stationary phase and death phase. Considering the impact of nutrients consumption in biomass building and hence H<sub>2</sub>S generation is one of the advantages of biomass modeling approach (Evans et al., 2015).

The main workflow of the SourSim model is depicted in Figure 8, where Pre-Processor is any reservoir model such as Eclipse 100, CMG IMEX, Chevron CHEARS, etc.

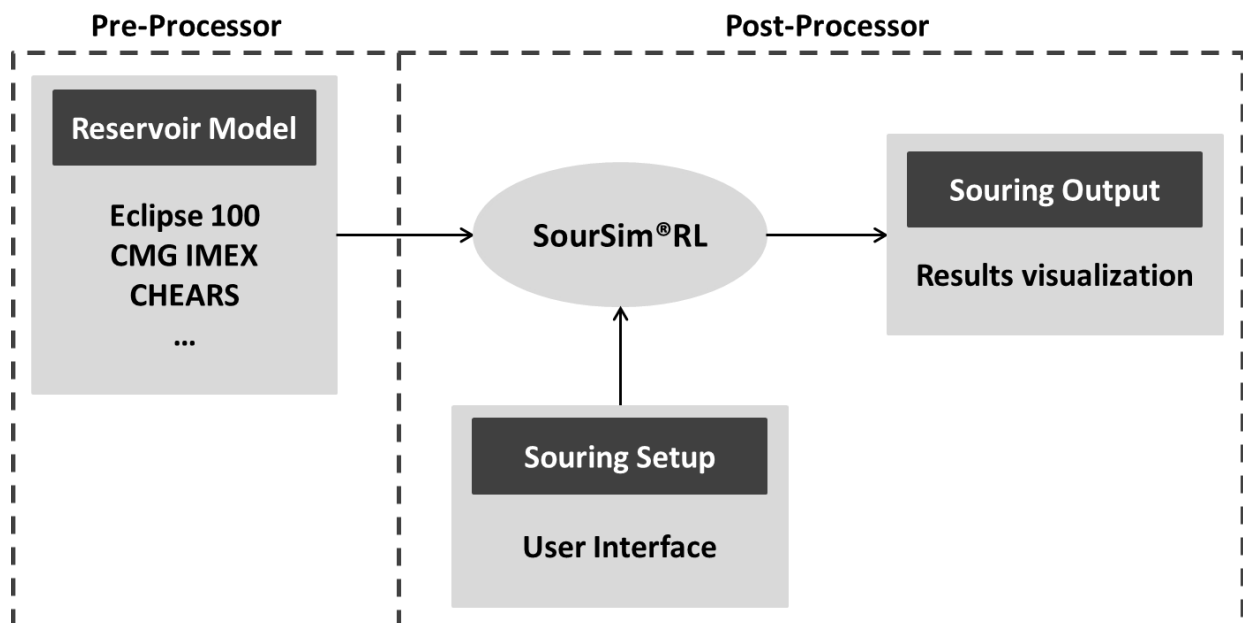


**Figure 8: Workflow of SourSim®RL**

## 2.3 Reservoir Souring Case Histories

Water-flooding with seawater is one of the most common techniques to maintain the reservoir pressure in offshore oilfields. As it was described previously in chapter 1, routine use of seawater injection causes the reservoir to sour. Industry has published numerous reports and reviews regarding the modeling of reservoir souring and its mitigation approaches in different reservoirs with varied injection strategies. Very little, however, is reported regarding the progress and monitoring of reservoir souring together with the analysis of governing factors based on field data. This chapter collects and discusses industry reported reservoir souring information from various fields in the North Sea based on published material. It should be noted that although reservoir souring is one of the major challenges in petroleum industry, there is no such a 'universal' template for reporting the results, which could be attributed to the incomplete understanding of the phenomenon and the factors governing H<sub>2</sub>S production. Reports also differ in their level of analysis varying from well based to field / platform based. While some of the Operators used their in-house models to evaluate and predict hydrogen sulfide production, others implemented the techniques described in chapter 2.

### 2.3.1 South Arne Field – Denmark

*Source:* (Robinson, Samuelsen, Lungaard, & Skovhus, 2010)

The South Arne field is located in North Western area of the Danish North Sea and produces oil from a chalk reservoir with a temperature of 115°C. Prior to the start of water injection repeated measurements indicated less than 3 ppm H<sub>2</sub>S in gas. The reservoir has undergone de-aerated, low-sulfate seawater (LSSW) injection for 9 years, and mixtures of LSSW with produced water in part of the field since 2004 and into all wells since 2009. Having experienced high H<sub>2</sub>S concentrations (35 ppm in gas) after the restart of a shut-in well, a thorough study was commenced to understand the causes of souring. Relatively high values of H<sub>2</sub>S were suspected either as a result of reservoir souring associated with seawater injection or microbial activities within the topside facilities.

In addition to the analysis of the sulfur isotopes in H<sub>2</sub>S, review of the historical H<sub>2</sub>S scavenger usage and pre-water injection well-test H<sub>2</sub>S measurements were also implemented to understand the source of souring. Historical (1999-2000) well-test data indicated that all the early producers had H<sub>2</sub>S concentrations of close to 3 ppm in gas phase, which was consistent with the historical minimum H<sub>2</sub>S scavenger usage. In 2008 the amount of H<sub>2</sub>S scavenger used was

significantly higher than the amount in 2000, while the export gas H<sub>2</sub>S content did not change considerably, i.e. no H<sub>2</sub>S was generated at the topside facilities. It was then concluded that increasing scavenger usage per unit of gas was tracking the reservoir souring development.

To understand how much of sulfate is used for microbial H<sub>2</sub>S generation, mass balances of sulfate and sulfide for the reservoir and production system were performed based on the analysis of produced water together with H<sub>2</sub>S concentrations in all phases.

Assuming 50 mg/l of sulfate in LSSW and in this case sulfate free formation water, sulfate ion contents in produced water were calculated in the event where no sulfate had been lost in the reservoir. The results, then, were compared with measured sulfate content in produced water where the discrepancies between these values (in %) indicated how much of sulfate had been used for H<sub>2</sub>S generation or precipitated as scale within the reservoir (Figure 9).

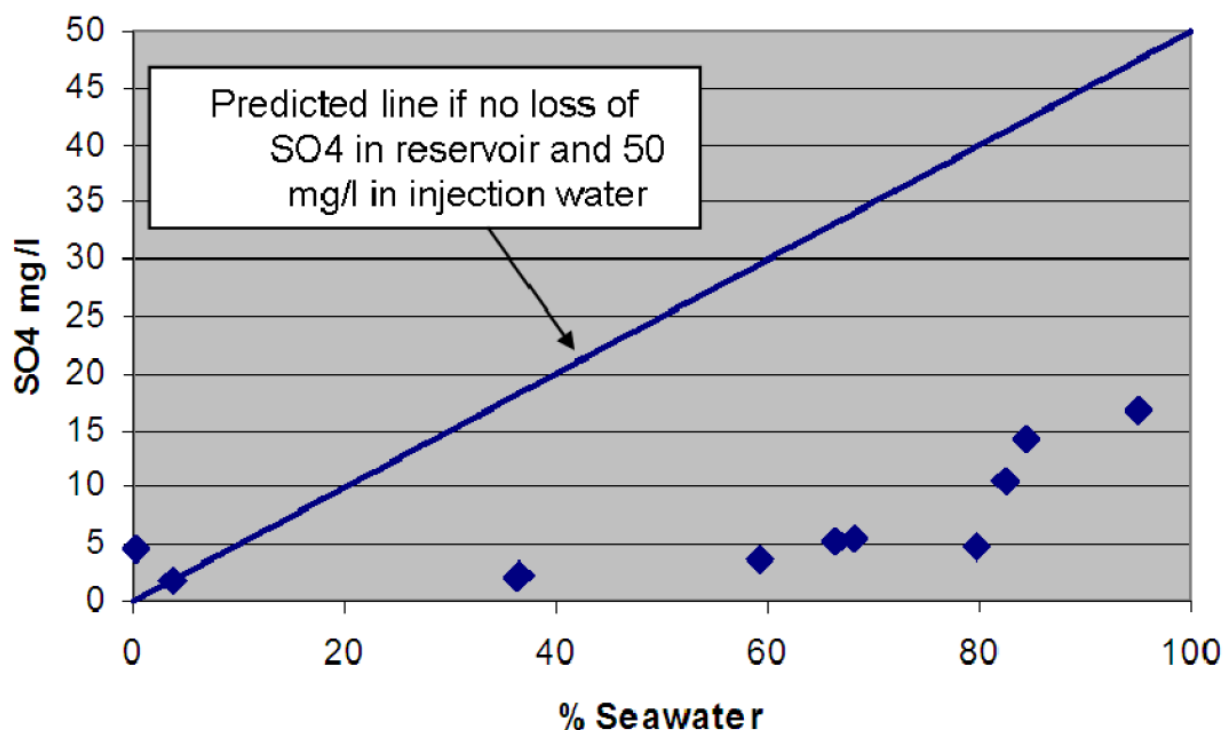


**Figure 9: Sulfate in produced water versus seawater cut (Source: Robinson et al. 2010)**

According to authors the amount of VFA in produced water from individual wells were high enough (188 mg/l) to encourage further growth of H<sub>2</sub>S. Moreover, microbiological measurements confirmed active in place SRA with relevant strains for H<sub>2</sub>S generation. Sulfate ion content, however, was a limiting factor inhibiting additional H<sub>2</sub>S generation.

With regards to scavenging potential of the reservoir, the South Arne chalk is almost pure calcite with minimal scavenging capacity. In addition, reservoir pressure is not high enough to prevent souring effect.

Taking all above mentioned parameters into account, it can be concluded that virgin reservoir temperature and limited sulfate amount were the factors inhibiting further H<sub>2</sub>S/sulfide generation.

### **2.3.2 Snorre Field (platform A)**

*Source:* (Mitchell, Hårvik, Anfindsen, & Hustad, 2010)

The Snorre A platform is located on the Norwegian North Sea and has been producing since 1992. In 1993 injection of de-aerated seawater was launched for pressure maintenance where it was routinely treated with biocide until nitrate injection was introduced in 2007. To meet the gas export specification of 2.5 ppmv H<sub>2</sub>S, scavenger injection in gas from the first stage separator was found to be necessary. The approach for monitoring of H<sub>2</sub>S production is somewhat similar to that of South Arne Field. Daily recorded scavenger usage, calculated amount of H<sub>2</sub>S scavenged and produced gas volumes are presented all together. This approach only demonstrates the development of reservoir souring in a field level and is failed when absolute amount of H<sub>2</sub>S produced is required either per wellbore or for a platform in aggregate.

### **2.3.3 Gullfaks Field**

Gullfaks field being one of the oldest fields on the Norwegian Continental Shelf has shown significant reservoir souring, thus being a subject for several papers targeting either the development of reservoir souring in the field [ (Mitchell et al., 2010); (Mitchell et al., 2017)] or its mitigation techniques (Sunde et al., 2004). Next in this chapter focus is given only on the development and monitoring of reservoir souring of the Gullfaks field.

The field was developed with three large production platforms; Gullfaks A starting production in late 1986, Gullfaks B joining in early 1988 followed by Gullfaks C in 1989. The Gullfaks reservoirs are heavily faulted and consist of several sandstone and overlying carbonate and shale formations. The drive mechanism for the main reservoirs is primarily water injection, with gas injection and water alternating gas injection (WAG) in some areas (factpages.npd.no). Although poor vertical communication between formations in the Gullfaks field (factpages.npd.no) may create a challenge for pressure maintenance, it can be useful when assessing H<sub>2</sub>S generation from individual formations.

Single well-test separator measurements are carried out to get the H<sub>2</sub>S concentrations (ppmv) in gas phase (Sunde et. al., 2004). All the above listed papers mention same calculation technique of H<sub>2</sub>S mass rate (kg/day) in gas, oil and water phases as well as a sum of these based on well-test and daily production data. The calculation of H<sub>2</sub>S in different phases was undertaken using equilibrium constants (K-values), which in turn account for pH, pressure and temperature (Waage et al., 2012). Further, to normalize the data total produced H<sub>2</sub>S (kg/day) in all three phases was divided either by produced water or injected seawater amounts observed at producers. The resulting concentration is referred as “sour water concentration” (Evans et al., 2015) or “souring index” (Mitchell et. al., 2017).

While Mitchell et al. (2010) presented platform level monitoring approach for Gullfaks C, Mitchell et al. (2017) “upgraded” the approach by demonstrating well level data interpretation. Although the authors claim about the challenge of interpreting large amount of spreadsheet based data, they came up with an interesting observation which could support the hypothesis discussed by Maxwell (2005). Figure 10 schematically illustrates observed souring development of several Gullfaks wells. The peak in H<sub>2</sub>S production shortly after injected water breakthrough followed by a decline is attributed to souring described by Mixing model (chapter 2.2.1), whereas delayed increase can be explained by Biofilm model (chapter 2.2.2).

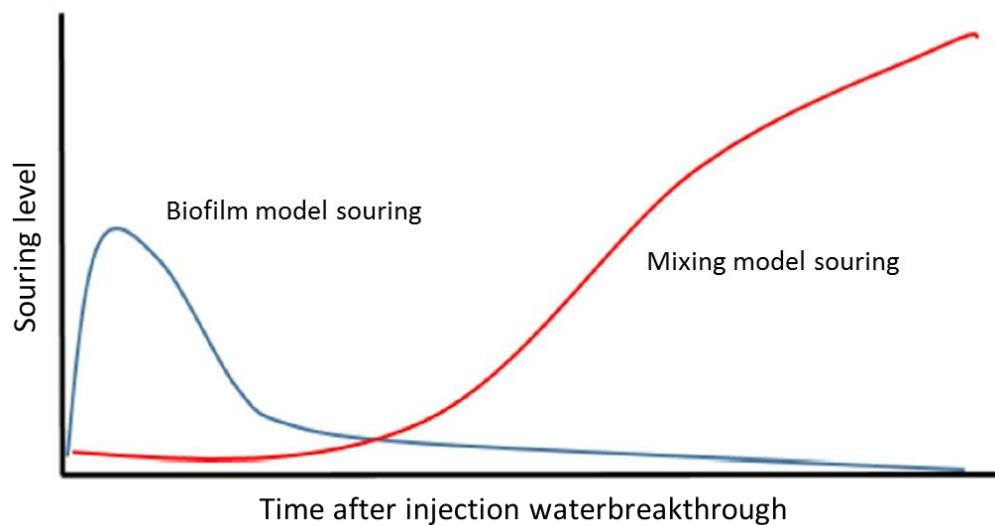


**Figure 10: Schematic illustration of observed dual souring mechanism**  
*Source:* (Mitchell, Skjevraak, & Waage, 2017)

The conclusion drawn from this observation was that the decrease in H<sub>2</sub>S level was not successive result of nitrate treatment as it had been claimed by Sunde et al. (2004), but it rather was a natural phenomenon that is described by two souring models jointly.



## 3 Methodology

This chapter briefly discusses the workflow of building the dashboard, different sources of extracted data, data cleaning and data manipulation for calculation of necessary parameters and downstream analysis. In addition, some of the calculations performed for the analysis are also covered.

### 3.1 Data Science Concept of the Present Thesis

*“A picture is worth a thousand words. An interface is worth a thousand pictures”*

– Ben Shneiderman

To visualize and understand reservoir souring correlations and gain insights from the available data it was decided to build an interactive dashboard that enables a robust monitoring and analysis. Successful implementation of TIBCO Spotfire tool for similar tasks within reservoir technology encouraged the idea of building the dashboard using this software for the current project. TIBCO Spotfire is a data visualization and analytics software that helps uncover insights for better decision-making. Several incorporated tools within Spotfire (HTML, CSS, JavaScript, R and Iron Python) were also involved to reach improved custom analysis and visualizations.

Figure 11 illustrates overall workflow for building the current dashboard. The data is collected from a variety of databases. Information flowing from the main databases, namely Oilfield Manager (OFM), individual EC (Energy Components) databases of each field in question and Norwegian Petroleum Directorate (NPD) are directly linked to Spotfire meaning that any updates in the databases are immediately reflected on the visualizations. Spotfire itself does not store the data coming from databases, but is simply reading the data directly from its source using corresponding connection URLs (Uniform Resource Locator) of databases. Consequently, if the user needs to retrieve the data from a new database, entering the connection URL, username, password, etc. in the “Information Manager” tool will do the job. On the other hand, data imported from time independent standalone tables (e.g. geographical location of wellheads and fluid composition of a well stream measured at the start of production) are first imported in TXT and/or CSV (comma separated values) formats and then embedded into the analysis.

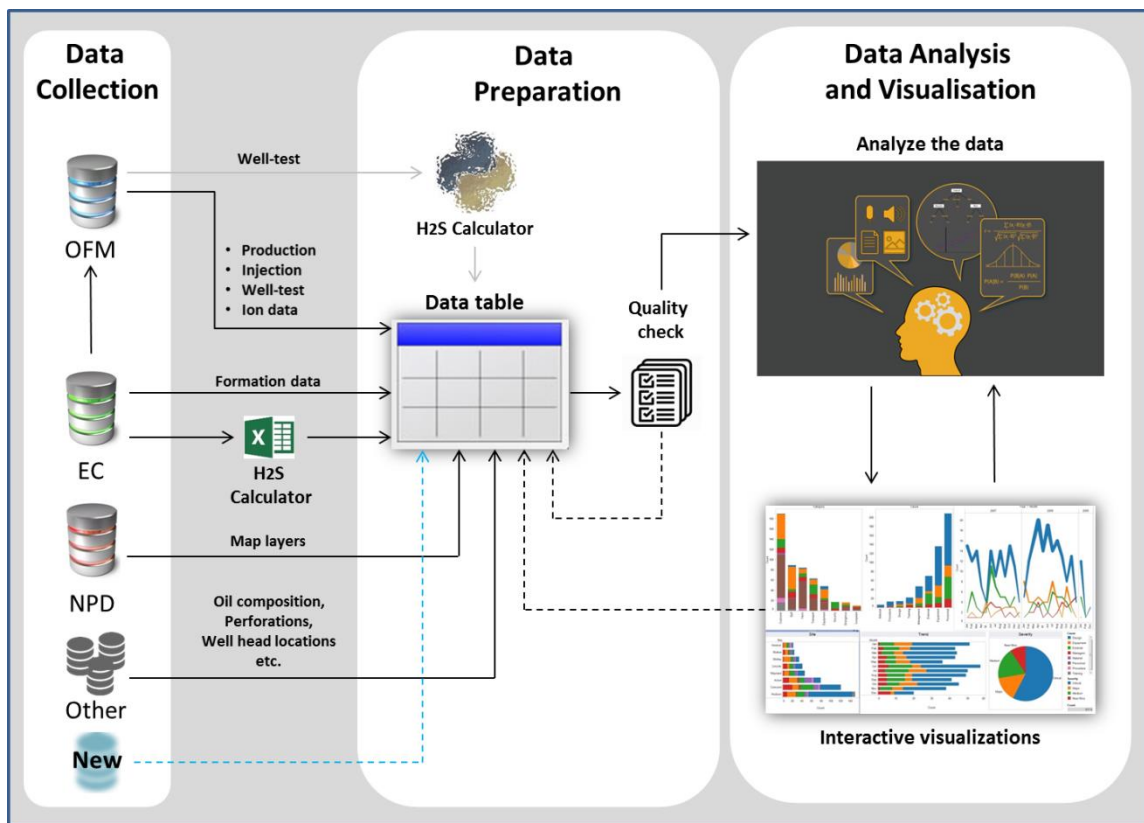


**Figure 11: Workflow for building the current dashboard**

All collected data are combined into one data table for flexible plotting and interactivity purposes during downstream filtering and analysis. In order to combine data from different data tables at least one column must match between them, meaning that data tables are joined on these columns. In most cases these identifier columns are either well-bore code, field name and/or date variables. This requires the data to have consistent shape and form prior to joining into one table. Therefore cleaning and transformation of data (pivoting, unpivoting, normalizations, adding and/or replacing columns and values etc.) that is coming from different sources has been performed before merging them together. Spotfire allows transforming the data either while uploading it or, later on, when the data has already been uploaded into Spotfire. An example of transformation, in this case unpivoting, of “Oil Composition” data table before merging it to main “Production” data table is given below. Unpivoting is a way of transforming table from short/wide to a tall/skinny format. It should be noted that although well names in tables 1, 2 and 3 are real, oil composition assigned to each well is fictitious.

**Table 1 – “Oil Composition” table prior to unpivoting**

Well	33/12-B-7	33/12-B 25	...	34/7-P-13
N2 (mole %)	0,280	0,620	...	0,370
CO2 (mole %)	0,190	0,460	...	0,320
C1 (mole %)	39,500	27,510	...	28,740
C2 (mole %)	7,630	7,860	...	5,530
C3 (mole %)	8,310	8,410	...	7,300
iC4 (mole %)	1,270	1,490	...	1,110
nC4 (mole %)	4,420	4,620	...	3,380
iC5 (mole %)	3,650	4,150	...	3,200
C6 (mole %)	3,110	3,280	...	2,560
C7 (mole %)	3,890	5,190	...	3,980
C8 (mole %)	3,840	5,420	...	4,150
C9 (mole %)	3,170	3,620	...	3,040
C10+ (mole %)	20,740	27,370	...	36,320

**Table 2 – “Oil Composition” table after unpivoting**

Well bore code	N2 (mole %)	CO2 (mole %)	C1 (mole %)	...	C9 (mole %)	C10+ (mole %)
33/12-B-7	0,280	0,190	39,500	...	3,170	20,740
33/12-B 25	0,620	0,460	27,510	...	3,620	27,370
...	...	...	...	...	...	...
34/7-P-13	0,370	0,320	28,740	...	3,040	36,320

The format of “Oil Composition” in Table 2 is now consistent with main “Production” data table. However, the identifier column (“Well bore code”) values have to exactly match with that in main “Production” data table where “Well bore code” is set based on POSC Caesar Association (PCA) standard for naming wells adopted by NPD (NPD guidelines for designation of wells and wellbores). Thus, all well bore code strings are modified (Table 3) as exactly in “Production” data table.

**Table 3 – Unpivoted “Oil Composition” table with NPD well bore code**

Well bore code	N2 (mole %)	CO2 (mole %)	C1 (mole %)	...	C9 (mole %)	C10+ (mole %)
NO 33/12-B-7	0,280	0,190	39,500	...	3,170	20,740
NO 33/12-B-25	0,620	0,460	27,510	...	3,620	27,370
...	...	...	...	...	...	...
NO 34/7-P-13	0,370	0,320	28,740	...	3,040	36,320

Finally, “Oil Composition” table (Table 3) is joined to “Production” data table on “Well bore code” identifier column using “Left outer” join method of SQL (Structured Query Language).

H<sub>2</sub>S is measured in gas phase (ppm) sampled at test separator during well tests. Statoil’s spreadsheet based H<sub>2</sub>S Calculator, which retrieves data from EC database, performs phase distribution calculations in order to determine the total amount of H<sub>2</sub>S in all phases (kg/day). Besides well tests, Spotfire currently imports H<sub>2</sub>S data (kg/day) from Excel H<sub>2</sub>S Calculator. Statoil has developed Python version of the H<sub>2</sub>S Calculator that has a number of advantages over the spreadsheet version (in terms of data manipulation and maintenance) and currently the process of packaging into a proper Python library is being performed. Importing partitioning data using Python H<sub>2</sub>S Calculator enables automatic interactivity with OFM data source, whereas importing it from a spreadsheet version requires manual updates of data within Spotfire each time when spreadsheet H<sub>2</sub>S Calculator is updated. Calculations performed behind Statoil’s H<sub>2</sub>S Calculator are presented later in chapter 3.3.1. Python script to extract the data from Excel H<sub>2</sub>S Calculator is enclosed in Appendix A.

To perform useful analysis the data must be reliable either it is measured or calculated. Quality check of measured H<sub>2</sub>S values during well-test was also carried out in the form of analytical outlier detection and removal rather than relying on commonly used statistical methods. Discontinuities in plots are then avoided, thus making it easier to fit mathematical models for future predictions. Detailed explanation of the method used in an example of one well is presented in chapter 3.3.1.

Having quality checked the data is supposed to be ready for visualization and analysis. However, most of the inconsistencies in data are discovered after getting them visualized meaning that some back and forth process between data processing and charting is inevitable.

## **3.2 Data Structuring for Visualization**

Several case histories from North Sea fields regarding H<sub>2</sub>S production monitoring were discussed in chapter 1.3. The reported data vary from field related features to well variables and thus represent different levels of information. Considering each level in one analysis, provided that sufficient information is available, may give more insight that would otherwise be lacking when only one level of analysis is carried out – be it wellbore, reservoir or field level.

Being motivated from this, it was decided to incorporate all levels in one analysis. Thus the dashboard illustrates the data in three interactive levels of visualization drilling down to field, formation and wellbore levels (Figure 12).



**Figure 12: Visualization levels**

It is believed that this approach gives an opportunity for finding analogue wells / fields and grouping them to analyze the similarities and distinctions with regards to H<sub>2</sub>S production thus being able to point out driving forces and/or limiting factors of H<sub>2</sub>S generation and production.

### **3.3 Calculations Involved Behind the Scenes**

#### **3.3.1 Outlier detection and removal**

Outliers are observation points which are distant from other observations. Common source for these outliers may be a transient malfunction of a physical apparatus while taking measurements or an error in data transmission or transcription. Other causes such as operators' mistakes when entering the data into the system/database are also possible.

Although there are several statistical methods of outlier removal, it was decided not to involve any of those but develop a subject matter method that considers the physics behind the observed H<sub>2</sub>S concentration. Since H<sub>2</sub>S concentration is measured in gas phase, one must remember that very low gas production volumes cause extremely high H<sub>2</sub>S concentration. Thus when removing any point as an outlier it should first be cross-checked with well rates.

One example is illustrated in Figure 13 where two extreme points (b) causes a huge increase in the cumulative H<sub>2</sub>S production accounted by the H<sub>2</sub>S calculator. When checking these exact points on well rates histogram (c), it can be seen that elevated H<sub>2</sub>S concentration may be the result of very low gas rate. Thus one should be careful when deciding to remove these points

from the analysis. The dashboard allows each user individually to choose to remove or leave any point in the analysis.

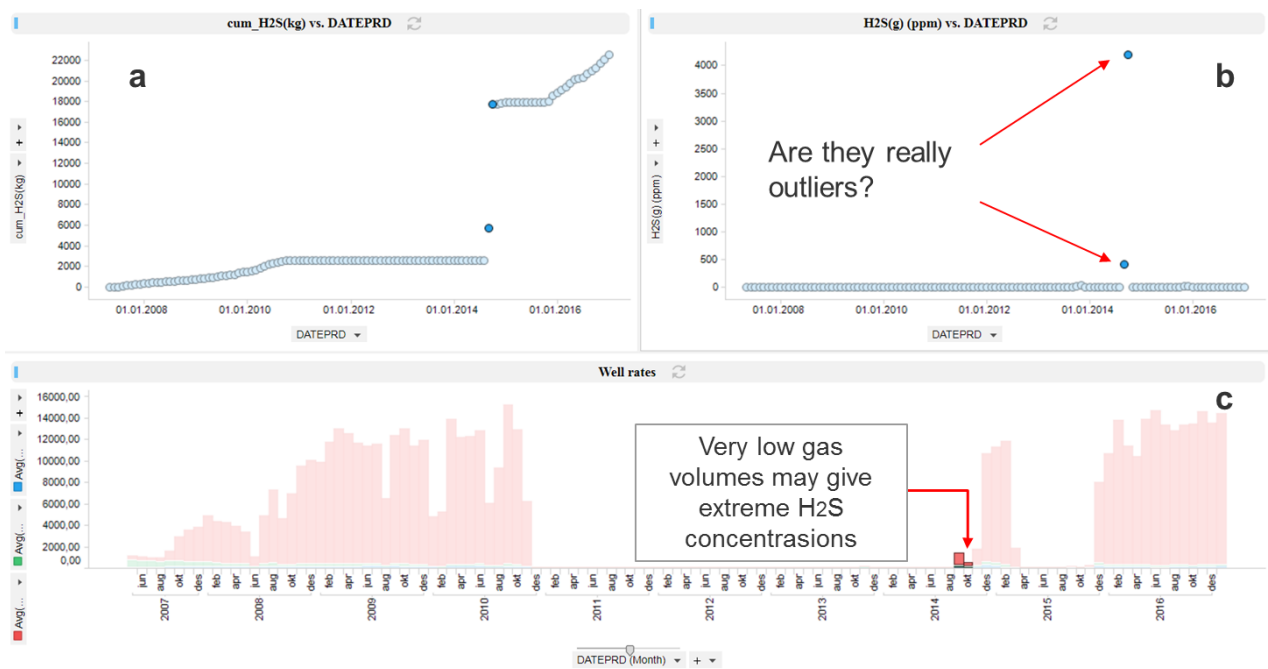


**Figure 13: Outlier detection**

**a)** Cumulative H<sub>2</sub>S; **b)** H<sub>2</sub>S concentration in ppm; **c)** Well rates (red – gas; green – oil; blue - water) – all variables are plotted against production date

The procedure of subject matter outlier removal is carried out as following. First the difference between consecutive measurements is calculated for each wellbore and visualized as a bar chart. Then user can set a plank (horizontal red line) individually for each wellbore in question where the values above this plank will be removed from the analysis. To return the removed points “Reset” button is also made available (Figure 14).

When comparing Figure 14-a with Figure 13-a obvious difference can be noticed. Besides retrieving high quality data for downstream analysis, another essential benefit of removing outliers is the reliability of the data when matching any developed model.

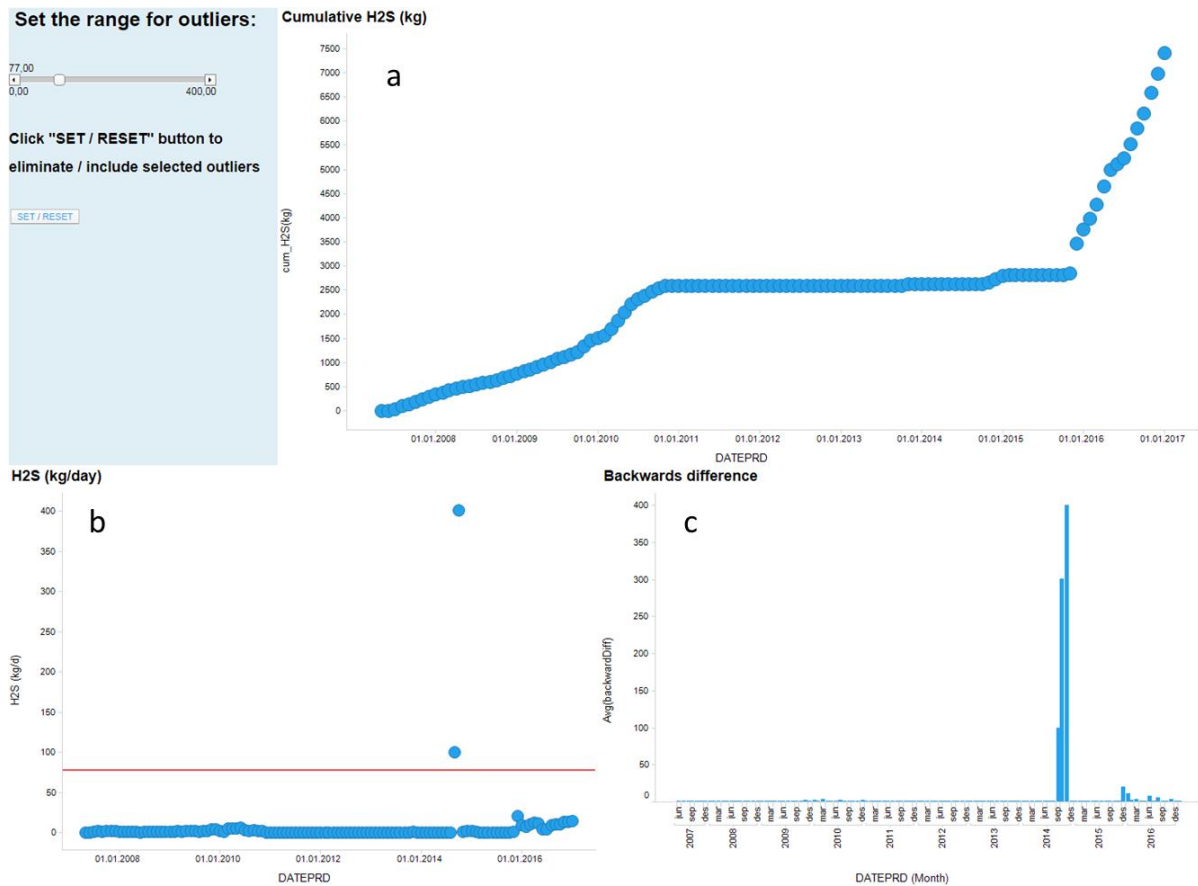


**Figure 14: Outlier removal procedure**

**a)** Cumulative H<sub>2</sub>S; **b)** H<sub>2</sub>S rate in kg/day; **c)** Backwards difference between consecutive rows of “H<sub>2</sub>S (kg/day)” column – all variables are plotted against production date

### 3.3.2 H<sub>2</sub>S Calculator

As it was previously mentioned H<sub>2</sub>S concentration (ppm) is measured in gas phase during well-tests. However to evaluate the impacts of reservoir souring total mass production rate from a well and/or from a field has to be considered. Thus, core task of H<sub>2</sub>S Calculators is to find mass rates of partitioned H<sub>2</sub>S in each – gas, oil and water phases and to combine them in order to get total H<sub>2</sub>S mass rate. Calculations assume equilibrium between phases which is quite reasonable at a test separator where the measurement of H<sub>2</sub>S is carried out. Both Excel and Python versions of H<sub>2</sub>S Calculator give identical results.

Assumption:  $H_2S_{(gas)} \leftrightarrow H_2S_{(water)} \leftrightarrow H_2S_{(oil)}$

$$H_2S_{gas} \left[ \frac{kg}{d} \right] = \frac{H_2S [ppm]}{1000000} * \frac{(P_{sc} * M_{W_{H_2S}})}{R * T_{sc}} * gas\ rate \left[ \frac{Sm^3}{d} \right] * 0,001 \quad (6)$$

$$H_2S\ Oil \left[ \frac{kg}{d} \right] = \frac{H_2S\ [ppm]}{1000000} * P_{sep} * K_{oilgas} * Oil\ rate \left[ \frac{Sm^3}{d} \right] \quad (7)$$

$$H_2S\ water \left[ \frac{kg}{d} \right] = \frac{H_2S\ [ppm]}{1000000} * P_{sep} * K_{wateroil} * M_{W_{H_2S}} * Water \left[ \frac{Sm^3}{d} \right] * (1 + K_{H_2S}/[H+]) \quad (8)$$

$$H_2S\ total \left[ \frac{kg}{d} \right] = H_2S\ gas \left[ \frac{kg}{d} \right] + H_2S\ oil \left[ \frac{kg}{d} \right] + H_2S\ water \left[ \frac{kg}{d} \right] \quad (9)$$

where:

$$P_{sc} = 101324\ Pa$$

$$T_{sc} = 15 + 273.15\ K$$

$$M_{W_{H_2S}} = 34\ g/mole$$

$P_{sep}$  – Separator pressure

$K_{oilgas}$  – Partitioning coefficient of  $H_2S$  between oil and gas phases

$K_{wateroil}$  – Partitioning coefficient of  $H_2S$  between water and oil phases

$K_{H_2S}$  – Dissociation constant of  $H_2S$  in water

$[H+]$  =  $10^{-pH}$  – Molar concentration of dissolved hydrogen ions which is a measure of acidity. This concentration can range from  $10^{-1}$  to  $10^{-14}$ . Having been scaled down to pH (power of Hydrogen) this range takes values from 1 to 14, where solutions with pH less than 7 are acidic and solutions greater than 7 are basic. Formation waters have pH values of roughly around 6.5.

Partitioning coefficients, also referred as K-values, are simulated for ten by ten matrixes of pressure and temperature values covering the possible range of conditions encountered in oilfields.

$H_2S$  Calculator allows setting a fixed default pH value for partitioning calculations, calculating it from  $CO_2$  [mole%], alkalinity [mg/l] and acidity ( $H_{ac}$  [mg/l]) or contrarily it can also be calculated from correlations as a function of pressure and temperature. Another assumption behind the calculations is that water from only one formation is considered when calculating pH, even if a well has water cut from different formations at the same time, i.e. mixture of formation waters.



### 3.3.3 Ion data analysis

Ion analysis is usually carried out to calculate the amount of seawater as a fraction of total produced water. In practice, there are different methods of calculating seawater cut (SWC) based on ion data, among which Ion Tracking method is used more commonly. In this work, calculation of SWC based on two different methods, namely Ion Tracking method and Statistical method, is discussed. Ishkov et al. (2009) proposed Reacting Ion method that is to find the seawater fraction in total produced water based on the concentrations of the dissolved mineral species in aqueous solutions. However this method is not considered in this work.

#### SWC calculations based on Ion Tracking method

Although OFM database provides seawater cut (SWC) for each wellbore, it was decided to reproduce the calculations and discuss the assumptions and accuracy of it. The database contains SWC information based on measured content of two ions – sulfate and magnesium separately. The calculation is performed using Ion Tracking method that is based on conservative ions. This method assumes no reactions are taking place in the reservoir while injection water is travelling towards producers. An example of simple reservoir case with seawater and water from one formation is given below:

$$C_{ion}^{meas} = SWC_{ion} * FW_{ion}^0 + (1 - SWC_{ion}) * SW_{ion}^0 \quad (10)$$

where:

$C_{ion}^{meas}$  – measured concentration of ion (in this case either sulfate or magnesium) in produced water;

$SWC_{ion}$  – seawater cut based on this ion;

$FW_{ion}^0$  – initial concentration of the ion in formation water;

$SW_{ion}^0$  – initial concentration of the ion in seawater.

Assuming conservative mixing, one can easily find SWC from equation (10):

$$SWC = \frac{C_{ion}^{meas} - FW_{ion}^0}{SW_{ion}^0 - FW_{ion}^0} \quad (11)$$

In reality, however, the ion may be involved in several chemical reactions within reservoir, e.g. in case of  $SO_4$  it can be precipitated as  $BaSO_4$  or more importantly take part in the

generation of H<sub>2</sub>S. Thus, this method engenders erroneous results for SWC which is a very important factor when assessing H<sub>2</sub>S production.

If it is assumed that SO<sub>4</sub> in the reservoir is lost only for H<sub>2</sub>S generation, then adding total H<sub>2</sub>S concentration in produced water to measured SO<sub>4</sub> when calculating SWC should give relatively accurate results:

$$SWC[SO_4 + H_2S] = \frac{(C_{SO_4}^{meas} + 3 * SI_{PW} \left[ \frac{mg}{l} \right]) - FW_{ion}^0}{SW_{ion}^0 - FW_{ion}^0} \quad (12)$$

where 3 is a conversion factor telling that for generation of one mole of H<sub>2</sub>S 1/3 mole of SO<sub>4</sub> was necessary. SI<sub>PW</sub> [mg/l] is the concentration of H<sub>2</sub>S in total produced water (PW):

$$SI_{PW}[mg/l] = \frac{H_2S[kg/day]}{SW[m^3/day]} * 1000 \quad (13)$$

To account for other possible reactions of SO<sub>4</sub> and more importantly for diluted/absorbed amount of produced H<sub>2</sub>S within the reservoir following averaging method is implemented.

### SWC calculations based on Statistical (average) ion method

First, SWC is calculated using above described Ion Tracking method for each ion separately (equation 14), except Barium since it is mostly involved in chemical reactions causing scaling. Also SWC from SO<sub>4</sub> is taken from equation 12 where it accounts for H<sub>2</sub>S generation.

$$SWC_i = \frac{C_{ion_i}^{meas} - FW_{ion_i}^0}{SW_{ion_i}^0 - FW_{ion_i}^0} \quad (14)$$

where subscript *i* stands for a specific ion under consideration.

If the absolute difference of initial concentration of ions in formation water and seawater is greater than half of the ion's initial seawater concentration (equation 15), than SWC value calculated from this specific ion is included in arithmetic averaging equation:

$$|SW_{ion_i}^0 - FW_{ion_i}^0| > \frac{SW_{ion_i}^0}{2} \quad (15)$$

$$Avr\_SWC = \sum_1^k \frac{SWC_k}{k} \quad (16)$$

where  $k$  is the ion with initial seawater and formation water concentrations satisfying the condition illustrated in equation (15).

Finally, corrected seawater cut based on ‘filtered’ average ions is represented as follows:

$$SWC[avr_{ion}] = \begin{cases} \sum_1^k \frac{(SWC_k + SWC[SO_4 + H_2S])}{k + 1}, & SWC_{SO_4} < \sum_1^k \frac{(SWC_k + SWC[SO_4 + H_2S])}{k + 1} \\ SWC_{SO_4}, & SWC_{SO_4} \geq \sum_1^k \frac{(SWC_k + SWC[SO_4 + H_2S])}{k + 1} \end{cases} \quad (17)$$

The difference between corrected seawater fraction calculated from averaging method and the one calculated taking into account  $H_2S$  produced (equation 12) gives adsorbed  $H_2S$  or more generally  $H_2S$  lost within the reservoir:

$$\text{adsorbed } H_2S = (SWC[avr_{ion}] - SWC[SO_4 + H_2S]) * SW_{SO_4}^0 \quad (18)$$

Usually adsorption capacity of a reservoir rock is determined from the mineralogical analysis of formation core samples. Nevertheless, lack of such data may, to some extent, be compensated by using ion data analysis.

### 3.3.4 Wellbore geo-location

Besides mapping of wellbore locations in order to get overview information, it was also considered to find a correlation between oil composition (for fields with high variety of composition within a reservoir) and  $H_2S$  generation and/or production from a specific area of a reservoir. However, no database has provided wellbore locations but only wellhead locations. Given wellhead locations (longitude and latitude) and deviation (X and Y) of wells it is quite straightforward to calculate wellbore locations as shown in equations (19) and (20):

$$\varphi_2 = \text{asin}(\sin\varphi_1 * \cos\delta + \cos\varphi_1 * \sin\delta * \cos\theta) \quad (19)$$

$$\lambda_2 = \lambda_1 + \text{atan2}(\sin\theta * \sin\delta * \cos\varphi_1, \cos\delta - \sin\varphi_1 * \sin\varphi_2) \quad (20)$$

where  $\varphi$  is latitude,  $\lambda$  is longitude,  $\theta$  is the bearing (clockwise from North),  $\delta$  is the angular distance  $d/R$ ,  $d$  being the distance as shown in Figure 15,  $R$  is the earth’s radius. All angles are in radians.

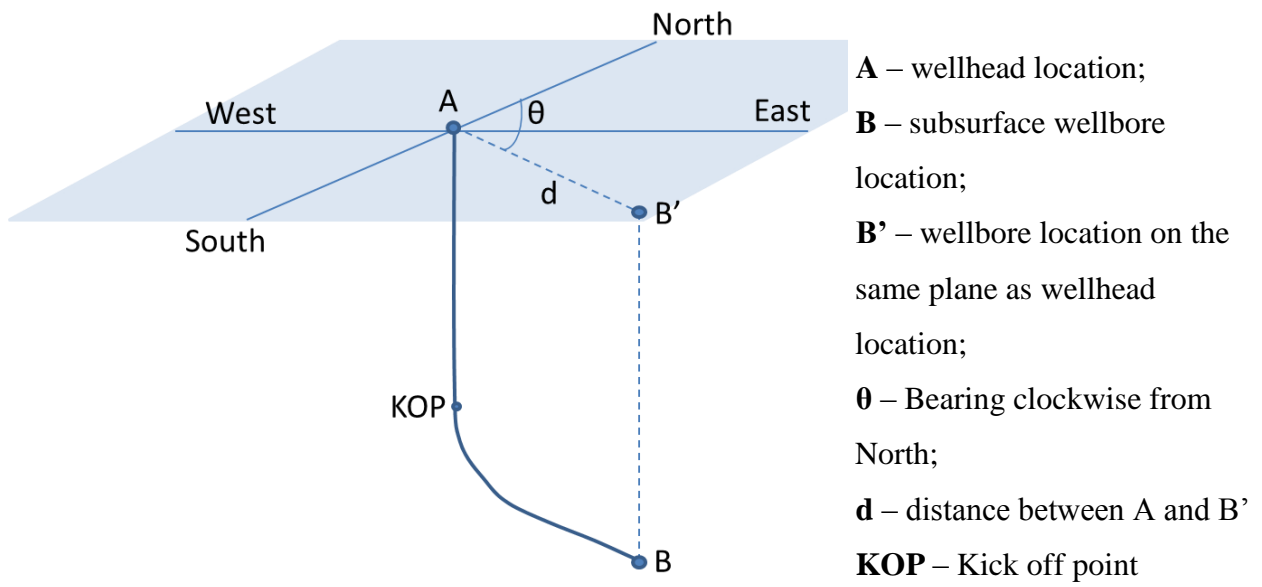


**Figure 15: Schematic illustration of a well**

Figure 15 gives a schematic illustration of a well with geographical parameters necessary to calculate wellbore location.

## 4 Results and Discussion

### 4.1 Field Level Visualization and Data Analysis

The dashboard contains 7 fields for the analysis. However, it is built in a way that once an access for a new field's database is awarded the dashboard can be updated with a click of a button to include the new field into the analyses. In aggregate the number of wellbores from all fields makes up over 800. The analysis in this section mainly considers the comparison of fields that are different in H<sub>2</sub>S production and have sufficient historical data, i.e. contain wells with frequent well tests.

Field level visualization presents general overview of souring development and its comparison against other fields.

#### 4.1.1 Cumulative H<sub>2</sub>S over the field lifetime

To get the overall picture of H<sub>2</sub>S production of an individual field, cumulative H<sub>2</sub>S is charted for the lifetime of fields. Field-wise cumulative values are sum of individual wells at a corresponding time. As it can be seen in Figure 16, the onset of H<sub>2</sub>S production in Field I has launched very early, around 2000 days after field start-up, as compared to other fields (roughly 5000 days).

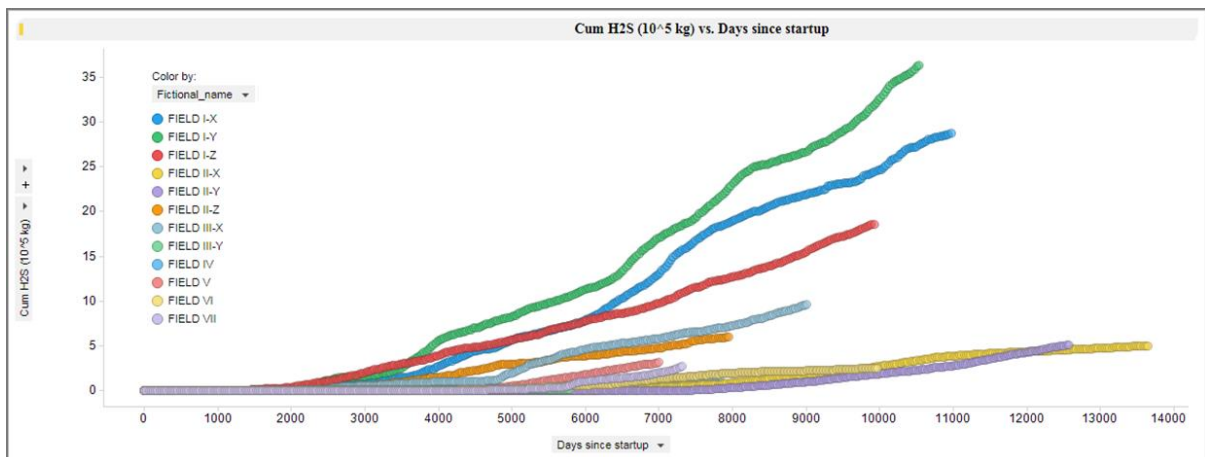


**Figure 16: Cumulative H<sub>2</sub>S production since field start-up**

Letters after the name of a field (e.g. X) define different platforms operating on the field

Another obvious difference is the amount of H<sub>2</sub>S produced where again Field I shows extreme results with approximately six times as much cumulative H<sub>2</sub>S (kg) as in the case of Field II. Figure 17 combines the cumulative H<sub>2</sub>S production graph and its concentration in produced seawater emphasizing Field I-A and Field II-B platforms in the illustration.

Earlier in chapter 3.3.3 it was shown how back calculation is performed to find the H<sub>2</sub>S concentration in total produced water (equation 13). To calculate the concentration of H<sub>2</sub>S in produced seawater it is sufficient to divide H<sub>2</sub>S mass rate to seawater rate seen at producers.

$$SI_{SW}[mg/l] = \frac{H_2S[kg/day]}{SW[m^3/day]} * 1000 \tag{21}$$

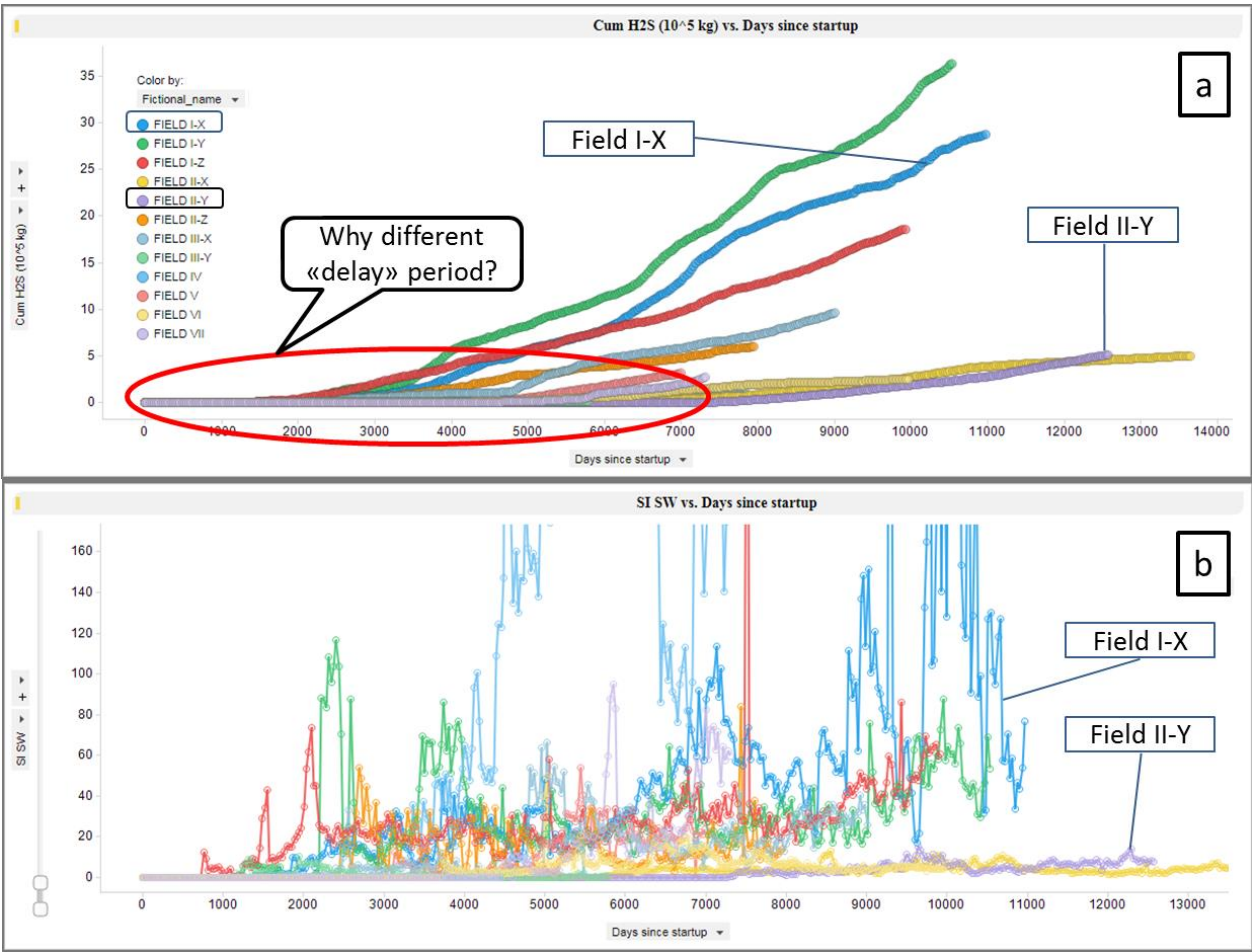


**Figure 17: a) Cumulative H<sub>2</sub>S production and b) H<sub>2</sub>S concentration in produced seawater since field start-up**

\*Same coloring applies for both charts

There are numerous factors affecting the time for H<sub>2</sub>S onset that might explain different delay period shown in Figure 17-a. While it can be related to different microbial growth conditions related to reservoir temperature, injection water (seawater and/or produced water

reinjection), injection zone i.e. either above or below oil water contact (which is believed to affect carbon source availability for H<sub>2</sub>S generation) and travel path distance between injectors and producers, another factors such as H<sub>2</sub>S partitioning, adsorption capacity of reservoir rock or permeability may also influence the amount of H<sub>2</sub>S production.

Figure 18 shows the development of cumulative H<sub>2</sub>S with respect to cumulative seawater, where H<sub>2</sub>S onset is observed after the seawater breakthrough. Analyzing this type of plots in a wellbore level can give good results, since it is not directly related to time unlike Figure 17-a, and reflects the effect of drainage patterns.

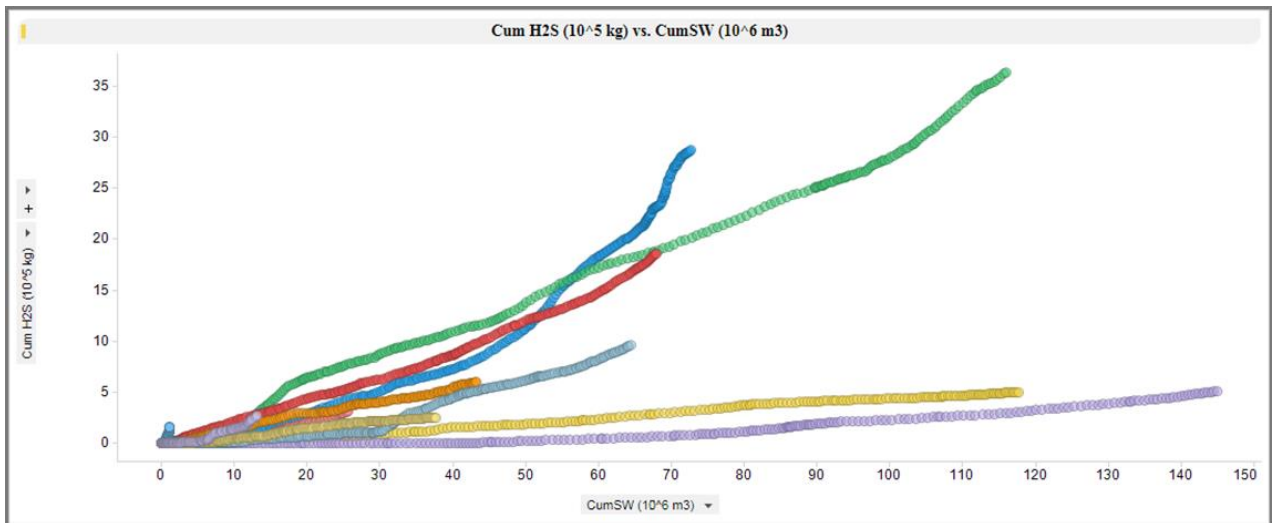


**Figure 18: Field level cumulative H<sub>2</sub>S vs. cumulative seawater chart**

## 4.2 Reservoir Level Visualization and Data Analysis

The analysis of H<sub>2</sub>S production on reservoir level is highly uncertain and more complicated owing to the data quality and availability. OFM database provides perforation data (“WELL (OFM)” data table) where one can find information telling what wellbore is producing from which formation (or formations) based on the start and end time of perforations. However in cases where a well is producing from more than one formation at a time the analysis requires the information about the ratio of production amount (gas, oil, water) from each formation individually. This information is not provided in this data table.

Information about the wellbore split into producing formations is given in EC database of each field. However, these split ratios are fixed in time and, most importantly, the source as well as reliability of these information are unclear. Most probably, they simply represent the ratio of height of perforated zone in one formation to the total height of perforations in all formations within a well, thus not accounting for the communication between formations. To get the correct ratio of production from different formations is very complicated, if possible at all.

Without access to individual EC database of each field, reservoir level analysis is limited to perforation data from OFM data source.

### 4.2.1 Water Cut vs. H<sub>2</sub>S per formation

To analyze the degree of correlation between water cut and H<sub>2</sub>S, perforation data from “WELL (OFM)” data table is merged with “Well Test” data table that contains the information about gas phase H<sub>2</sub>S concentration.

Figure 19 presents H<sub>2</sub>S gas phase concentration plotted against water cut where each color represents different reservoirs. It can be noticed that very high water cut resulted in extreme H<sub>2</sub>S concentrations within the reservoirs.



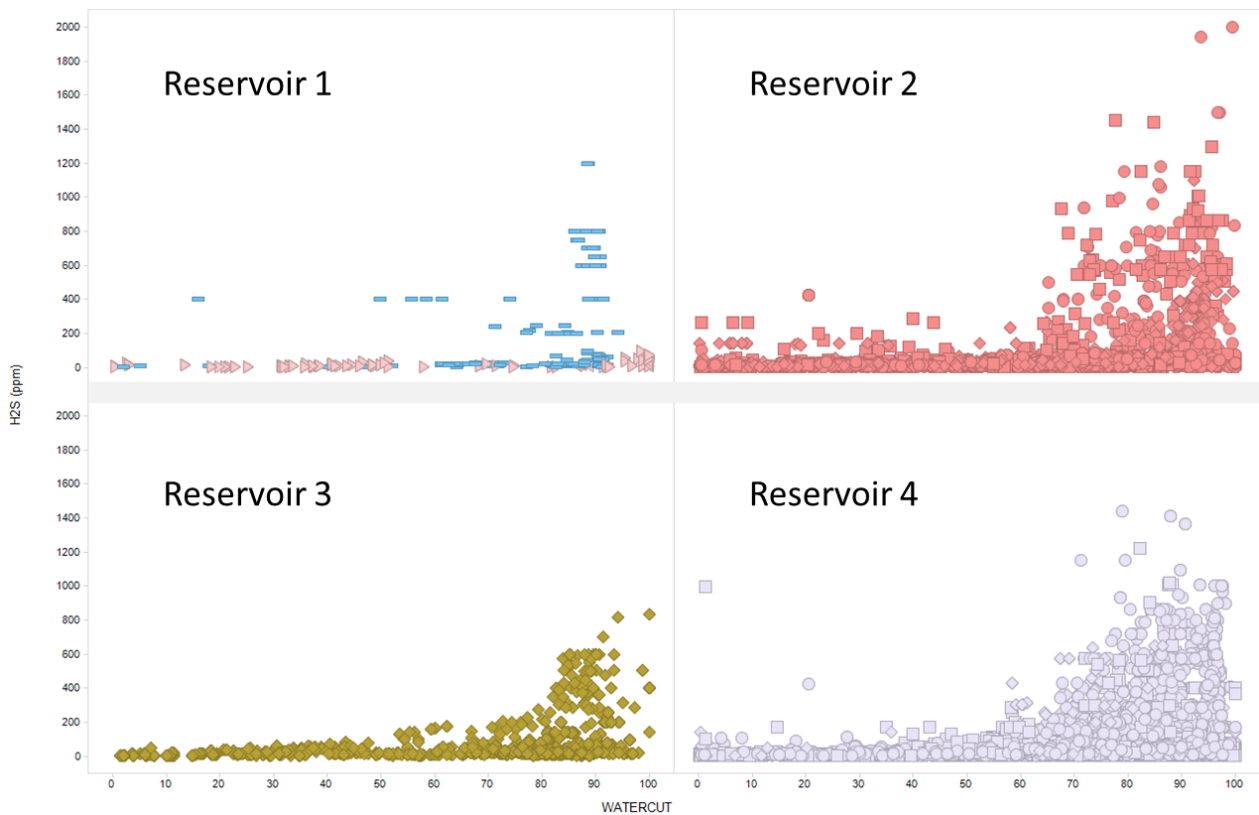
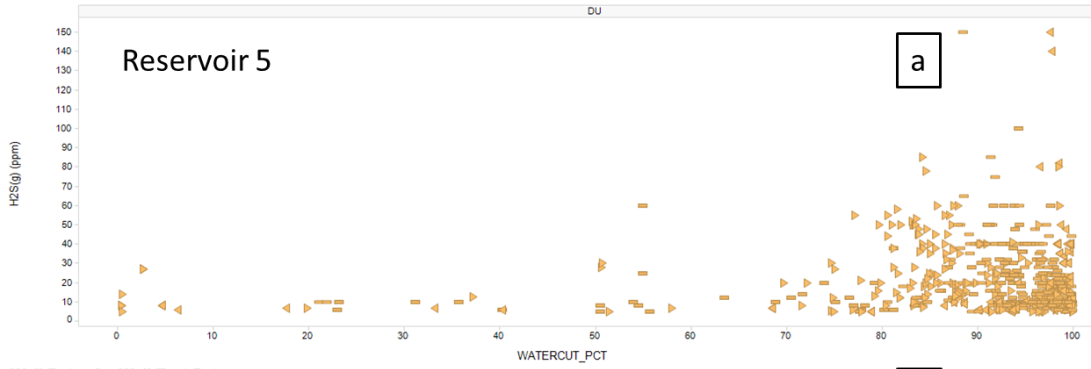


**Figure 19: H<sub>2</sub>S concentration (ppm) vs. water cut trellised by reservoir**

Although above plots show good correlation between water cut and H<sub>2</sub>S (ppm), one should be very careful to draw a conclusion based on these plots. The reason for this is that the gas fraction concentration of H<sub>2</sub>S cannot be regarded as representative for the generated and produced amount of H<sub>2</sub>S. At the stage where water cut is greater than 70-80% the volume of gas at test separators may be reduced as compared to the early production period, which can then result in elevated concentrations of H<sub>2</sub>S in gas phase as shown in Figure 20. This phenomenon was also briefly discussed on a wellbore level in chapter 3.3.1 when covering outlier detection example.

To assess the total H<sub>2</sub>S produced from a specific formation more robust results can be achieved when plotting seawater cut against total H<sub>2</sub>S produced (in kg/day) and/or against the concentration of total H<sub>2</sub>S either in produced water or seawater (SI\_PW or SI\_SW respectively). It is observed that most of the formations produce bulk of H<sub>2</sub>S when seawater cut is around 70-80%. Figure 21 exemplifies this observation (a) and compares it with previous type of plot where H<sub>2</sub>S concentration in gas phase (ppm) is used for the analysis (Figure 19).

TDEV\_H2S vs. WATERCUT\_PCT (Filter by formation)



Well Rates for Well Test Data

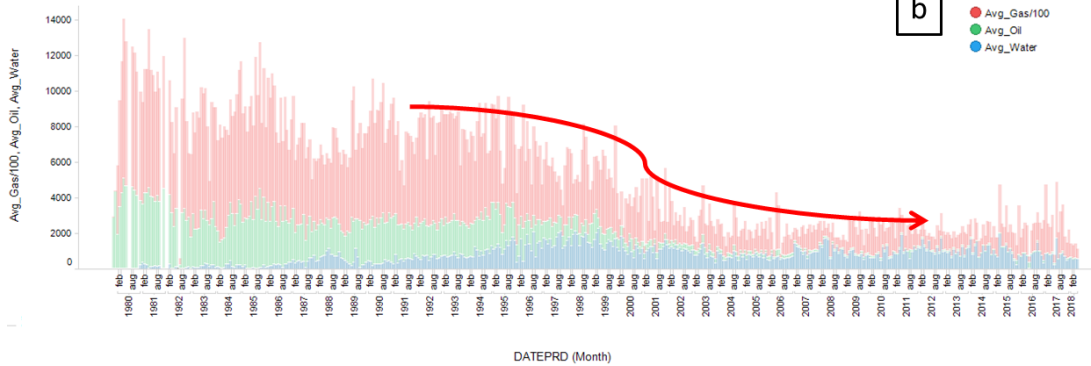
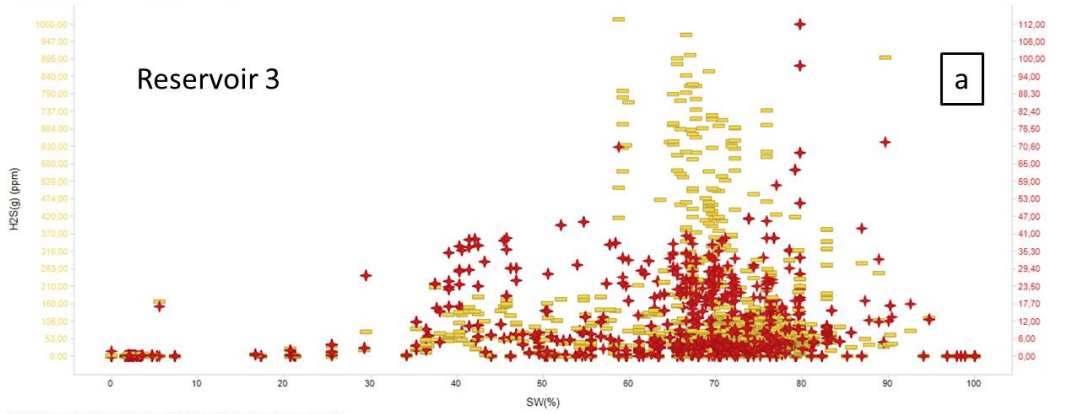


Figure 20: Decreased gas rate effect on H<sub>2</sub>S concentration

H<sub>2</sub>S(g) (ppm), H<sub>2</sub>S (kg/d) vs. SW(%)



H<sub>2</sub>S (ppm) vs. WATERCUT (Filter by formation)

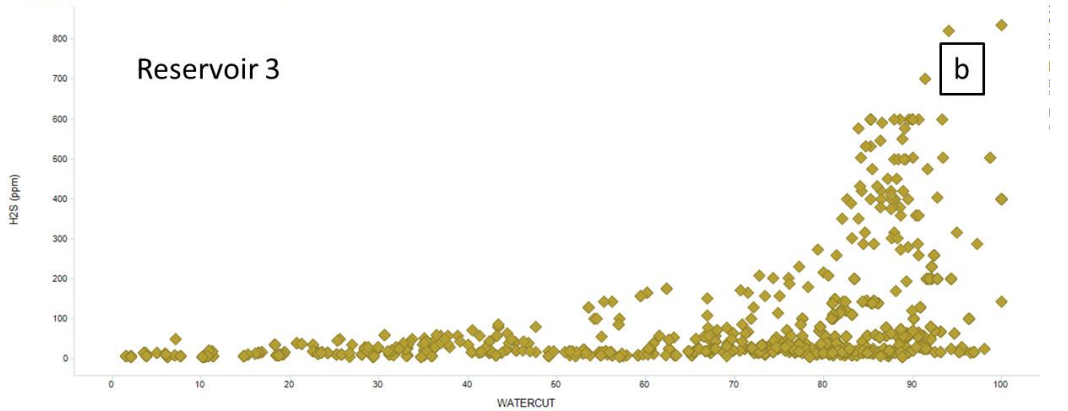
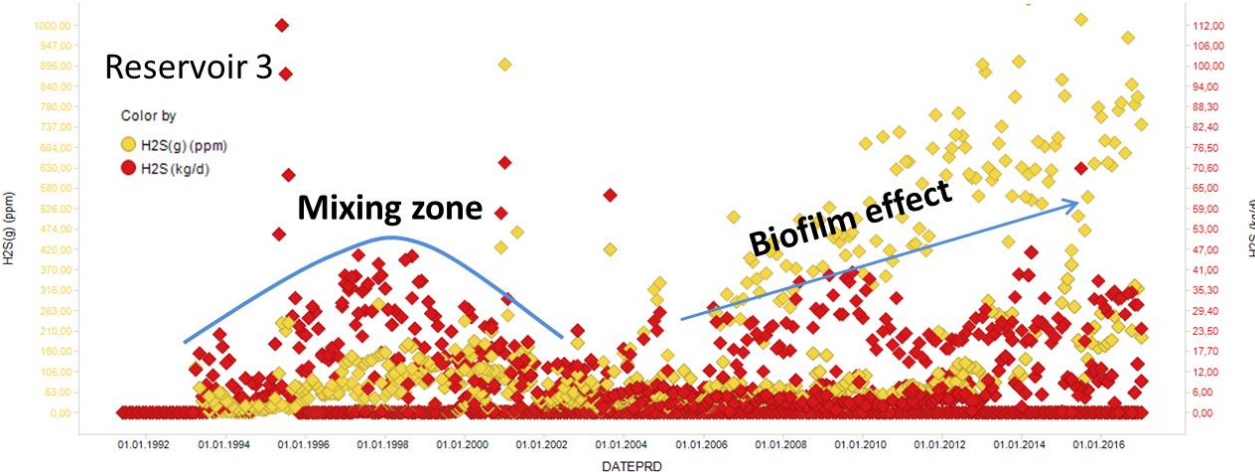


Figure 21: Comparison of total H<sub>2</sub>S produced against gas phase concentration

In spite of observed clear correlations between seawater cut and H<sub>2</sub>S production, the insight from these correlations is not fully understood yet. One observation is that it clearly supports the concept of “delayed H<sub>2</sub>S” where first seawater does not produce H<sub>2</sub>S generated as a result of reservoir cooling (SRB activation in biofilm). Low concentration of H<sub>2</sub>S seen with seawater breakthrough can instead be attributed to mixing zone generated H<sub>2</sub>S (Figure 22).



**Figure 22: Dual reservoir effect in formation level**

With access to the EC database for a specific field formation level analysis is believed to give improved and more reliable results. Furthermore, by properly joining production (OFM), wellbore split (EC) and injection (OFM) data tables it will be possible to examine the relationship between injected volumes (both water and gas) with produced H<sub>2</sub>S per formation.

### 4.3 Wellbore Level Visualization and Data Analysis

Wellbore level part of the dashboard involves more detailed analysis due to both data availability and quality. To start with, field level cumulative plot (Figure 16) is drilled down to wellbore level, generating plots for the development of cumulative H<sub>2</sub>S with time for all wellbores. Figure 23 illustrates Field I wellbores' cumulative H<sub>2</sub>S where it can be noticed that field-wise extreme amounts of H<sub>2</sub>S is not the result of all wells producing increased values but instead there some certain wells with extremely high H<sub>2</sub>S content in production fluids.

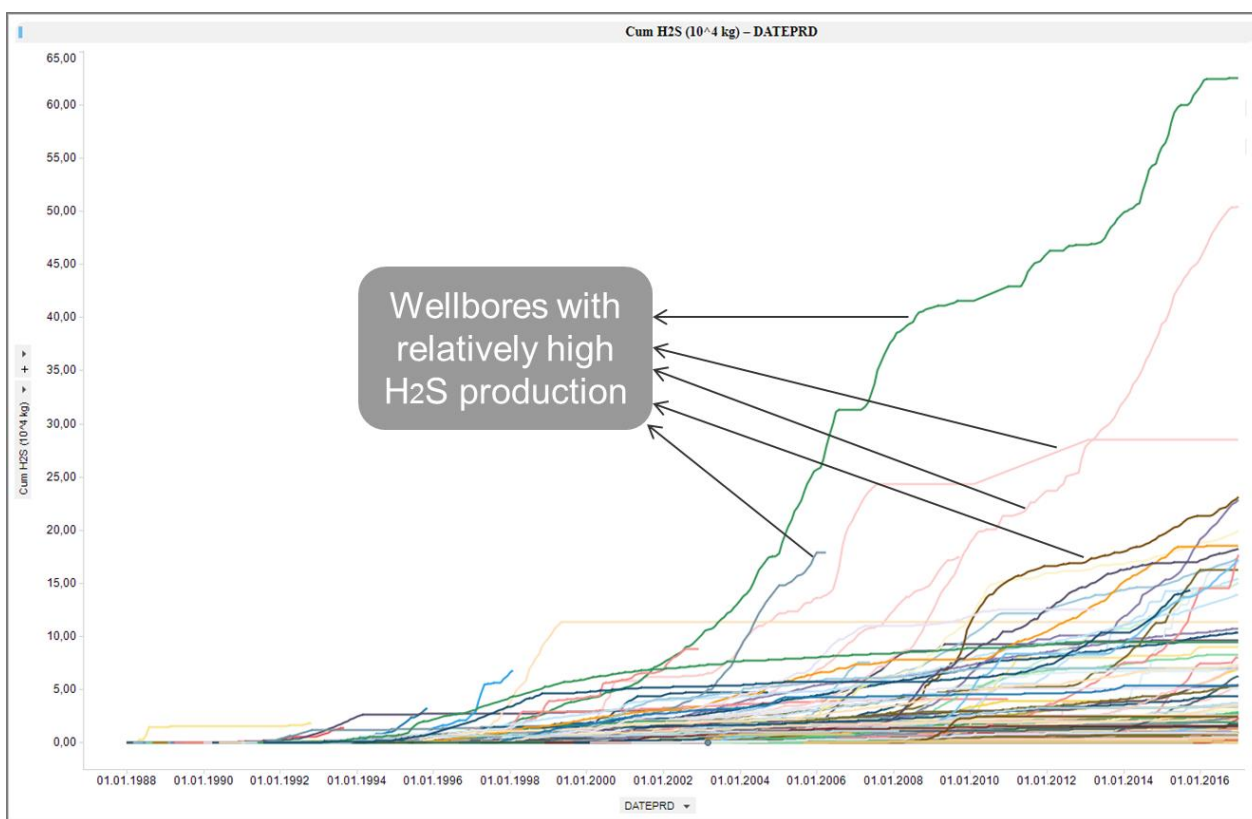


**Figure 23: Field I-X cumulative H<sub>2</sub>S production per well-bore**

Due investigation of these distinct wellbores including their comparison both with analogue wellbores and with those that are different in H<sub>2</sub>S production development (low H<sub>2</sub>S content) is believed to yield essential factors contributing and/or prohibiting H<sub>2</sub>S generation and production.

#### 4.3.1 Cumulative H<sub>2</sub>S vs. Cumulative Seawater

When plotting measured H<sub>2</sub>S concentration in gas phase (ppm) against seawater cut (Figure 24), elevated concentrations of H<sub>2</sub>S appear as produced seawater fraction increases. The

correspondence between produced seawater and H<sub>2</sub>S production is observed in plots of cumulative production of H<sub>2</sub>S and seawater has been generated for all wellbores (Figure 25).

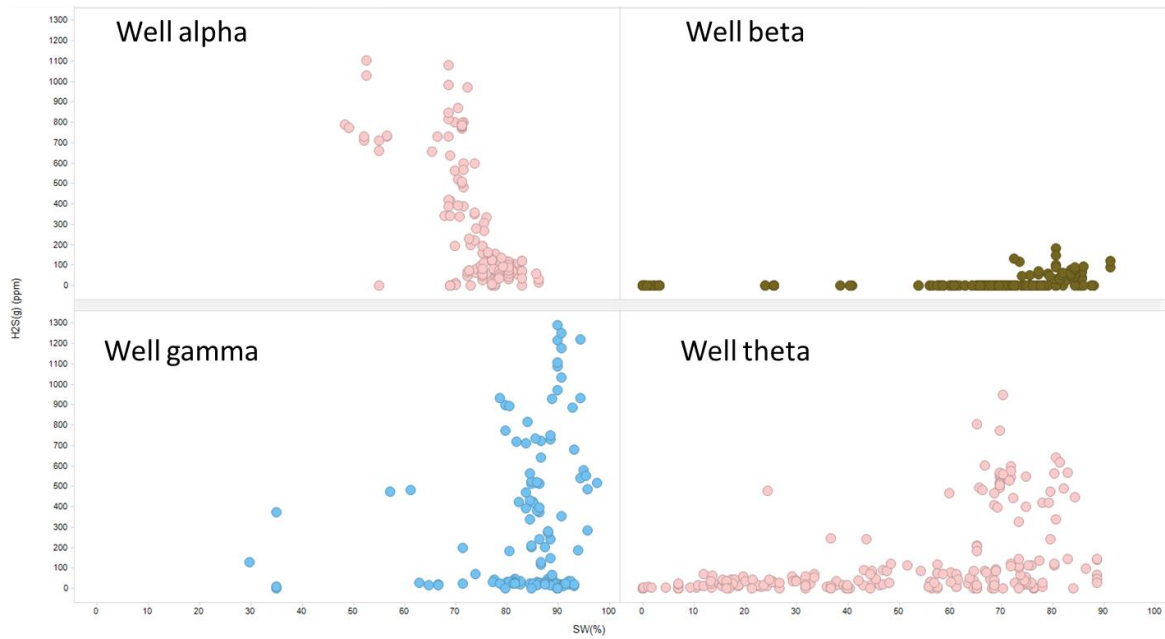


**Figure 24: H<sub>2</sub>S concentration in gas phase (ppm) vs. SWC**

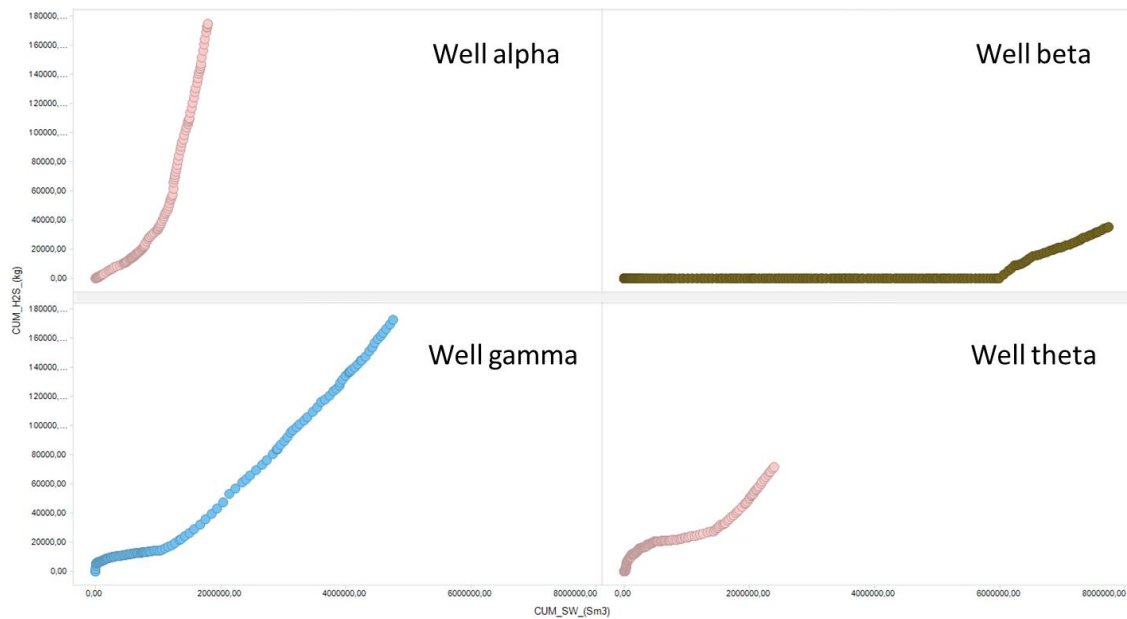


**Figure 25: Cumulative H<sub>2</sub>S (kg) vs. cumulative seawater production**

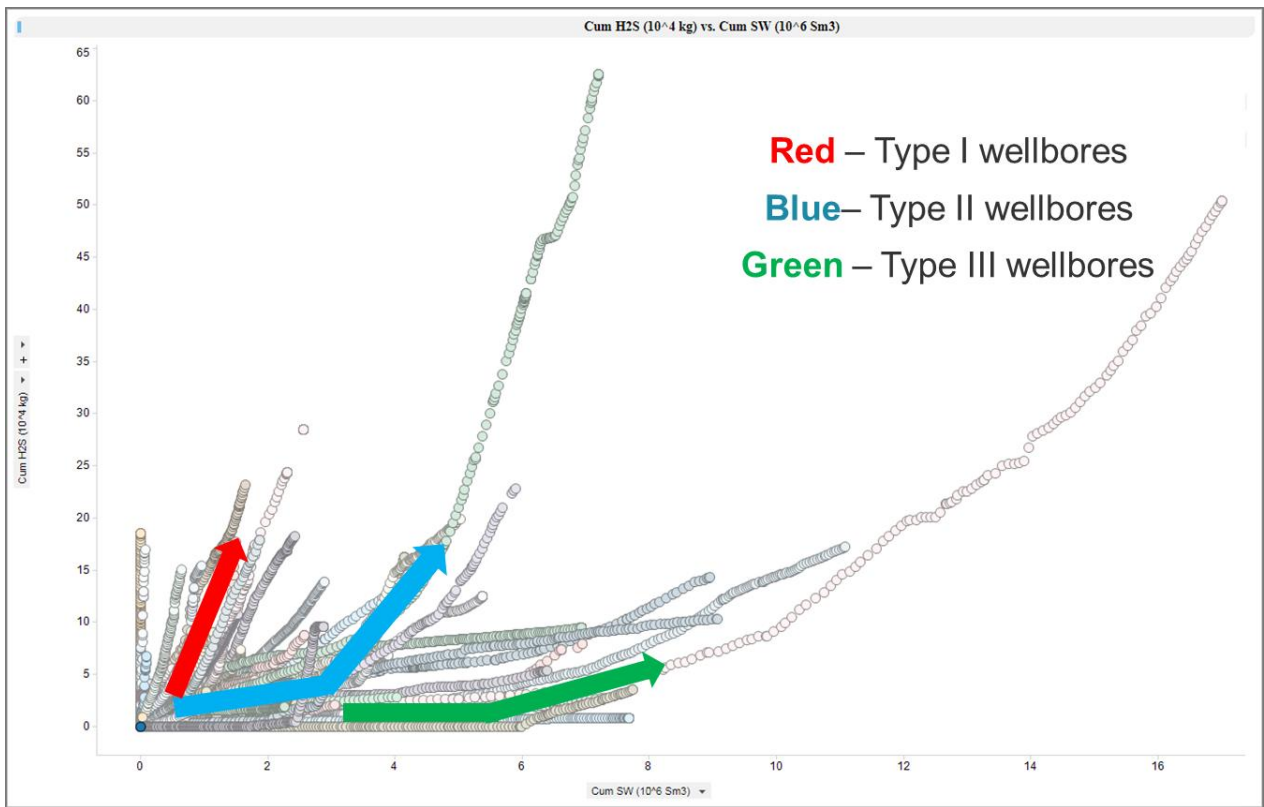


**Figure 26: Cumulative H<sub>2</sub>S vs. Cumulative seawater production for all wellbores of Field I**

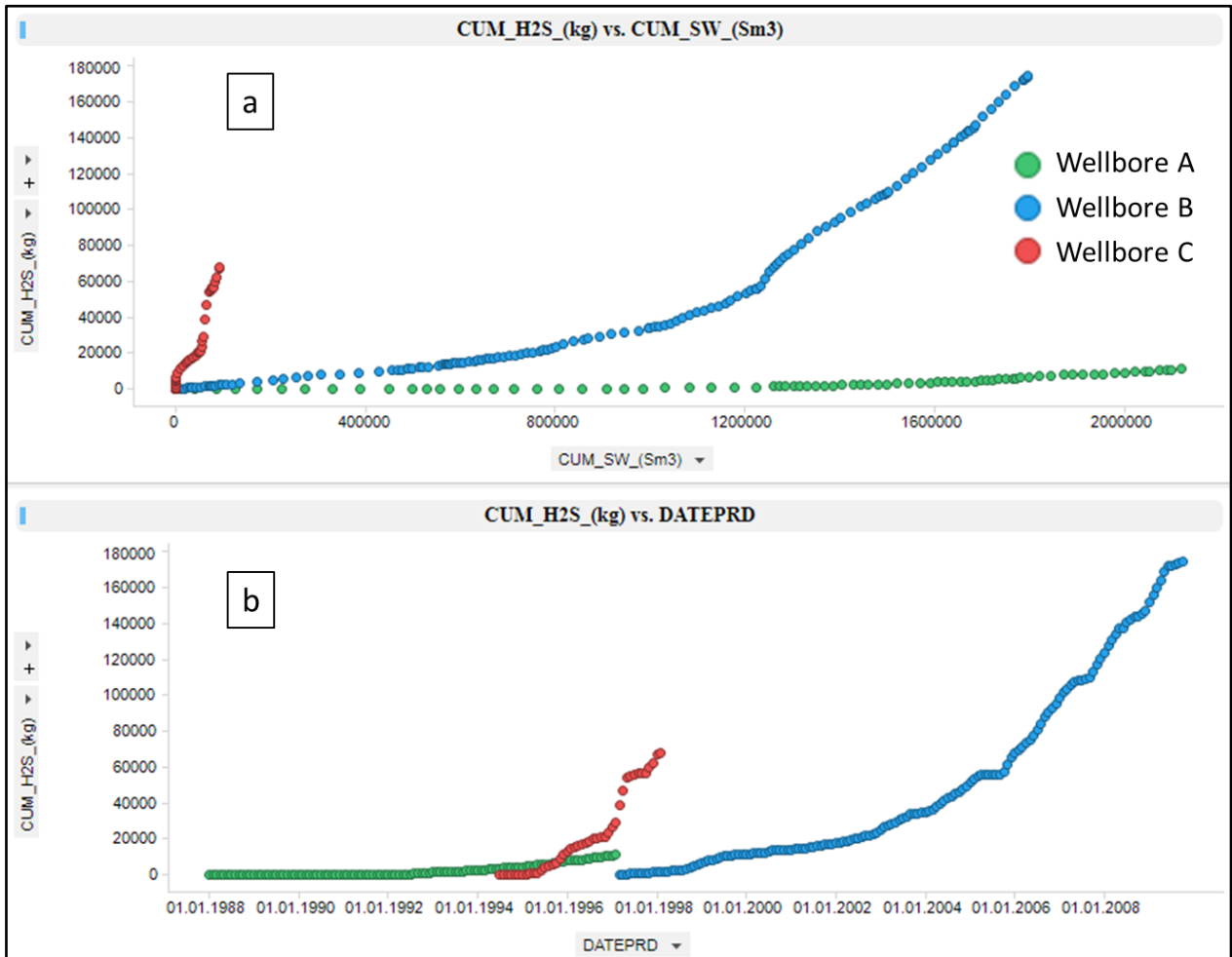
As indicated by the red, blue and green arrows in Figure 26, wellbores follow three clearly defined trends. To understand this natural separation, wellbores are clustered into three “Types” for further analysis. Although there is still no full comprehension of why wellbores follow somewhat predefined trends, it is thought that the grouping of wellbores is related to different drainage patterns.

Figure 27 exemplifies wellbores belonging to three different “Types”, where the distinction in terms of H<sub>2</sub>S development is obvious. Wellbore A with a fairly long delay period has the onset of H<sub>2</sub>S roughly after 1500 on-stream days (after 1992). Wellbore B which shows gradual increase in H<sub>2</sub>S production is a sidetrack from mother well A. This moderate escalation in H<sub>2</sub>S amount from the start of the wellbore’s life can be due to already flooded near wellbore zone. Wellbore C which initially was an injector supplying seawater above oil water contact has later been converted to a producer. It can be seen that observed H<sub>2</sub>S development of this wellbore supports the biofilm theory, which says that H<sub>2</sub>S is generated in a biofilm around injectors (chapter 2.2.2). Thus, after conversion of the wellbore from an injector to a producer it has drained the reservoir zone that meets all conditions for H<sub>2</sub>S generation such as reduced



temperature as a result of cold seawater flooding and availability of both sulfate and carbon sources.

Although most of the wellbores can be classified into a specific “Type”, there are some with a hybrid form of a cumulative H<sub>2</sub>S vs. cumulative seawater curve (Figure 26), i.e. showing a trend that is a combination of either two or all “Types”. To understand the development of these trends all – production, injection and H<sub>2</sub>S development charts are tied into one analysis (chapter 4.3.2).



**Figure 27: Wellbore examples of each “Type”**

- a) Cumulative H<sub>2</sub>S vs. cumulative seawater production
- b) Cumulative H<sub>2</sub>S development with time

### 4.3.2 Injection – Production data joint analysis

In order to analyze seawater breakthrough time and its impact on H<sub>2</sub>S production, injection and production data is combined into one visualization together with the development of H<sub>2</sub>S throughout wellbore life (Figure 28). Plots such as in Figure 28 can be visualized by

performing few filtration steps, where user starts by selecting a field to work with. It is made possible to analyze only one producer supported by one or more injectors at a time. Thus selection option for producers is limited to one wellbore, whereas multiple number of injectors can be picked up. Depending on the number of injectors supporting a producer, several vertical delimiters can be introduced for each individual injector. Delimiters, i.e. vertical lines, are controlled by interactive sliders that cover all production life of a wellbore. The entire page including filtration options can be found in Appendix C.

It should be noted that dashboard does not provide the information about injector – producer communication, in other words the user is expected to know which injector (or list of injectors) is supporting a specific producer.

In case of one injector and one producer pair it is relatively easier to analyze and interpret the H<sub>2</sub>S development of a wellbore with regards to seawater breakthrough. Furthermore, the influx towards the producer can be estimated on the basis of the cumulative production (voidage replacement). However when the producer is supported by several injectors simultaneously it becomes a complicated task to detect breakthrough time and explain H<sub>2</sub>S development based on only these plots. Therefore, to achieve improved interpretation it is highly recommended to work in cooperation with reservoir simulations.



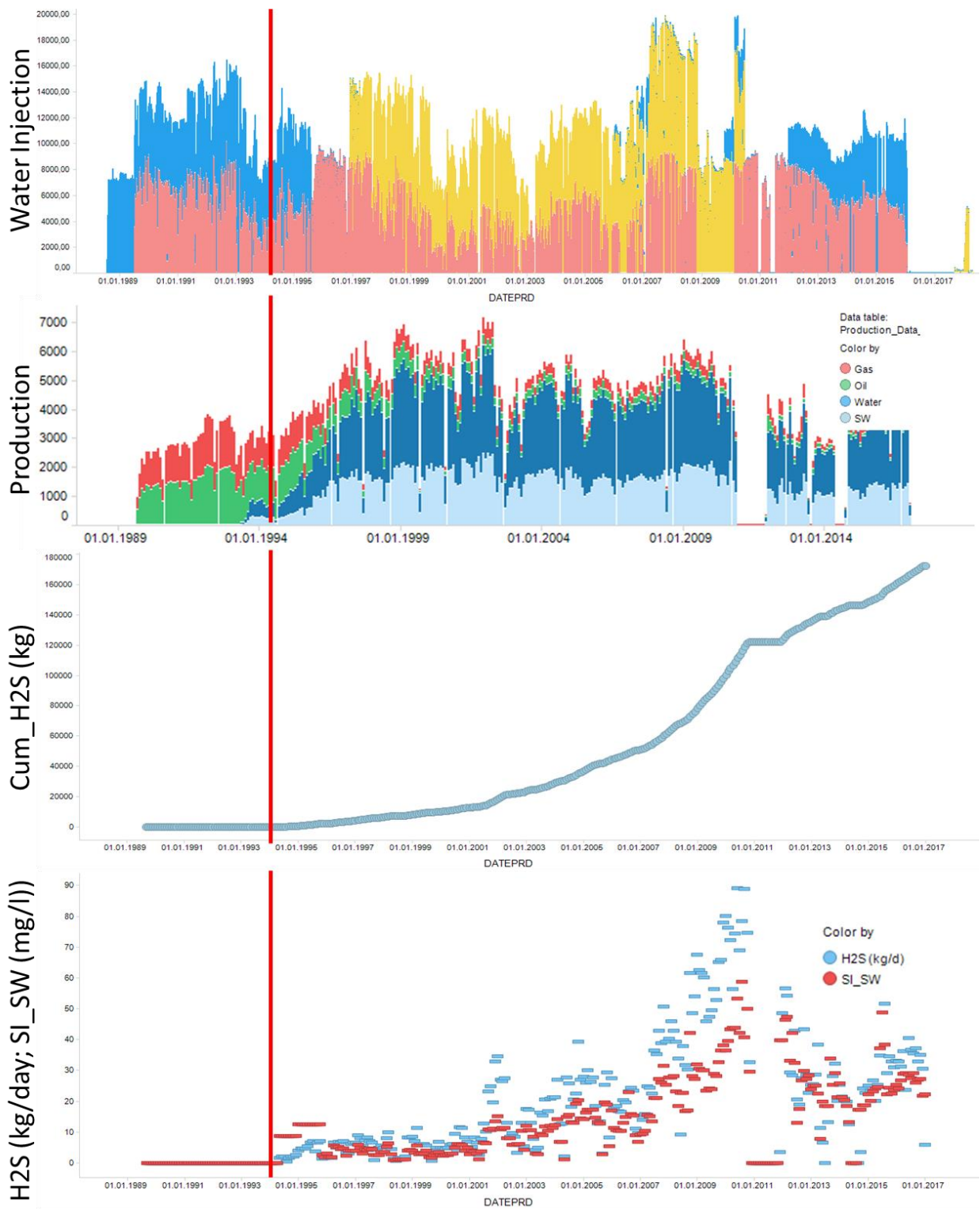


**Figure 28: Injection – Production data joint analysis**

### 4.3.3 Wellbore location on map

It was initially thought that areal variety of oil composition throughout a field might have some effects on the amount of H<sub>2</sub>S generated, especially for highly faulted fields like Field I. To evaluate this factor, wellbore location is calculated as described in chapter 3.3.4 and cumulative H<sub>2</sub>S is mapped per wellbore as a bubble chart, where the size of each bubble corresponds to the amount of total produced H<sub>2</sub>S at a given time, i.e. the bigger the size of the bubble, the more H<sub>2</sub>S is produced by that time (Figure 29).

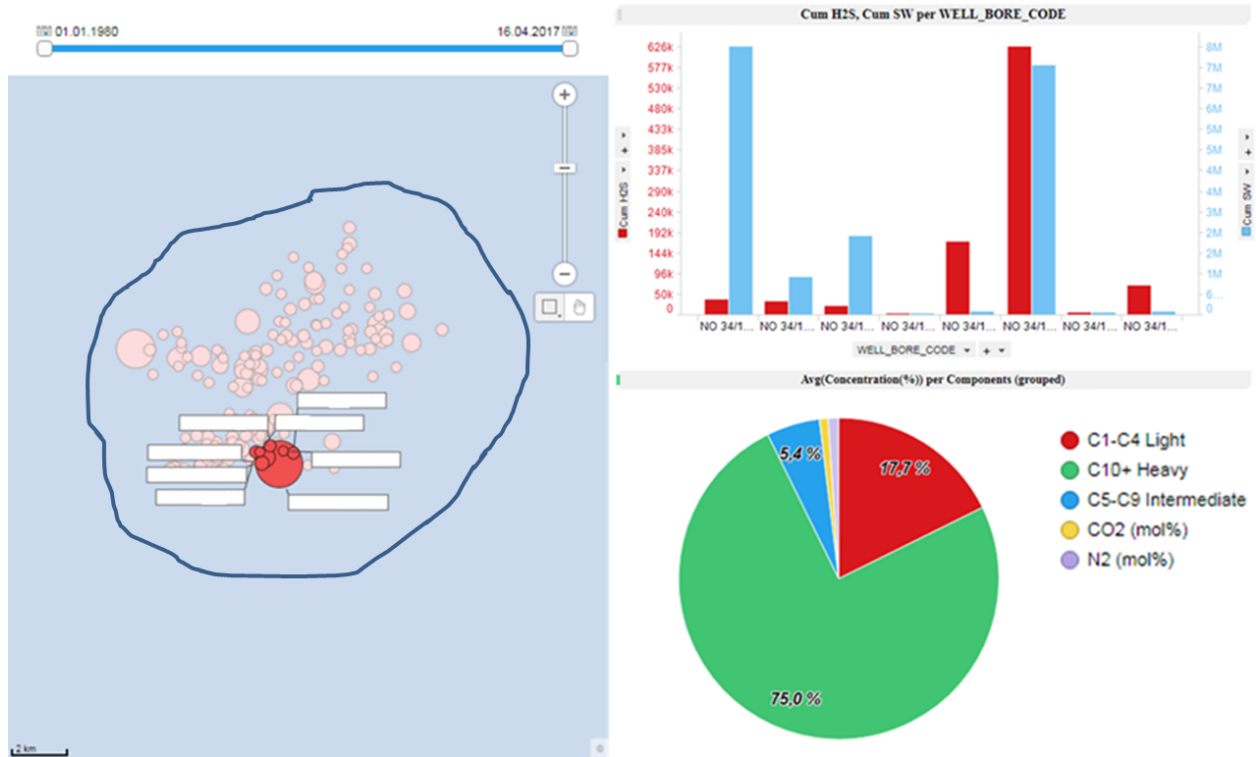


**Figure 29: Map chart (Field I example), cumulative H<sub>2</sub>S and seawater, oil composition for the entire history**

Field and NCS block map layers are turned off for confidentiality purposes.

For a chosen group of wellbores on the map, on demand details, namely cumulative H<sub>2</sub>S and cumulative seawater in the form of bar chart as well as average concentration of grouped components (C1-C4; C5-C9; C10+) in the form of pie chart can be illustrated. User has the flexibility of setting the range for production time simply by dragging the slider to visualize the amount of accumulated H<sub>2</sub>S and seawater during the chosen time period. As an example, Figure 30 demonstrates the time period of 1998-2008, where size of the bubbles on the map chart and cumulative amounts on the bar chart represent the values corresponding to the selected time period (plugged and not yet drilled wellbores disappear from the map).

Oil composition data is taken in the beginning of well life meaning that it is fixed in time. Consequently, effects of drainage and changes in reservoir PVT conditions that cause gradual changes in composition are not considered. Thus, this type of comparison may not give valuable insight, unless data for time dependent oil composition per wellbore is included into the analysis.

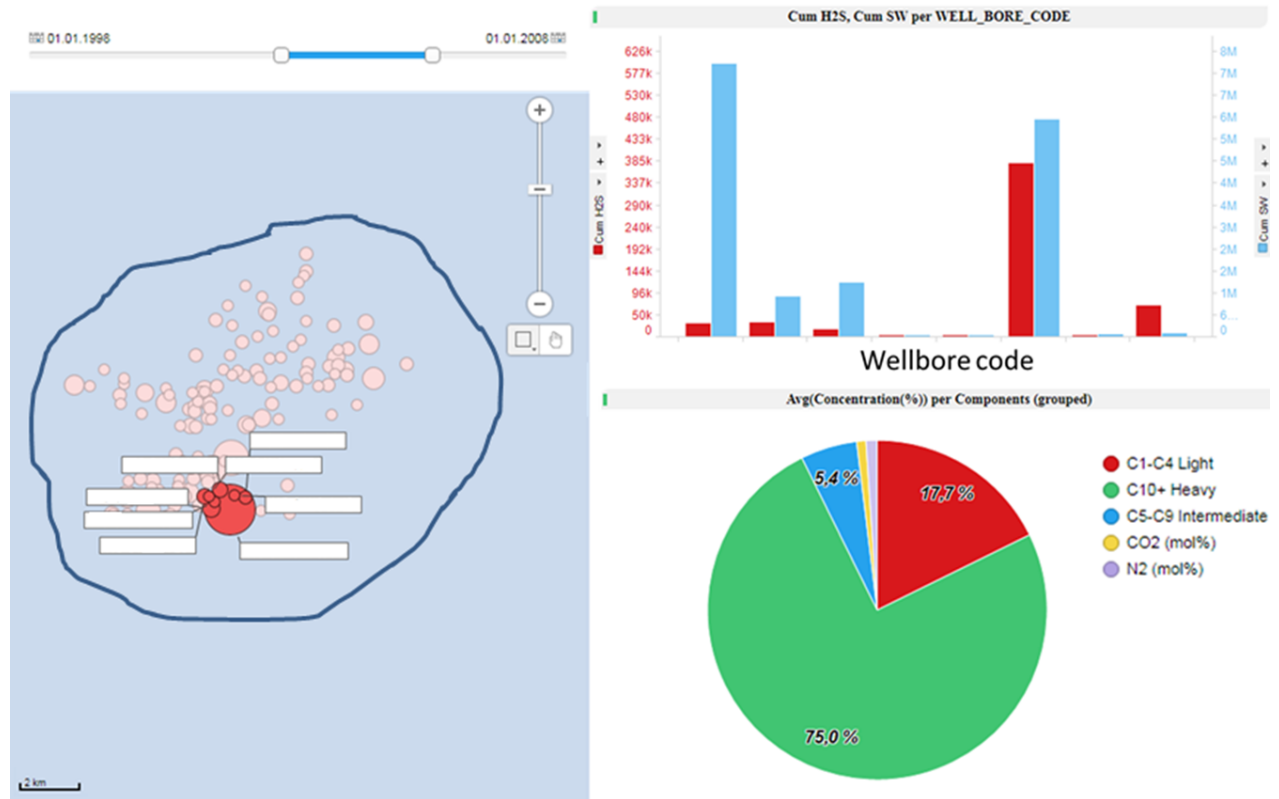


**Figure 30: Map chart, cumulative H<sub>2</sub>S and seawater, oil composition for 1998-2008 period**

#### 4.3.4 Ion data analysis

As it was presented previously in chapter 3.3.3 the main objective of performing ion analysis is to calculate seawater fraction produced along with formation water. In this chapter the results of proposed statistical (average) method of seawater fraction calculation based on all ions is presented. It also covers the effect of implementing the method on future analysis and history matching of developed models.

Ion analysis involves the method implemented by Robinson et.al. (2010) in South Arne field H<sub>2</sub>S assessment (chapter 2.3.1). Figure 31-a illustrates sulfate mass balance, where straight line represents predicted concentration of sulfate ions in seawater assuming no loss within the reservoir. It should be noted that X axis used for this plot is seawater cut calculated from statistical method. For this particular example, pure formation water, i.e. 0% seawater, corresponds to no sulfate in it, whereas 100% seawater cut contains 2750 mg/l of sulfate ions.

Scattered circles, on the other hand, show true measured concentration of sulfate ions in total produced water. Thus, in case of no sulfate loss within the reservoir, one would expect overlap of measured and predicted values. However, there are fairly noticeable discrepancies between these values (especially after 50% SWC). Provided that all sulfate lost in the reservoir was converted to  $H_2S^2$ , one can conclude that the difference between predicted line and measured values (red arrow from each point) can be attributed to the amount of  $H_2S$  generated within the reservoir.

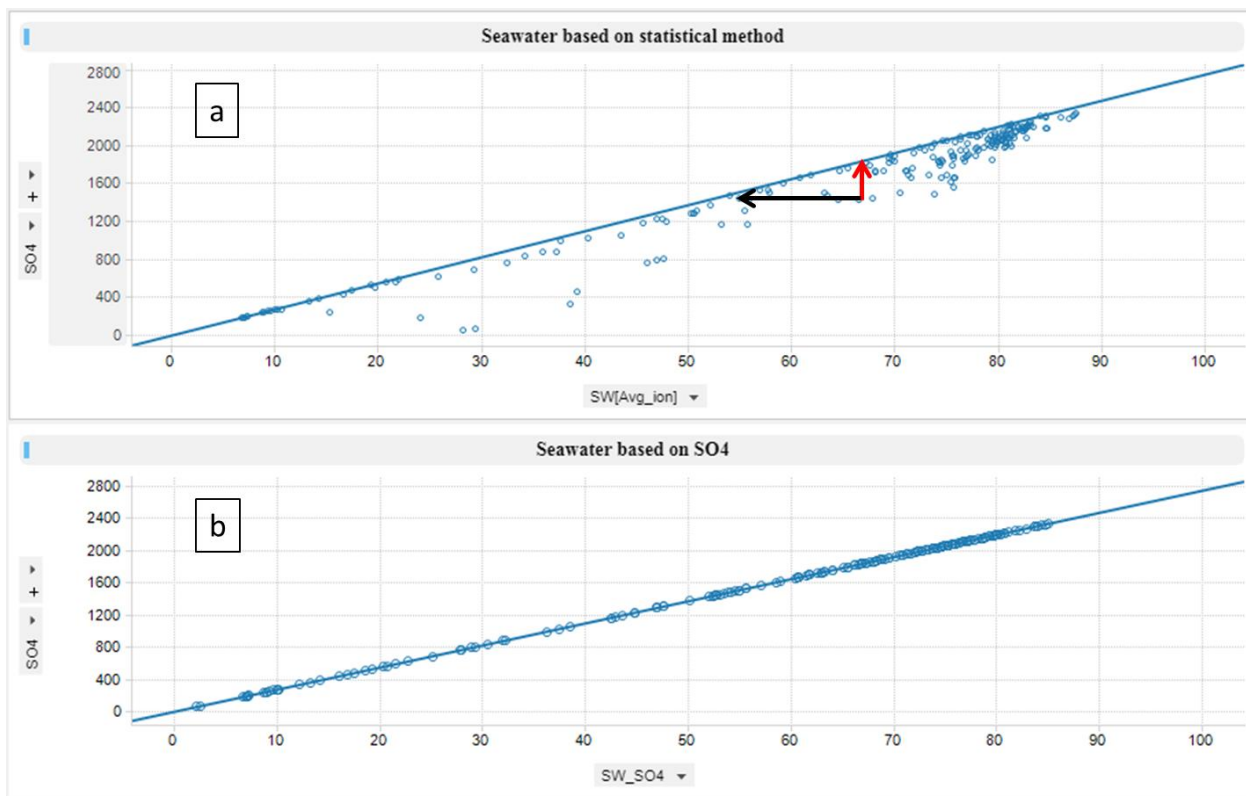


**Figure 31: Sulfate mass balance**

However, before moving forward to the analysis of generated  $H_2S$  care should be taken with regards to the accuracy of seawater fraction calculated based on statistical method (X axis in Figure 31-a). Equation 17 in chapter 3.3.3 shows that input data for statistical method (Average Ion) is seawater and formation water ion compositions as well as the concentration of  $H_2S$  in total produced water. While pure seawater ion composition is fairly accurate, involving only negligible uncertainties of measuring device (measured before injection), formation water ion composition is measured at the start of production life, when it is believed that formation water is not the mixture of different waters. However, later in well's lifetime it might produce water from different formations and this issue has to be dealt with when calculating produced seawater

<sup>2</sup> This assumption might not be valid when considerable scaling (e.g. accumulation of  $BaSO_4$ ) is in place.

fraction. To assure that formation ion composition in the equation is the true representative of produced formation water, X axis in Figure 31-a should be set to SWC calculated only from measured sulfate ions, which should then shift scattered circles onto the predicted line (Figure 31-b) meaning that mass balance is fulfilled. In case they do not overlap, SO<sub>4</sub> concentration in formation water should be adjusted. This tuning procedure has to be performed for each ion of formation water and to do this dashboard provides a separate page with interactive input boxes (Appendix C).

Having tuned formation water composition for each ion, it can now be considered that all input variables into seawater calculation based on statistical method are fair representatives of the actual data, meaning that the difference between predicted line and measured concentration of sulfate should represent the concentration of H<sub>2</sub>S generated within the reservoir. Consequently, comparison of this concentration of H<sub>2</sub>S against produced amount should in turn give an idea about the retained H<sub>2</sub>S in the reservoir due to retention in terms of adsorption/precipitation.

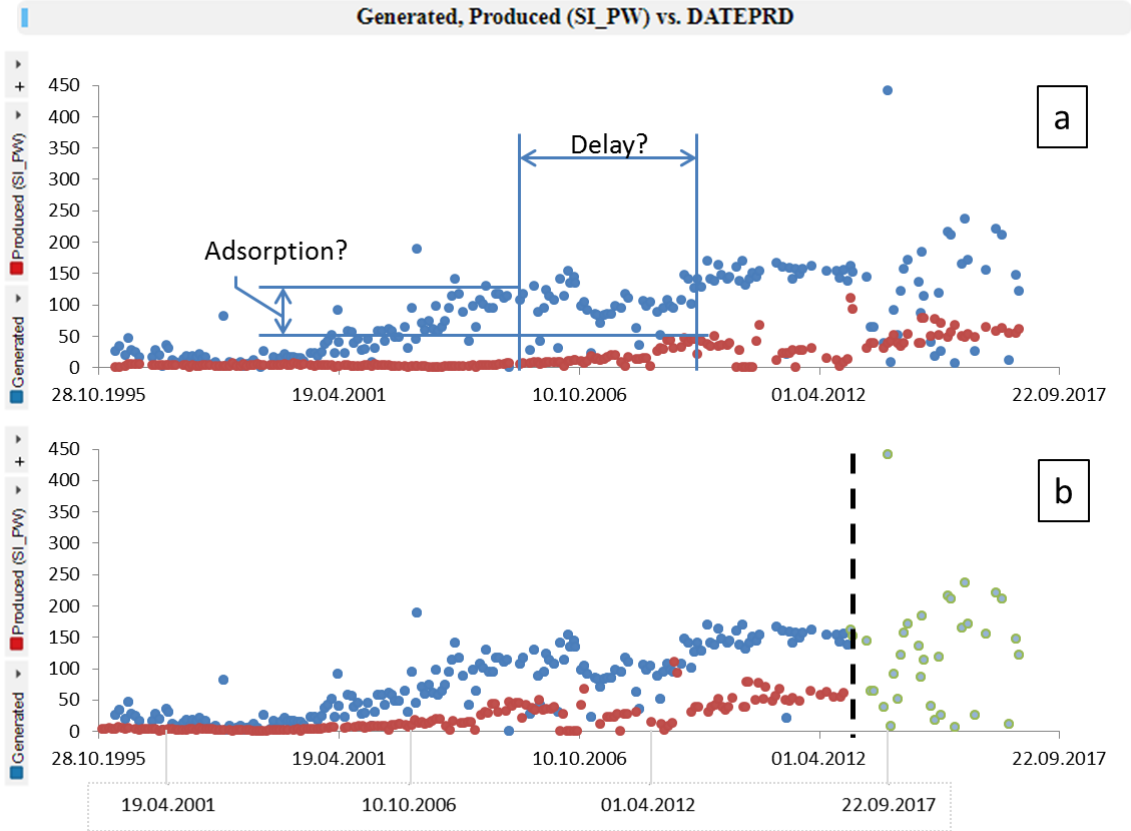


**Figure 32: Well X generated and produced H<sub>2</sub>S**

Blue and red circles in Figure 32-a represent total generated and produced amounts of H<sub>2</sub>S respectively and the difference between them can be regarded as scavenged H<sub>2</sub>S. However the interpretation of this figure still involves some uncertainties. One interesting observation is that

the produced amount of H<sub>2</sub>S seems to follow generated amount with some delay in time, which can be attributed to distance between H<sub>2</sub>S generated area (in this case most likely biofilm close to injectors) and the producer. If time axis for produced H<sub>2</sub>S is shifted to past exactly as much as the delay period, one can notice a discrepancy between generated and produced H<sub>2</sub>S amounts that can be regarded as scavenged (adsorbed) H<sub>2</sub>S within the reservoir.

As it can be seen in Figure 32-b, produced H<sub>2</sub>S data is shifted to the past (lowermost X axis). Remaining generated H<sub>2</sub>S data (green circles) on the right-hand side of vertical dashed line would then be the upper bound prediction for H<sub>2</sub>S to be generated, meaning that even in case of full reservoir rock saturation, i.e. no discrepancy between generated and produced data points, production of H<sub>2</sub>S is not expected to exceed these values.

Before drawing any conclusion about delay period and adsorption of H<sub>2</sub>S these plots have to be analyzed very thoroughly for other wells that show similar H<sub>2</sub>S development, for which the developed dashboard can serve as a very handy tool. Below in Figure 33 two other examples are presented.

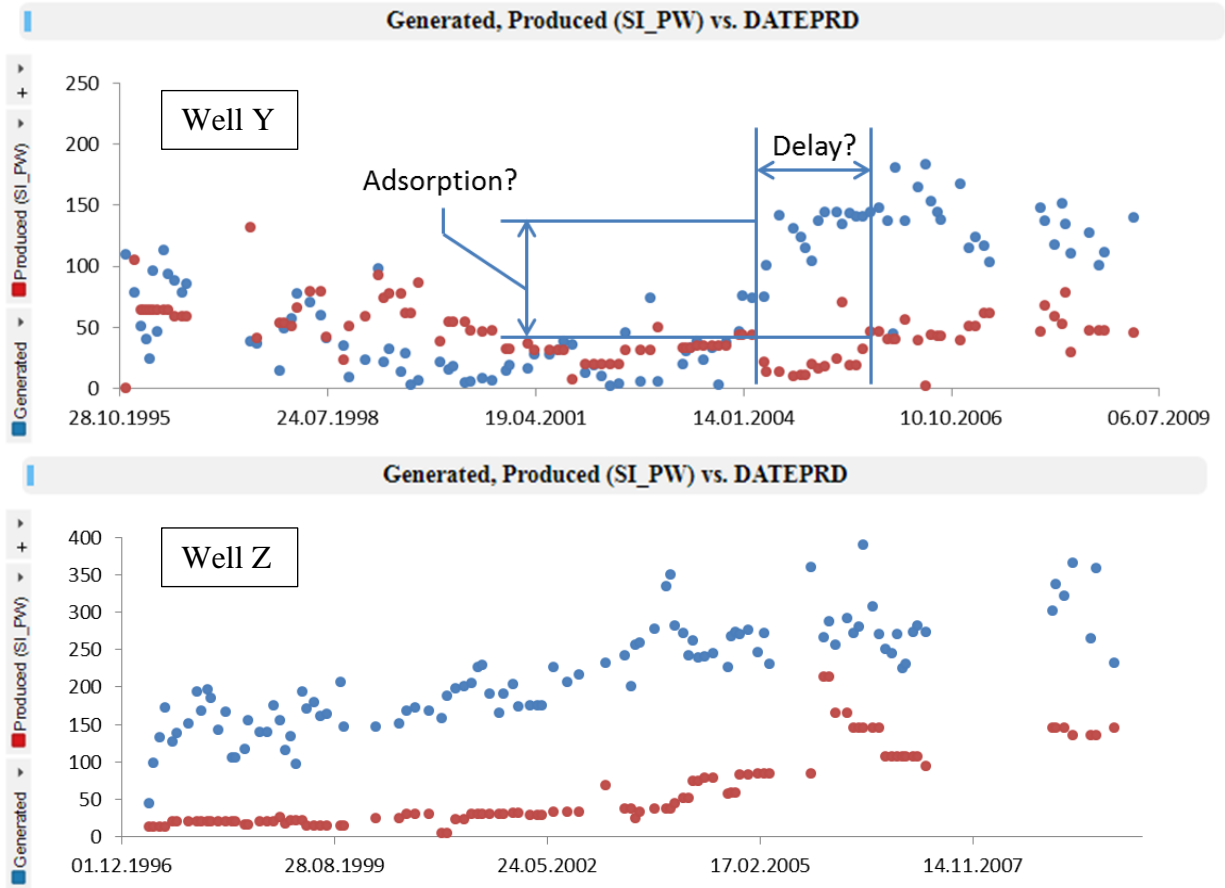


**Figure 33: Other well examples on generated and produced H<sub>2</sub>S comparisons**

While well Y can be interpreted in a similar manner as well X, it is very difficult to say something in case of well Z regarding delay period that might be because of short travel distance. In order to thoroughly comprehend the trends of generated and produced H<sub>2</sub>S, tracer data indicating supporting injectors and travel path distance has to be incorporated. It is also challenging to correctly define delay period owing to H<sub>2</sub>S saturation, which is expected to increase over time. Moreover, this analysis may prove inefficient for sidetracked wells that produce H<sub>2</sub>S immediately at the start of production time. Nevertheless, despite mentioned complexity and potential limitations of the analysis this may be extremely useful for quality checking of developed models for H<sub>2</sub>S production forecast such as SourSim RL and/or “Multivariate Statistical Modeling” (internal project). This requires determining only few wells showing distinct delay phases, e.g. well X, and comparing models’ prediction against upper bound H<sub>2</sub>S prediction from ion analysis (green circles in Figure 32).



### 4.3.5 Effect of different SWC calculations on the analysis

Having calculated more accurate seawater fraction (Figure 34 – SW[Avg\_ion]), it can now be incorporated in all further analysis including cumulative H<sub>2</sub>S – cumulative seawater. It is clear that calculating SWC based on only sulfate ions results in reduced seawater fraction, thus showing less cumulative seawater than it actually is (Figure 35). The more H<sub>2</sub>S is produced, i.e. the more sulfate is converted, the more erroneous is the SWC that is based on only sulfate.

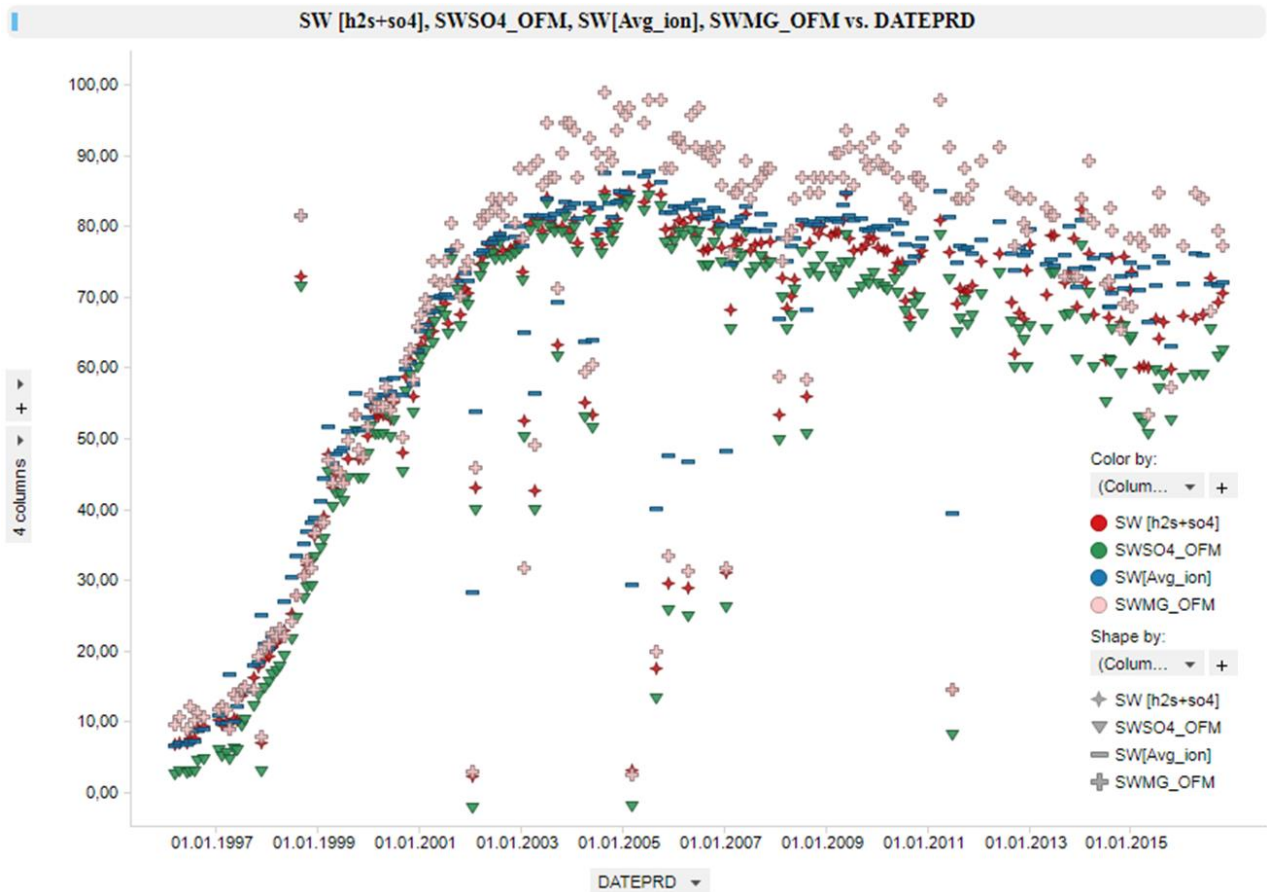


**Figure 34: Well X seawater fraction calculated from different methods**

**SW [H<sub>2</sub>S +SO<sub>4</sub>]** – Seawater fraction based on sulfate and hydrogen sulfide

**SW [Avg\_ion]** – Seawater fraction from statistical method

**SWSO<sub>4</sub>\_OFM** and **SWMG\_OFM** – Seawater fractions extracted from OFM database that are calculated based on only sulfate and magnesium respectively

The effect of increasing error in calculated seawater fraction becomes very pronounced when considering cumulative seawater. On the other hand, seawater fraction calculated only from magnesium ions seems to follow more closely SWC calculated from statistical method.



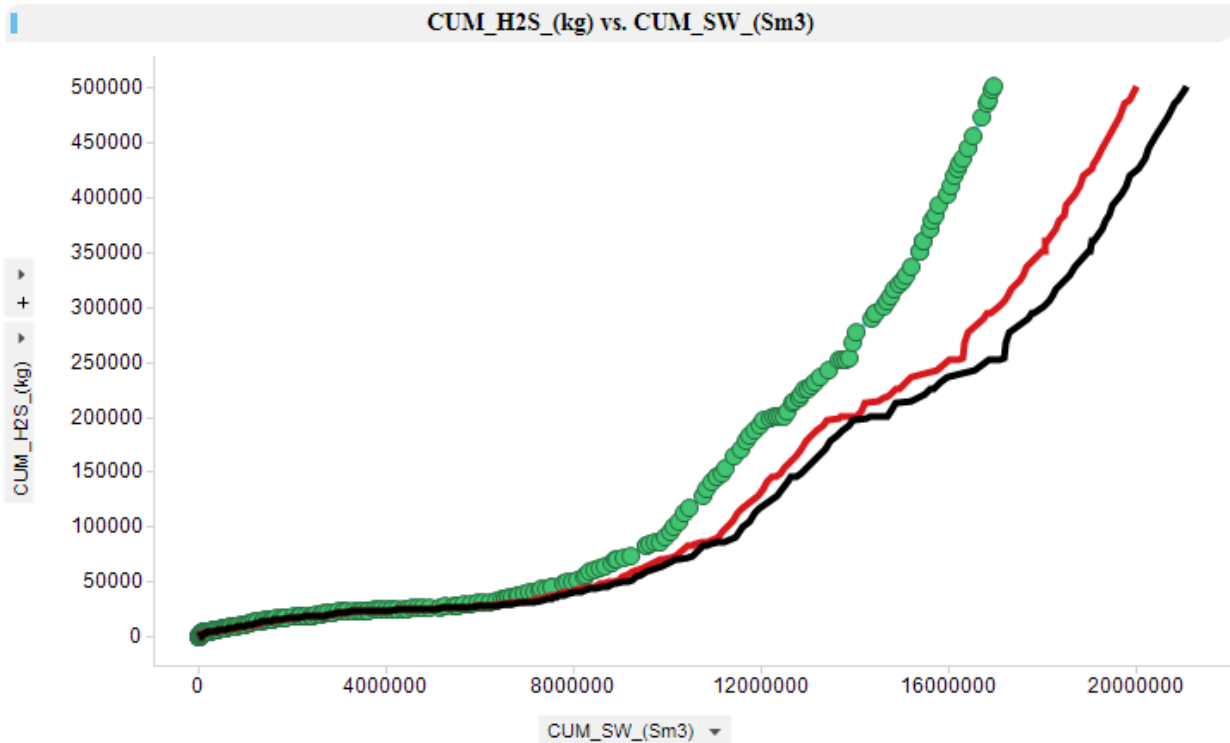


**Figure 35: Well X cumulative H<sub>2</sub>S vs. cumulative seawater**

**Green** – Cumulative seawater is calculated using SWC based on sulfate only (OFM)

**Black** – Cumulative seawater is calculated using SWC based on magnesium only (OFM)

**Red** - Cumulative seawater is calculated using SWC based on statistical method

There is no doubt that having correct and high quality data is fundamental for history matching of any developed model. To perform any reliable predictions model should at least reproduce “correct history”, which in this case is represented by cumulative H<sub>2</sub>S and cumulative seawater.

## 4.4 Incorporating H<sub>2</sub>S production models (correlations) in the dashboard

The potential for using historical data for predictions of H<sub>2</sub>S development in a wellbore level has been investigated in another master thesis work within the Reservoir Souring project (Mburu, 2018).

Cumulative production of H<sub>2</sub>S and seawater plots (e.g. Figure 35) have proved useful and modeling of the same relationship is believed to increase the understanding of reservoir souring when comparing production from several wells. When reservoir pressure is fairly well maintained (as in the case of NCS fields included in the analysis) the reservoir volume taken out by production from a well is replaced by influx from the surroundings, namely influx from aquifer and water injectors, with minor contribution from gas injection and lateral movement of oil. This idea, i.e. the concept of voidage replacement, served as a basis for modeling of cumulative production of H<sub>2</sub>S and seawater as a function of cumulative liquid production (sum of produced oil and water), normalized using a ‘reference volume’ – the cumulative liquid production up to the first observation of H<sub>2</sub>S in a well (Meisingset, 2017).

Meisingset (2017) has developed a mathematical expression to reproduce the cumulative H<sub>2</sub>S vs. cumulative seawater curve (Figure 35; model uses seawater cut calculated from sulfate ions only), where the slope of the plot is modeled as a function of cumulative liquid production (CumL):

$$\frac{d(CumH_2S)}{d(CumSW)} = f(CumL) \quad (22)$$

where  $f(CumL)$  increases with time from 0 to 0,2 kg per cubic meter of seawater:

$$f(CumL) = 0,2 * \left[ \frac{K_2 + (1 - K_2) * f_1(CumL)^{K_3}}{f_1(CumL)^{K_3} + (1 - f_1(CumL)^{K_4})} \right] \quad (23)$$

where

$$f_1(CumL) = 1 - K_1^{(1 - \frac{CumL}{V_{ref}})} \quad (24)$$

where constants K<sub>1</sub>-K<sub>4</sub> were selected and optimized by ‘trial and error’ method to obtain a general match with V<sub>ref</sub>, which in turn is equal (or similar) to the cumulative liquid production of a well up to the first H<sub>2</sub>S observation in the well stream.

With the intention of simplifying of the current model, a slightly modified version of it with fewer constants has lately been developed (Uleberg & Meisingset, 2018) and further investigated (Mburu, 2018):

$$f(CumL) = 0,2 * \left[ \frac{K_1 + (1 - K_1) * (PV)}{(PV - 1) + K_2 * PV^{K_3}} \right] \quad (25)$$

where PV is pore volume:

$$PV = CumL/V_{ref} \quad (26)$$

By combining the equations 22 and 25 the expression for cumulative H<sub>2</sub>S as a function of cumulative liquid can be derived:

$$d(CumH_2S) = 0,2 * \left[ \frac{K_1 + (1 - K_1) * (PV)}{(PV - 1) + K_2 * PV^{K_3}} \right] * d(CumSW) \quad (27)$$

or:

$$\begin{aligned} [CumH_2S]_{n+1} &= [CumH_2S]_n + \\ &+ 0,2 * \left[ \frac{K_1 + (1 - K_1) * (PV)}{(PV - 1) + K_2 * PV^{K_3}} \right] * ([CumSW]_{n+1} - [CumSW]_n) \end{aligned} \quad (28)$$

where indexes [n] and [n+1] represent current and next time steps correspondingly.

Constant K<sub>1</sub> in the modified model (eq. 25) represents the initial slope of the cumulative H<sub>2</sub>S vs. cumulative seawater curve, whereas K<sub>2</sub> and K<sub>3</sub> control the exponential part and the maximum H<sub>2</sub>S amount respectively.

To illustrate the potential of the dashboard latest ‘simplified model’ is integrated into the analysis for Field I wellbores. Appendix D provides the python script written for extracting ‘reference volume’ for each wellbore and consequently running the model. It should be noted that for ‘Type I’ wellbores where H<sub>2</sub>S production is observed very early, the definition of ‘reference volume’ becomes meaningless. In this case, the best option for implementation of the mathematical expression is then to allow the ‘reference volume’ and the constant representing the initial H<sub>2</sub>S production rate (K<sub>1</sub>) to be modified to match the measured cumulative H<sub>2</sub>S production. For this purpose input boxes for manipulation of all constants are made available in the dashboard.

Meisingset (2017) reported ‘matched reference volumes’ for wellbores with early H<sub>2</sub>S breakthrough, which varied from less than 0.01 to more than 0.5 mill. m<sup>3</sup>. Decadic logarithm (log<sub>10</sub>) average of reference volumes found to be -0,8466, corresponding to an average volume of

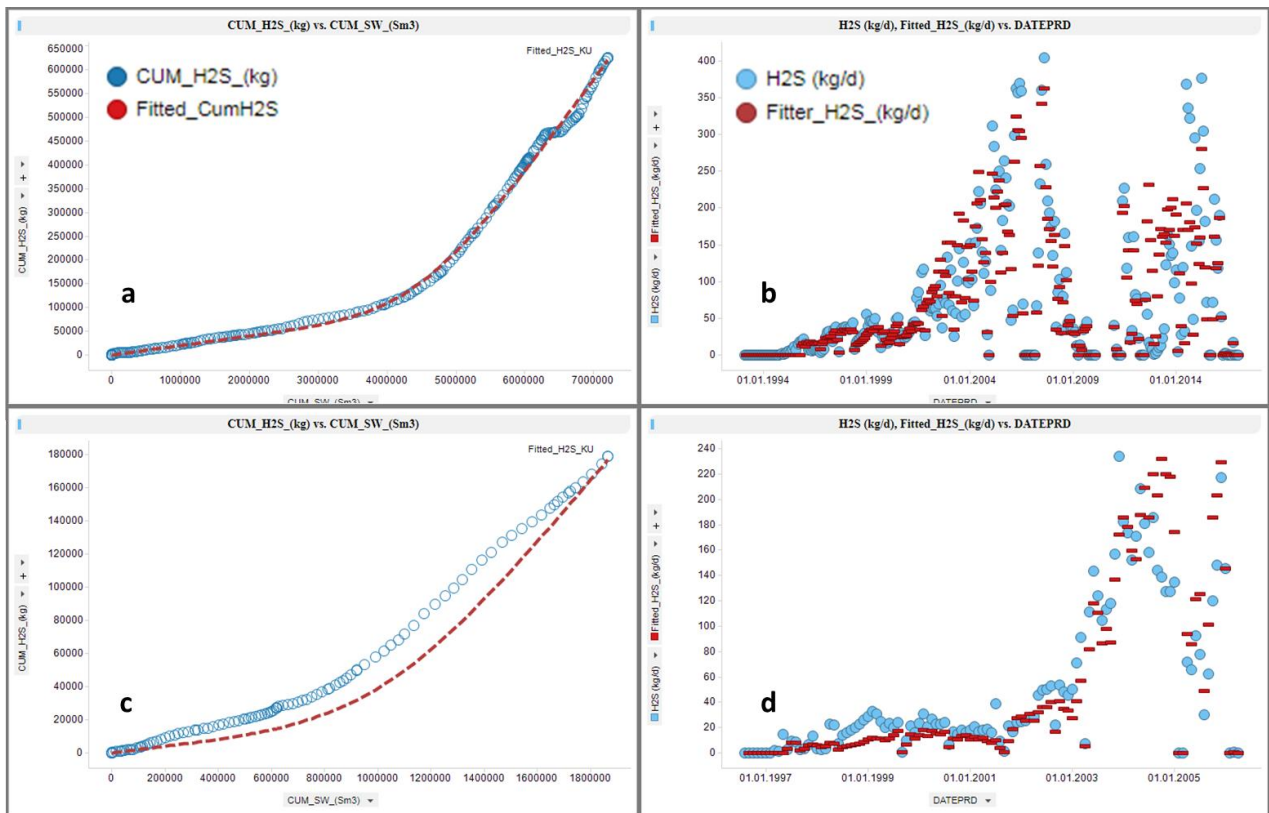


**Figure 36: Simplified model match in example of Type II wellbores**

a; c – Historical and matched cumulative H<sub>2</sub>S vs. cumulative seawater production  
 b; d - Historical and matched H<sub>2</sub>S rates

142 000 m<sup>3</sup>. As a typical ‘minimum reference volume’ for ‘Type I’ wellbores, 140 000 m<sup>3</sup> is suggested to use (Meisingset, 2018).

Figure 36 demonstrates historical (blue) and matched (red) cumulative H<sub>2</sub>S vs. cumulative seawater production (‘a’ and ‘c’) alongside with historical and matched H<sub>2</sub>S rates (‘b’ and ‘d’) in the example of two ‘Type II’ wellbores. Optimized set of constants for these types of wellbores used in the calculations is provided by Mburu (2018) (Appendix D). Meisingset (2017) and Mburu (2018) reported that for the wellbores with elevated early H<sub>2</sub>S production the higher priority is given for matching the late part of cumulative H<sub>2</sub>S vs. seawater plots (Figure 36-c).

As shown in Figure 37, using the same set of constants (K<sub>1</sub> - K<sub>3</sub>) for all ‘Types’ of wellbores does not raise a good match of the model for ‘Type I and III’ wellbores, thus requiring the modification of constants to reproduce the historical cumulative H<sub>2</sub>S vs. seawater curves.

For history matching of these plots, i.e. cumulative H<sub>2</sub>S vs. cumulative seawater curves, the question addressed in the previous chapter (4.3.4) regarding the different methods of seawater fraction calculation becomes crucial, meaning that models should match ‘accurate history’ to predict the future accurately.

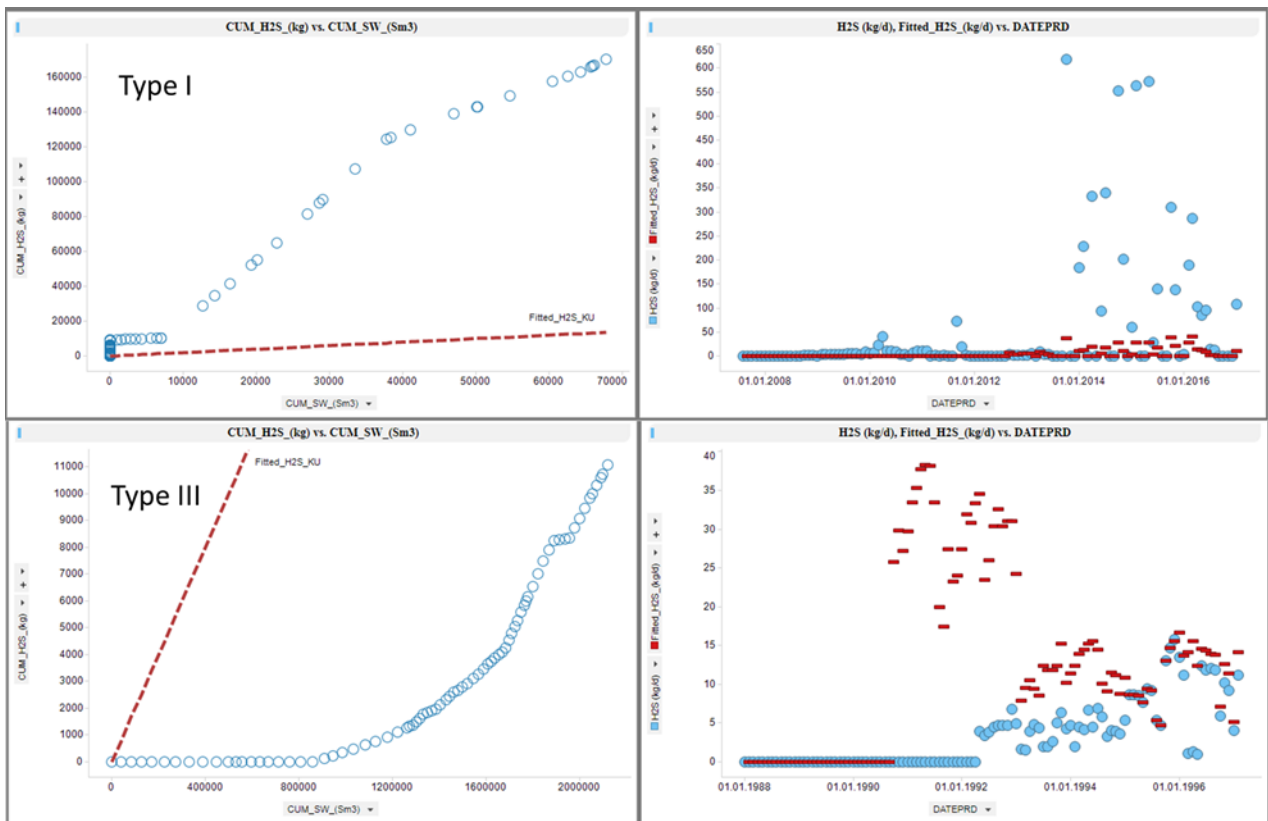


**Figure 37: Simplified model match for Type I and III wellbores**

Having matched correct historical data of cumulative H<sub>2</sub>S, curves can then be extrapolated into the future to get the predictions of H<sub>2</sub>S rate for the upcoming years. Since the mathematical equations are the function of cumulative liquid (produced water and oil), extrapolation of the models require predicted oil and water rate that can be taken either from simulations or decline curve analysis (DCA).

**Present status of the mathematical models:**

- Field sensitive set of constants, i.e. a new optimized set of constants should be found for each field;
- Although universal set of constants for ‘Type II’ wellbores for a specific field can be implemented, it is required to manipulate with constants in order to be able to fit the model to historical data of ‘Type I’ and ‘Type III’ wellbores;
- Optimization of constants was made by ‘trial and error’ method, trying to get a best possible visual match in the plots. No curve fitting algorithm was used.

## 5 Conclusion

### 5.1 Summary and Recommendations

Prior to building the dashboard a thorough literature review including several models for H<sub>2</sub>S generation/production as well as industry reports for H<sub>2</sub>S monitoring in the example of North Sea oilfields was performed.

Developed dashboard is, currently, in its initial phase. Spotfire is connected and directly extracting the necessary data from OFM, EC (only Field I) and NPD databases. In case a new data source is required to connect to the dashboard, having the connection URL, username and password allows extracting necessary data. Presently, dashboard extracts H<sub>2</sub>S production data from Excel H<sub>2</sub>S Calculator. Extracting it from newly developed Python version of H<sub>2</sub>S Calculator has numerous advantages in terms of data maintenance, thus one of the future work is to connect Python H<sub>2</sub>S Calculator into Spotfire. However, it should be noted that Spotfire does not support Python scripts directly. Therefore it was decided to run Python scripts from TERR established within Spotfire and based on initial investigations either “PythonInR” or “reticulate” packages are suggested to perform this task.

Dashboard is presented in three different levels of visualization, namely field level, reservoir level and wellbore level. Field level that is sum off all wells within a field serves as a general overview and comparison between fields. Reservoir level presents H<sub>2</sub>S production per reservoir. However, this level of analysis involves high uncertainty due to data quality and availability, thus it needs improvements and extensions that can be done once the access to individual EC databases is granted. One of the suggested analyses would be the investigation of reservoir wise water and gas injection versus H<sub>2</sub>S production.

Wellbore level contains more detailed analysis as compared to previous ones. First, wellbore geo-location was calculated based on wellhead location and deviation data, which then used to map H<sub>2</sub>S development to find a correlation between areal variety in oil composition and H<sub>2</sub>S production within a field. Furthermore, cumulative H<sub>2</sub>S and cumulative seawater plots are

generated for all wellbores in question. According to these graphs wellbores are grouped into three categories (types) according to drainage patterns, where:

- Type I – wells with early H<sub>2</sub>S production;
- Type II – wells showing a short delay in H<sub>2</sub>S appearance at the producers followed by a moderate increase
- Type III – wells with slow development of H<sub>2</sub>S

In order to examine injection water communication, production, injection and H<sub>2</sub>S development data was integrated into a single visualization. However to investigate these effects the user is expected to know communication pathways between injectors and producers.

Ion data visualization and analysis is also carried out to find more accurate seawater fraction that is an essential input variable for H<sub>2</sub>S prediction models such as the one discussed in chapter 4.4. Seawater fraction calculated from proposed statistical method seems to be close to magnesium based seawater cut; whereas sulfate based calculations show fairly reduced amounts. It would be worthwhile to incorporate seawater fraction calculated from statistical method into further analyses and prediction models, since it does not involve assumptions of conservative ions (chapter 3.3.3). It is also highly advisable to automate tuning of formation ion composition involved in statistical method of seawater calculation, since currently it is done manually for each individual wellbore.

Observed behavior of generated (based on ion data) and produced H<sub>2</sub>S raises very interesting, yet uncertain, information about retardation (adsorption) and delay of H<sub>2</sub>S. Prior to drawing any conclusions plots like Figure 32 should further be investigated.

Last but not least, mathematical models for matching cumulative H<sub>2</sub>S and seawater production curves are also investigated and a simplified empirical model (eq. 25) is included into the dashboard analysis, thus giving the opportunity of forecasting H<sub>2</sub>S production.

Combining all aforementioned it can be said that the goal of building a dashboard for visualization, evaluation and modeling of wellbore and field H<sub>2</sub>S production is satisfactorily achieved and web-player version of the dashboard is also made available for end users with limited Professional Spotfire experience.

## 5.2 Future Development of the Dashboard

*“There is nothing so useless as doing efficiently that which should not be done at all”*

– Peter Drucker

Despite the fact that the dashboard is in the initial phase of development, it has been proven to be a very useful tool for H<sub>2</sub>S production evaluation. Alongside all other features for H<sub>2</sub>S production analysis the dashboard can serve as a user friendly version of python H<sub>2</sub>S Calculator for people with less experience of coding.

In Figure 38 the future workflow of dashboard in terms of H<sub>2</sub>S production forecast and control is illustrated. First trial of the workflow has shown promising potentials for H<sub>2</sub>S monitoring, thus it is highly recommended to develop the workflow for the use of end users.

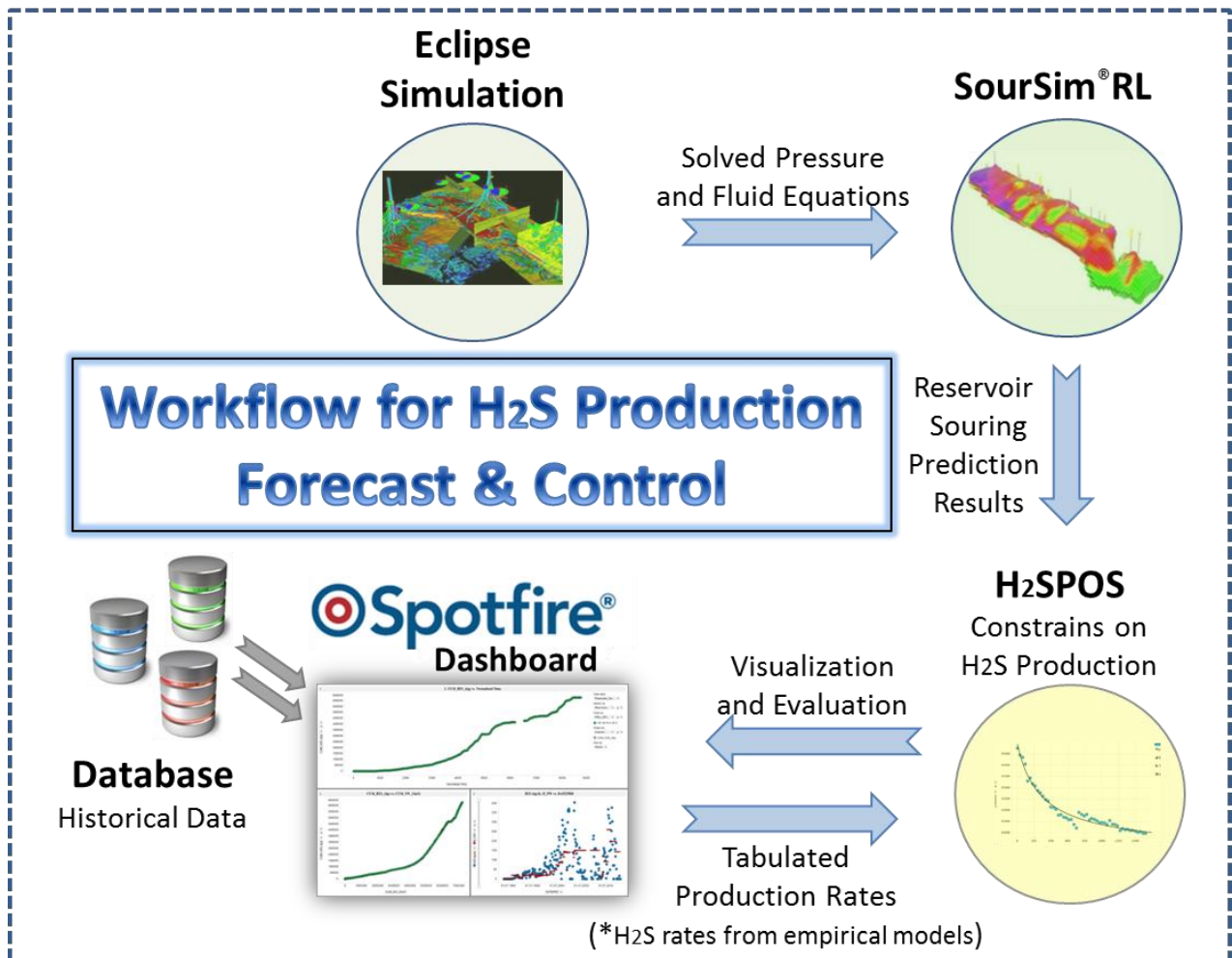


**Figure 38: Workflow for H<sub>2</sub>S Production Forecast and Control**

\*Alternative H<sub>2</sub>S production rate input predicted from mathematical expressions



As it was previously described in chapter 2.2.5, SourSim<sup>®</sup>RL is the post-processor where it receives the results of pressure and fluid equations from Eclipse (or any other) reservoir simulation software. Having been predicted, the results of H<sub>2</sub>S production forecast is then sent to in-house developed H<sub>2</sub>S production optimization software (H<sub>2</sub>SPOS), where, on the other hand, it also receives tabulated historical data of production rates, namely water, oil, gas and seawater rates from Spotfire dashboard. The main task of H<sub>2</sub>SPOS is then to impose constraints on the maximum level of H<sub>2</sub>S production, which will consequently reflect on oil and gas production rates. If group of wells are selected, then it will cut back on the wells with the highest H<sub>2</sub>S amounts to meet the maximum allowed H<sub>2</sub>S level set for selected group of wells. The same procedure can be performed for input of H<sub>2</sub>S production rate from mathematical expressions (e.g. eq. 25). Finally, the results from H<sub>2</sub>SPOS are then sent and visualized in the Spotfire dashboard for further evaluation of new well targets.

To minimize the number of softwares in the chain and thus optimize the workflow, the option of H<sub>2</sub>SPOS integration into Spotfire dashboard as in the case of python H<sub>2</sub>S Calculator can be considered.

## 6 Bibliography

- Bastin, E., Anderson, F., Greer, E., Merritt, C., & Moulton, G. (1926). The Problem of Natural Reduction of Sulphates. *Bull. Am. Assoc. Petrol. Geol.*, *10*, 1270-1299.
- Beeder, J., Nilsen, R., Rosnes, J., Torsvik, T., & Lien, T. (1994). Archaeoglobus fulgidus Isolated from Hot North Sea Oil Field Waters. *Applied and Environmental Microbiology*, *60*(4), 1227-1231.
- Beeder, J., Torsvik, T., & Lien, T. (1995). Thermodesulforhabdus norvegicus gen. nov., sp. nov., a Novel Thermophilic Sulphate-Reducing Bacteria from Oil Field Water. *Archives of Microbiology*, *164*(5), 331-336.
- Bernard, O., & Magot, M. (2005). *Petroleum Microbiology*. Washington, DC: American Society for Microbiology.
- Birkeland, N.-K. (2005). Sulfate-Reducing Bacteria and Archaea. In B. Ollivier, & M. Magot, *Petroleum Microbiology* (pp. 35-54). Washington DC: American Society for Microbiology.
- Burger, E. D., Jenneman, G. E., Bache, Ø., Jensen, T. B., & Soerensen, S. (2005). *A Mechanistic Model to Evaluate Reservoir Souring in the Ekofisk Field*. The Woodlands, Texas: Society of Petroleum Engineers. doi:10.2118/93297-MS
- Burger, E. D., Jenneman, G., Vedvik, A., Bache, O., & Voldum, K. (2006). *Forecasting the Effect of Produced Water Reinjection on Reservoir Souring in the Ekofisk Field*. San Diego, California: NACE International.
- Burger, E., Jenneman, G., & Carroll, J. (2013). *On the partitioning of Hydrogen Sulfide in Oilfield Systems*. Woodlands, Texas: Society of Petroleum Engineers. doi:<https://doi.org/10.2118/164067-MS>
- Eden, B., P.J. Laycock, & M. Fielder. (1993). *Oilfield Reservoir Souring*. HMSO, UK Health and Safety Executive.
- Evans, P., & Dunsmore, B. (2006). *Reservoir Simulation of Sulfate-Reducing Bacteria Activity in the Deep Sub-Surface*. Houston, Texas: NACE International.
- Evans, P., Nederlof, E., & Richmond, W. (2015). *Souring Development Associated with PWRI in a North Sea field*. Galveston, Texas: Society of Petroleum Engineers.

- factpages.npd.no*. (n.d.). Retrieved March 31, 2018, from [www.npd.no](http://www.npd.no):  
<http://factpages.npd.no/factpages/Default.aspx?culture=en>
- Haghshenas, M. (2011). *Modeling and Remediation of Reservoir Souring*. Austin, Tex: The University of Texas at Austin.
- Herbert, B. (1987). *Reservoir Souring (pp. 63-71)*. (E.C.Hill, J.L.Shennan, & R.J.Watkinson, Eds.) London, UK: The Institute of Petroleum.
- Herbert, B., Gilber, P., Stockdale, H., & Watkinson, R. (1985). *Factors Controlling The Activity Of Sulphate-Reducing Bacteria In Reservoirs During Water Injection*. Society of Petroleum Engineers.
- Håland, K., Barrufet, M., Rønningsen, H., & Meisingset, K. (1999). *An Empirical Correlation Between Reservoir Temperature and the Concentration of Hydrogen Sulfide*. Houston, Texas: Society of Petroleum Engineers.
- Immanuel, O., Abu, G., & Stanley, H. (2015). *Mitigation of Biogenic Sulfide Production by Sulfate Reducing Bacteria in Petroleum Reservoir Souring*. Lagos, Nigeria: Society of Petroleum Engineers.
- Ishkov, O., Mackay, E., & Sorbie, K. (2009). *Reacting Ions Method to Identify Injected Water Fraction in Produced Brine*. Woodlands, Texas: Society of Petroleum Engineers.
- Johnson, R. J., Folwell, B. D., Wirekoh, A., Frenzel, M., & Skovhus, T. L. (2017). Reservoir Souring - Latest developments for application and mitigation. *Journal of Biotechnology*, 256, 57-67. doi:<https://doi.org/10.1016/j.jbiotec.2017.04.003>
- Khatib, Z. I., & Salanitro, J. (1997). *Reservoir souring: analysis and experience in sour waterfloods*. Richardson, Tex: Society of Petroleum Engineers. doi:<https://doi.org/10.2118/38795-MS>
- Larsen. (2002). *Downhole nitrate applications to control sulfate reducing bacteria activity and reservoir souring*. Denver, Colorado: NACE International.
- Ligthelm, D.J. de Boer, R.B. Brint, & Schulte W.M. (1991). *Reservoir Souring: An Analytical Model for H<sub>2</sub>S Generation and Transportation in an Oil Reservoir Owing to Bacterial Activity*. Aberdeen, United Kingdom: Society of Petroleum Engineers. doi:<https://doi.org/10.2118/23141-MS>
- Maxwell, S., & Spark, I. (2005). *Souring of Reservoirs by Bacterial Activity During Seawater Waterflooding*. The Woodlands, Texas: Society of Petroleum Engineers. doi:<https://doi.org/10.2118/93231-MS>

- Mburu, A. (2018). *Well modeling of H<sub>2</sub>S production on a field in the North Sea*. Stavanger: Master thesis.
- Meisingset, K. K. (2017). *Field I well correlation for cumulative H<sub>2</sub>S production*. Internal report.
- Meisingset, K. K. (2018). *Personal communication*. Stavanger: Equinor.
- Mitchell, A. F., Hårvik, A.-M. B., Anfinsen, H., & Hustad, B. M. (2010). *A Review of Reservoir Souring for Three North Sea Fields*. Houston, Texas: NACE International.
- Mitchell, A. F., Skjevraak, I., & Waage, J. (2017). *A Re-Evaluation of Reservoir Souring Patterns and Effect of Mitigation in a Mature North Sea Field*. Montgomery, Texas: SPE. doi:<https://doi.org/10.2118/184587-MS>
- NPD guidelines for designation of wells and wellbores*. (n.d.). Retrieved April 19, 2018, from [www.npd.no](http://www.npd.no): [http://www.npd.no/Global/Norsk/5-Regelverk/Tematiske-veiledninger/Bronner\\_betegnelser\\_og\\_klassifisering\\_e.pdf](http://www.npd.no/Global/Norsk/5-Regelverk/Tematiske-veiledninger/Bronner_betegnelser_og_klassifisering_e.pdf)
- OilPlusLTD. (n.d.). (OilPlus LTD) Retrieved May 20, 2018, from [www.oilplusltd.com](http://www.oilplusltd.com): <https://oilplusltd.com/services/reservoir-souring-modelling>
- Pedersen, K. (2000). Exploration of deep intraterrestrial microbial life: current perspectives. *FEMS Microbiology Letters*, 185(1), 9-16.
- Reduction potential*. (n.d.). Retrieved March 15, 2018, from wikipedia: [https://en.wikipedia.org/wiki/Reduction\\_potential](https://en.wikipedia.org/wiki/Reduction_potential)
- Robinson, K., Samuelsen, W., Lungaard, E., & Skovhus, T. (2010). *Reservoir Souring in a Field with Sulphate Removal: A Case Study*. Florence, Italy: Society of Petroleum Engineers. doi:<https://doi.org/10.2118/132697-MS>
- Rosnes, J., Torsvik, T., & Lien, T. (1991). Spore-Forming thermophilic Sulphate Reducing Bacteria Isolated from North Sea Oil Field Waters. *Applied Environmental Microbiology*, 57(8), 2302-2307.
- Sunde, E., Lillbø, B.-L. P., Bødtker, G., Torsvik, T., & Thorstenson, T. (2004). *H<sub>2</sub>S Inhibition By Nitrate Injection on the Gullfaks Field*. Houston, Texas: NACE International.
- Sunde, E., Thorstenson, T., Torsvik T., Vaag J.E., & Espedal, M.S. (1993). *Field-Related Mathematical Model To Predict and Reduce Reservoir Souring*. New Orleans, Louisiana: Society of Petroleum Engineers. doi:<https://doi.org/10.2118/25197-MS>
- Uleberg, K., & Meisingset, K. K. (2018). *Field I well modified correlation for cumulative H<sub>2</sub>S production*. Internal report (not published).

- Vance, I., & Thrasher, D. R. (2005). Reservoir Souring: Mechanisms and Prevention. In O. Bernard, & M. Magot, *Petroleum Microbiology* (pp. 123-142). Washington, DC: American Society for Microbiology.
- Waage, J., Brurås, H. A.-M., & Mitchel, A. F. (2012). *Reservoir Souring: How to Minimize the Impact Based on Current Knowledge?* Geilo, Norway: Tekna Oilfield Chemistry Symposium.

## **Nomenclature**

<b>CSV</b>	Comma separated values
<b>DCA</b>	Decline curve analysis
<b>EC</b>	Energy Components
<b>GOR</b>	Gas oil ratio
<b>H<sub>2</sub>S</b>	Hydrogen sulfide
<b>H<sub>2</sub>SPOS</b>	Hydrogen sulfide production optimization software
<b>LSSW</b>	Low-sulfate seawater
<b>NPD</b>	Norwegian Petroleum Directorate
<b>OFM</b>	Oilfield Manager
<b>ppmv</b>	Parts per million per volume
<b>SI_PW</b>	Produced water souring index
<b>SI_SW</b>	Seawater souring index
<b>SRA</b>	Sulfate-reducing archae
<b>SRB</b>	Sulfate-reducing bacteria
<b>SRP</b>	Sulfate-reducing prokaryotes
<b>SWC</b>	Seawater cut
<b>TERR</b>	TIBCO Enterprise Runtime for R
<b>TVS</b>	Thermal viability shell
<b>URL</b>	Uniform resource locator
<b>VFA</b>	Volatile fatty acids
<b>WAG</b>	Water alternating gas

## Appendix A – Python script for extracting H<sub>2</sub>S data from Excel H<sub>2</sub>S Calculators

*# import necessary packages*

```
import pandas as pd
import numpy as np
import matplotlib.pyplot as plt
import glob
import os
import datetime
```

*# read the data from Excel H2S Calculators*

```
list_dfs = []
for file in glob.glob(r"D:\...\Calculator" + "/H2S*.xlsm"):
    xls = pd.ExcelFile(file)
    well_names = xls.sheet_names[18:]

    for well in well_names:
        df = pd.read_excel(xls, sheet_name=well, skiprows=[0, 1, 2, 3, 4, 5, 6, 7], usecols="T:Y,AA:AF")
        df.dropna(how='all', axis=1, inplace=True)
        df.dropna(how='all', axis=0, inplace=True)
        df_new = df.assign(FIELD_NAME=os.path.basename(xls).split(' 1MND')[0].split('NY ')[1])
        list_dfs.append(df_new)

platform = pd.concat(list_dfs, ignore_index=True)
```

*# clean the data after merging*

```
pd.to_datetime(platform['DATEPRD'], yearfirst=True, format="%Y-%m-%d")
platform = platform[platform['WELL_BORE_CODE'] != 'No Data']
```

*# temporary auxiliary column*

```
platform['diff'] = platform['DATEPRD'].groupby(platform['WELL_BORE_CODE']).diff()
/ np.timedelta64(1, 'D')
platform['diff'] = platform['diff'].fillna(0)
```

*# find well-bore-wise cumulative oil, water and liquid productions*

```
platform['CUM_OIL_VOL'] = (platform['BORE_OIL_VOL (Sm3/d)']*platform['diff']).\
    groupby(platform['WELL_BORE_CODE']).cumsum()
platform['CUM_WAT_VOL'] = (platform['BORE_WAT_VOL (Sm3/d)']*platform['diff']).\
    groupby(platform['WELL_BORE_CODE']).cumsum()
platform['CUM_LIQ_VOL'] = platform['CUM_OIL_VOL'] + platform['CUM_WAT_VOL']
```

*# find well-bore-wise cumulative SW and H2S*

```
platform['CUM_SW_(Sm3)'] = (platform['BORE_OIL_VOL
(Sm3/d)']*platform['diff']*platform['SW(%)']/100).\
```

```
groupby(platform['WELL_BORE_CODE']).cumsum()
platform['CUM_H2S_(kg)'] = (platform['H2S (kg/d)']*platform['diff']).\
groupby(platform['WELL_BORE_CODE']).cumsum()
```

*# find Souring Indexes*

```
platform['SI_PW'] = platform['H2S (kg/d)']*1000/platform['BORE_WAT_VOL (Sm3/d)']
platform['SI_SW'] = platform['H2S (kg/d)']*1000/(platform['BORE_WAT_VOL
(Sm3/d)']*platform['SW(%)']/100)
```

*# number of days since the start-up of each well-bore*

```
platform['n_days'] = platform['diff'].groupby(platform['WELL_BORE_CODE']).cumsum()
```

*# number of days in production (i.e. without shut-in period)*

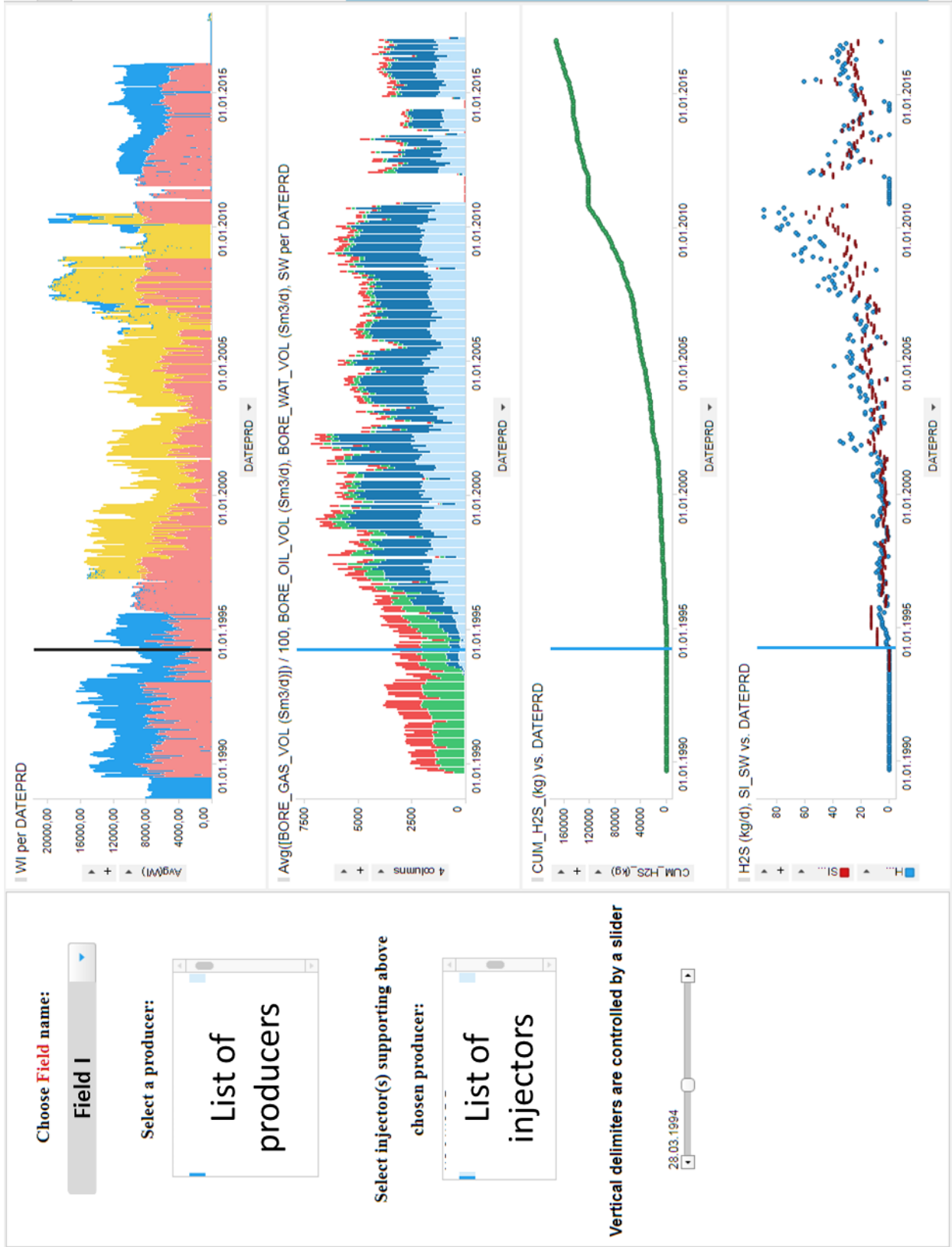
```
platform['days_in_prod'] = np.where((platform['BORE_OIL_VOL (Sm3/d)'] == 0) &
                                     (platform['BORE_WAT_VOL (Sm3/d)'] == 0) & (platform['BORE_GAS_VOL (Sm3/d)']
                                     == 0),
                                     (platform['n_days']-platform['diff']), platform['n_days'])
```

*# export to cvs file*

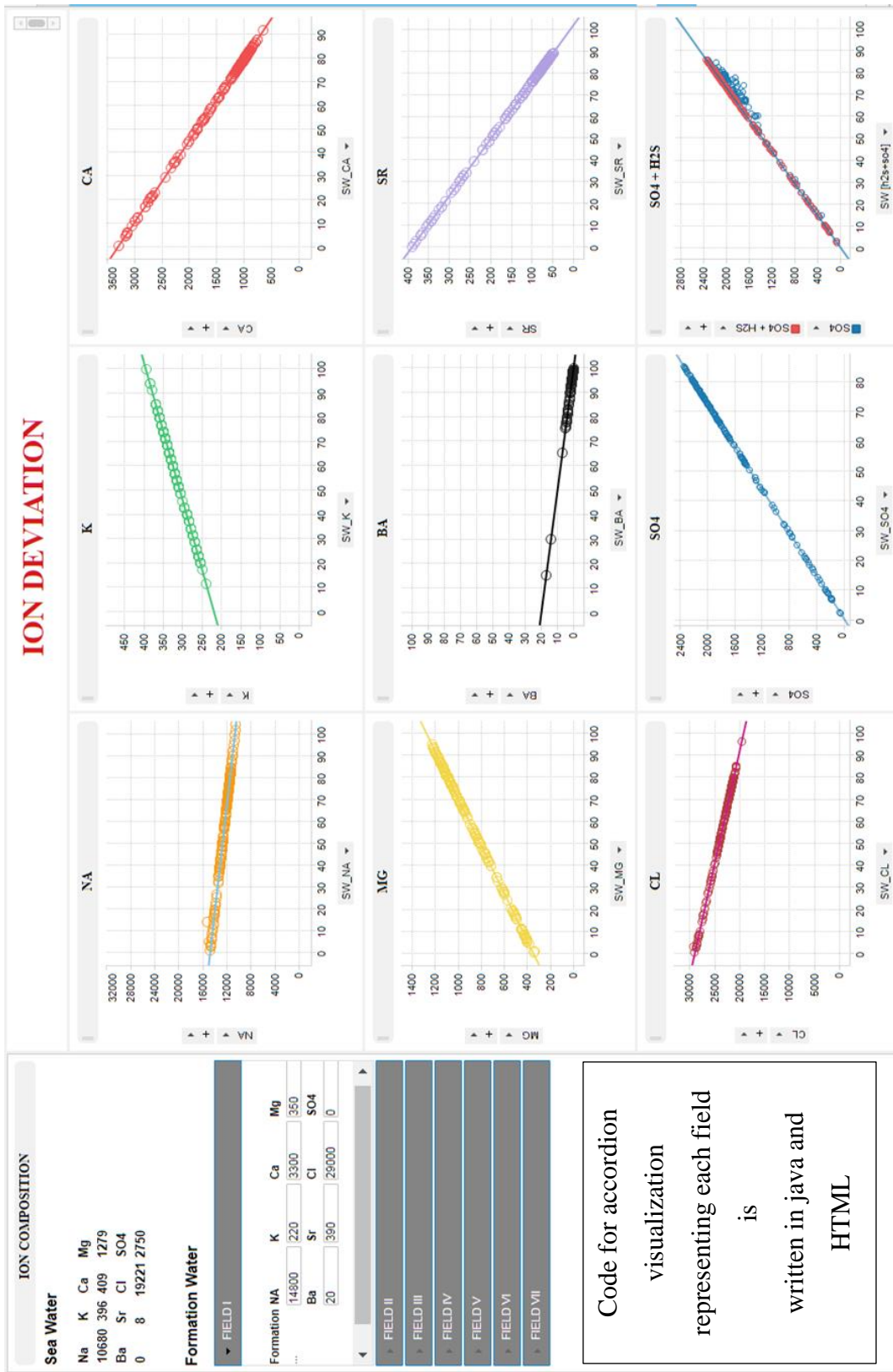
```
platform.to_csv("Production_Data.csv")
```



# Appendix B – Dashboard page for injection – production data joint



# Appendix C



Dashboard page for formation ion composition adjustment

## Appendix D – Python script for extracting ‘reference volumes’ for each wellbore and running the model

```
# import necessary packages
import pandas as pd
import numpy as np

# read the data into pandas data frame
df1 = pd.read_excel('F:\Statoil Documents\Production_Data_v2.xlsx')
df = df1.dropna(subset = ['WELL_BORE_CODE'])

# drop all rows with zero valued H2S (kg/d)
df_test = df[(df['H2S (kg/d)'] != 0.0)]
df_test = df_test.groupby(['WELL_BORE_CODE']).first()

# create a list for storing reference volumes of each wellbore
wbc_previous = ""
V_refs = []
for i, row in df.iterrows():
    wbc_current = row['WELL_BORE_CODE']
    if wbc_previous != wbc_current:
        if row['H2S (kg/d)'] > 0:
            V_refs.append(140000) # minimum reference volume for 'Type I' wellbores
        else:
            if wbc_current in df_test.index:
                V_refs.append(df_test.loc[wbc_current, 'CUM_LIQ_VOL'])
            else:
                V_refs.append(np.nan)
        else:
            V_refs.append(V_refs[len(V_refs)-1])
    wbc_previous = wbc_current
df.loc[:, 'V_ref'] = V_refs

# Set of constants for 'Type II' wellbores, proposed by Mburu (2018)
K1 = 0.1
K2 = 5.4*(10**11)
K3 = -8.8
m = 0.2

# Run the model
df.loc[:, 'PV'] = df['CUM_LIQ_VOL'] / df['V_ref']
df.loc[:, 'F(CumL)'] = K1 + (1 - K1)*(df['PV'] - 1) / (df['PV'] - 1 + K2*pow(df['PV'],K3))
```